BIRZEIT UNIVERSITY

Faculty of Pharmacy, Nursing and Health Professions

Master Program in Industrial Pharmaceutical Technology

Formulation of Metoprolol Tartrate bi-layer tablets by using 3D Printing Technology

تشكيل أقراص طرطرات الميتوبرولول ثنائية الطبقة باستخدام تكنولوجيا الطباعة ثلاثية الأبعاد

This thesis was submitted in partial fulfillment of the requirements for the Master's degree in Industrial Pharmaceutical Technology from the Faculty of Graduate Studies at Birzeit University, Palestine

By

Mariana Jubraeil Musallam

MSc. Pharmacy – Birzeit University - Palestine

Supervisor: Dr. Hani Shtayeh

May 2020

Birzeit University

Faculty of Graduate Studies

Faculty of Pharmacy, Nursing and Health Professions

Master in Industrial Pharmaceutical Technology

Formulation of Metoprolol Tartrate bilayer tablet by using 3D printing technology

Prepared by: Mariana Musallam

Registration number: 1165097

Supervisor: Dr. Hani A. Shtayeh

Master thesis submitted and accepted, Date: 28th May,2020

The names and signatures of the examining committee are as follows:

Dr. Hani A. Shtayeh	Head of committee	Signature:
Dr. Feras I. Kanaze	First Examiner	Signature:
Dr. Moammal S. Qurt	Second Examiner	Signature:

Remark

This Thesis was done at faculty of Pharmaceutical sciences at Ghent university under

the supervision of PhD researcher **Aseel Samaro** and Prof. Dr. Apr. **Chris Vervaet.**

Dedication

This work is dedicated to the soul of **my father** may God Almighty bless him.

Acknowledgments

First and foremost, I would like to thank God Almighty for giving me the knowledge, ability, opportunity, and strength to deal with this project and to persevere and complete it satisfactorily. Without his blessings, this achievement would not have been possible.

I wish to express my deepest appreciation to my supervisor, **Associated Professor Hani Shtayeh**, who persistently guided and encouraged me to the right way, even when the road got tough. Without his continuous corporation, the goal of this work would not been released.

I would like to acknowledge the invaluable help that my great supervisor, **Aseel Samaro**, provided during my research, without her help this project would not see the light.

I am indebted to **Prof. Chris Vearvate** who hosted me at his labs, provided me with the materials and equipment, and followed up my work at Ghent university.

The financial and technical assistance from the Entrepreneurship and innovation unit presented by **Mr. George Yerousis** and **Mr. Atef Shkokani** as well as **Dr. Iyad Tumar** is highly appreciated.

List of abbreviations

3D	Three-Dimensional Printing
ABS	Acrylonitrile Butadiene Styrene
ASA	Amino salicylate
API	Active Pharmaceutical Ingredient
BCS	Biopharmaceutical Classification System
°C	Celsius degree
CAD	Computer-aided design
CAP	Captropril
DC	Direct compression
DSC	Differential scanning calorimetry
ER	Extended Release
EP	European Pharmacopeia
EVA	Ethylene-vinyl acetate
FDA	Food and Drug Administration
FDM	Fused Deposition Modelling
FFF	Freeform fabrication technology
GI	Gastrointestinal tract
GLI	Glipizide

ΔH	Enthalpy
HCl	Hydrochloric acid
HCV	Hepatitis C virus
HDPE	High-density polyethylene
HME	Hot-melt extrusion
HMPC	Hydroxypropyl Methylcellulose
HPC	Hydroxypropyl cellulose
IR	Immediate release formulation
J	Jol
KN	Kilo newton
LOD	Loss On Dry
LOM	laminated objects manufacturing technology
MFI	Melt flow index
MIT	Massachusetts Institute of Technology
MPT	Metoprolol Tartrate
N	Number
NA	Not Applicable
NIF	Nifedipine
Pa	Pascal
PC	Polycarbonate

PCL	Polycaprolactone
PEG	Polyethylene glycol
PEI	polyetherimide
PEO	Polyethylene oxide
PLA	Polylactic acid or polylactide
P.M	Physical mixture
PPSF	Poly phenyl- sulfone
PVA	Polyvinyl alcohol
PVP	Polyvinylpyrrolidone
QC	Quality control
R^2	Correlation coefficient value
RPM	Rounds Per Minute
RSD%	Relative standard deviation
SL	Stereolithography
SR	Sustained-release formulation
STDEV	Standard Deviation
SSEs	Single-Screw extruders
T_d	Degradation temperature
T_g	Glass transition temperature
T_m	Melting temperature

T_{max}	Maximum temperature
TA	Texture Analyzer
TCP	Tricalcium phosphate
TEC	Triethyl citrate
TSEs	Twin-screw extruders
UK	United Kingdom
USA	United states of America
USP	United States Pharmacopeia
UV	Ultra Violet
V	Version
VA	Vinyl acetate
w/w	Weight by weight

List of Figures

List of Tables

List of Equations

Contents

Abstract

The Aim of this research was to manufacture individualized bilayer tablets with dual release of Metoprolol tartrate using 3D printing technology, FDM technique.

3DP technology used to personalized the dose. Bilayer tablet manufactured due to the need of loading and maintenance dose. MPT was used as a model drug due to its low T_m and BCS classification (class I). Also, it was not manufactured in direct compression or as capsules.

Different polymers used to prepare the desired tablets. After examination, MPT: CAPA® 6506 (40:60%, w/w) filament used to prepare the sustained release layer, while MPT: Eudragit: Polyox^{TM} (25:52.5:22.5%, w/w) filament used to prepare the immediate release one.

Filaments extruded and their mechanical properties studied by applying the tensile test using texture analyzer. Tablets printed and their dimensions, weight variation, hardness, content uniformity and friability calculated. All the results were satisfactory.

Crystallinity content in the filaments and printed tablets evaluated using DSC and they were acceptable. Printing parameters modified and the effect on the tablets` morphology observed. Moreover, the effect of printing parameters on the dissolution rate and kinetics investigated.

Regarding the in vitro dissolution, it was applied for the mono tablets and bilayer tablets (n=3). For SR mono tablets, phosphate buffer used PH 6.8, a semi linear curve obtained and 94.11% of the drug released within 24 hours. And they showed Korsmeyer- Peppas with an anomalous release model.

For IR tablets two formulas were printable [MPT+ Klucel EF (25:75%, w/w) and MPT: Eudragit EPO: POLYOX^{TM} (25:52.5:22.5%, w/w)] the test applied, using HCl buffer PH 1.2. The first formula showed slow release since 100% of the drug released within an hour, while the second one showed a faster release since 100% of the drug released within the first 15 minutes.

Considering bilayer tablets, HCl PH 1.2 used for the first 2 hours and phosphate buffer PH6.8 used for the last 22 hours, it was found that 40% of the API released within the first hour as a loading dose, where 87% released withing the 24 hours.

Direct compression technology performed for the same formulas; it was found that the SR formula was not compressible. Whereas, MPT: Eudragit EPO: POLYOX^{TM} (25:52.5:22.5%, w/w) showed a complete release within 30 minutes.

To conclude, this work proved that FDM is a good method to prepare individualized medicine and Bilayer tablets. In addition, it can be a fundamental for future similar researches.

الملخص

تهدف هذه الدراسة إلى تصنيع أقراص طرطرات الميتوبرولول ثنائية الطبقة والتحرر الدوائي بواسطة تكنولوجيا الطباعة ثلاثية الأبعاد بتقنية نمذجة الترسيب المدمج.

تستخدم تكنولوجيا الطباعة ثلاثية الأبعاد لتخصيص الجرعة الدوائية، وتم تصنيع الأقراص ثنائية الطبقة لحاجة المريض إلى الجرعة الفورية والمستدامة. تم اختيار المادة الفعالة طرطرات الميتوبرولول لأنها تملك درجة ذوبان منخفضة، وتصنف ضمن المجموعة الأولى من نظام تصنيف الصيدلانيات البيولوجية. لم يتم تصنيعها من قبل على شكل أقراص بواسطة تقنية الكبس أو على شكل كبسولات.

استخدمت عدة بوليمرات لتحضير الأقراص المطلوبة. بعد الفحص والتحقق تم اعتماد MPT: CAPA® 6506 (40:60%, w/w) كحبر صيدلاني للطبقة مستدامة التحرر الدوائي، بينما استخدم :MPT: Eudragit Polyox™ (25:52.5:22.5%, w/w) لطبقة التحرر الدوائي الفوري.

تم تحضير الحبر الصيدلاني عن طريق جهاز البثق، وفحص خصائصة الميكانيكية باستخدام اختبار الشد. تم طباعة الأقراص الدوائية وفحص أقطارها، وأوزانها، ودرجة صلابتها، ومحتوى المادة الفعالة فيها ودرجة تفتتها. وكانت النتائج وفق المعايير المطلوبة.

بعدها تم تقييم درجة التبلور في الأحبار الصيدلانية والأقراص الدوائية المطبوعة باستخدام جهاز مسعر المسح التبايني، وكانت النتائج مقبولة. وتم التغيير في اعدادات الطباعة ودراسة تأثيرها على تشكيل الأقراص ومورفولوجيتها. علاوة على ذلك، تم دراسة التغيير في اعدادات الطباعة وأثره على سرعة الذوبان وحركية الدواء.

وفيما يتعلق بذوبان الأقراص في المختبر، تم تطبيق الاختبار على ثلاث أقراص من الأقراص مستدامة التحرر الدوائي، وسريعة التحرر الدوائي، وثنائية الطبقة. تم استخدام محلول الفوسفات درجة حموضته 6.8، والحصول

على منحنى شبه خطي وتحرر دوائي بنسبة 94.11% خلال 24 ساعة، واتبعت هذه الأقراص نموذج Korsmeyer– Peppas with anomalous release model للتحرر الدوائي.

فيما يخص الأقراص سريعة التحرر الدوائي، فكانت هناك نوعين فقط من الأحبار الصيدلانية لهما القابلية للطباعة وهما [MPT+ Klucel EF (25:75%, w/w) and MPT: Eudragit EPO: POLYOX^{TM} (25:52.5:22.5%, w/w))]، تم تطبيق اختبار الذوبان باستخدام محلول حمض الهيدروكلوريك ذو درجة الحموضة 1.2. وكانت الخلطة الأول بطيئة اذ تم تحرر الدواء كاملا 100% خلال ساعة، بينما الخلطة الثانية كان التحرر الدوائي فيها كاملا خلال 15 دقيقة.

بالنسبة للأقراص ثنائية الطبقة، فاستخدم محلول حمض الهيدروكلوريك درجة حموضته 1.2 أول ساعتين من الاختبار ومحلول الفوسفات درجة حموضته 6.8 خلال ال22 ساعة الأخيرة. ووجد أن 40% من المادة الفعالة تم اطلاقها كجرعة أولية خلال الساعة الأولى وتم اطلاق 87% من المادة الفعالة خلال 24 ساعة.

تم تحضير نفس الخلطات وكبسها لمقارنة نتائج ذوبان الدواء. ووجد أن الطبقة المستدامة كانت غير قابلة للكبس بينما الطبقة سريعة التحرر الدوائي تحرر الدواء فيها خلال 30 دقيقة.

وفي النهاية، تم الاثبات بهذا البحث أن تقنية نمذجة الترسيب المدمج نجحت في انتاج أقراص فردية الجرعات وثنائية الطبقة، وبالإضافة إلى ذلك يمكنه أن يكون قاعدة أساسية لأبحاث مماثلة بالمستقبل.

1. Introduction

1.1 Oral drug delivery: Tablet dosage form

A drug can be identified as an agent intended for use in treatment, diagnosis, cure, or prevention of diseases in humans or animals[1]. It reaches organs through drug delivery systems which are "Approaches, systems, technologies, and formulations for transporting a pharmaceutical compound in the body as needed to safely achieve its desired therapeutic effect". They are designed to improve the bioavailability of the drugs and to modify the time and/or site of their release [1].

Medication can be administrated by a different route of administration such as oral, sublingual, parenteral, transdermal, topical, conjunctival, intraocular, intranasal, aural, intrarespiratory, rectal and vaginal [2].

The oral route is considered as the most natural, uncomplicated, convenient, and safe means of administering drugs. Also, this route does not need specific supplies nor knowledge for its application. It is compliance for both patients and physicians consequently leads to successful therapy [2],[3].

In the oral route, the drug passes different parts from the digestive tract starting from the oral cavity to the pharynx, to the esophagus, to the small and large intestines as shown in Figure 1. Moreover, Unabsorbed substances leave over the anal sphincter. The small intestine is considered as the most significant part because most of the drug absorptions happen there [3].
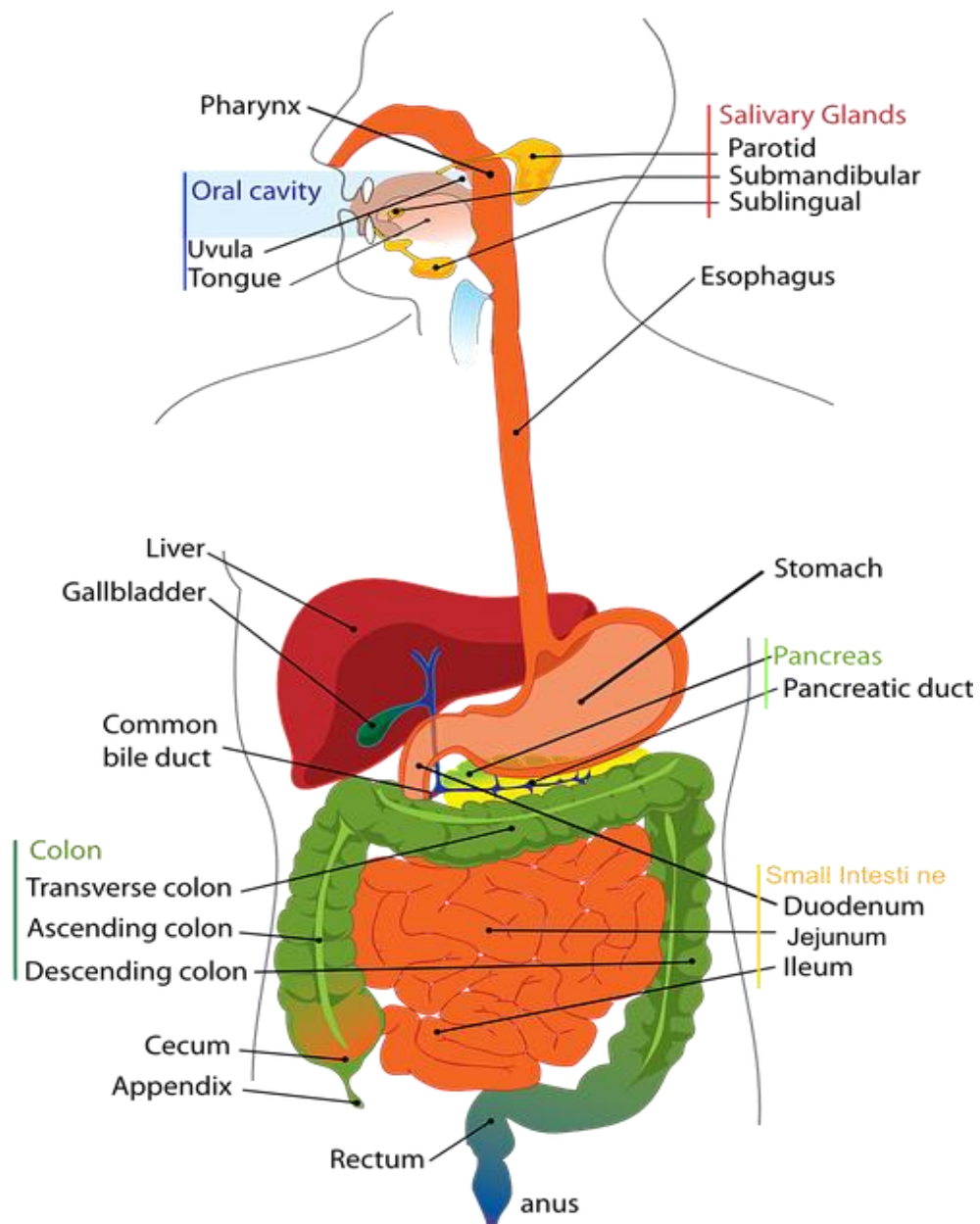
Figure 1: Gastrointestinal tract anatomy [145]

The drug disintegrates, crosses the gastrointestinal epithelium and dissolves in the gastrointestinal tract (GI) [2]. Due to the large surface area of the intestine, the Active Pharmaceutical Ingredient (API) can be absorbed effectively. Moreover, before the APIs move to the circulation system, they pass the first-pass effect in the lever that leads to (in)activation of the API [2].

Oral route disadvantages can be summarized as it is unsuitable for unconscious patients and slower onset action compared with parenteral one. Since there is a chance for irregular absorption of the drugs because this route may depend on the type of food present in the GI. Hormones, pathological states, and other drugs can affect it. Also, the destruction of some drugs by the acidic PH in the stomach or the GI enzymes [2],[3].

The common orally administered dosage forms in use are: tablets, capsules, syrup, solutions, elixirs, suspension, gels, and magmas. While tablets and capsules are the most used dosage forms [2].

Tablets and capsules can be intended as immediate-release formulation and/or modified-release to vary or extend the release such as controlled release sustained release and extended releases [4].

1.1.1 Immediate release

Immediate release formulation (IR) is intended to release the medication in a short period after administration. Where the API released fast and generally result to the maximum plasma concentration (C_{max}) in short period of time. The time of action is defined as the time where the concentration is below the minimum toxic concentration and above the minimum effective concentration which called the therapeutic window as shown in Figure 2 [4].

In the immediate release, the time where plasma concentration present in the therapeutic range is short, so frequency doses needed, which is not preferred by patients. Thus, that may lead to insufficient treatment and/or subtherapeutic and toxic doses [5].

1.1.2 Sustained release

The sustained-release formulation (SR) is intended to allow the frequency of dosing to be reduced compared with immediate-release dosage forms. However, it is one of the major challenges in pharmaceutical industries. Consequently, the maximum plasma concentration is lower compared with immediate-release but it stays for a longer time in the therapeutic range. This leads to less frequent doses that improve patient compliance as shown in Figure 2 [4], [5].

Sustained-release formulations have many advantages such as; better control of drug absorption, improve patient conveniences, increase the safety margin of high potency drugs, reduction of fluctuation in steady-state level and reducing the resources spent to dispense, administer and monitor patients [5].

On the other hand, sustained-release formulation may have a risk of toxicities (dose dumping/ physiological formulation variables), reduced potential for dosage adjustment of drugs and retrieval of drug difficult in case of toxicity, poisoning or hypersensitive reactions [5].
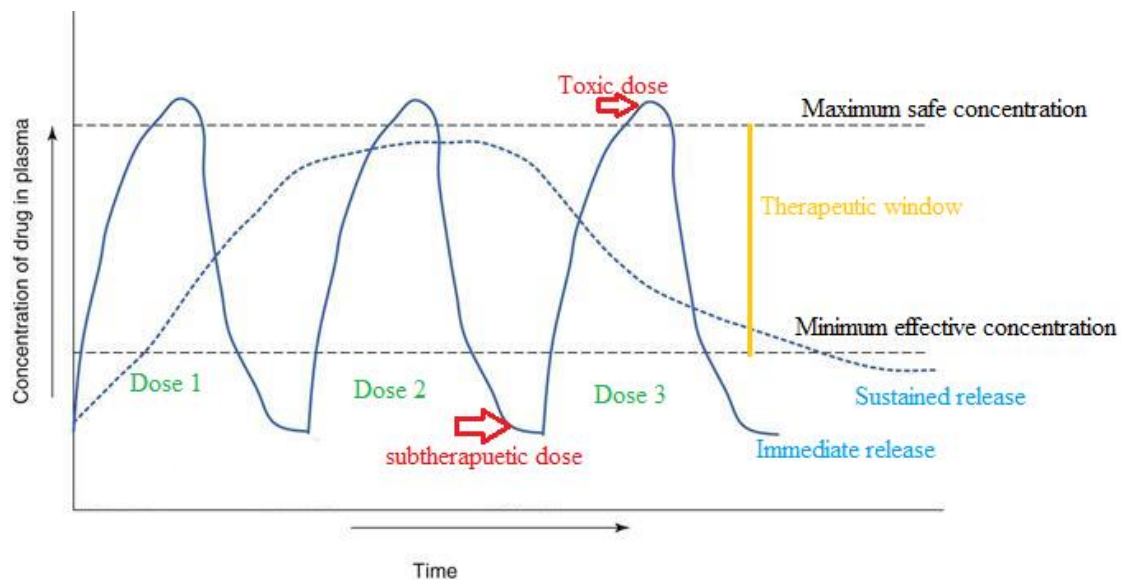
Figure 2: Plasma concentration time profile for immediate release (dotted line) and sustained release (continuous line)

1.2 Hot Melt Extrusion

1.2.1 Introduction

Hot-melt extrusion (HME) is an old manufacturing technique that returned to early 1930s and was mainly used for plastic, rubber and food industries [6]. The HME advantages over the traditional solid dosage forms manufacturing have triggered the interest to use it as a new technology within the pharmaceutical industry. This technology presents its viability and robust in producing a variety of drug delivery systems. For example, it is used for pellets, capsules, films, tablets and implantable reservoirs [7]. Also, the ability to produce solid dispersion that enhances the bioavailability, without using any type of liquid [8]. Thus, it can be an alternative technique for spray drying [7].

HME is a process of forcing raw materials out of a well-defined die under control conditions like pressure, temperature, feeding and mixing rates to produce a stable product with constant density and shape [8],[9].

Recently, HME is combined with Fused Deposition Modelling (FDM) printing to manufacture personalized medicine that is a modern trend in the 21st century. Personalized medicine depends on tailoring treatments (such as drug release profile, dose strength, specific color, shape, and flavor) to the characteristics preferences and needs of individual patients [7], [10].

Recently, HME has been integrated with Fused Deposition Modelling (FDM) 3DP technology, as shown in Figure 3. This process of integration has many advantages. Those advantages can be summarized in increasing drug solubility and bioavailability due to the good molecular level mixing in extrusion, uniform structure of the dosage form and personalized product attitudes [7].
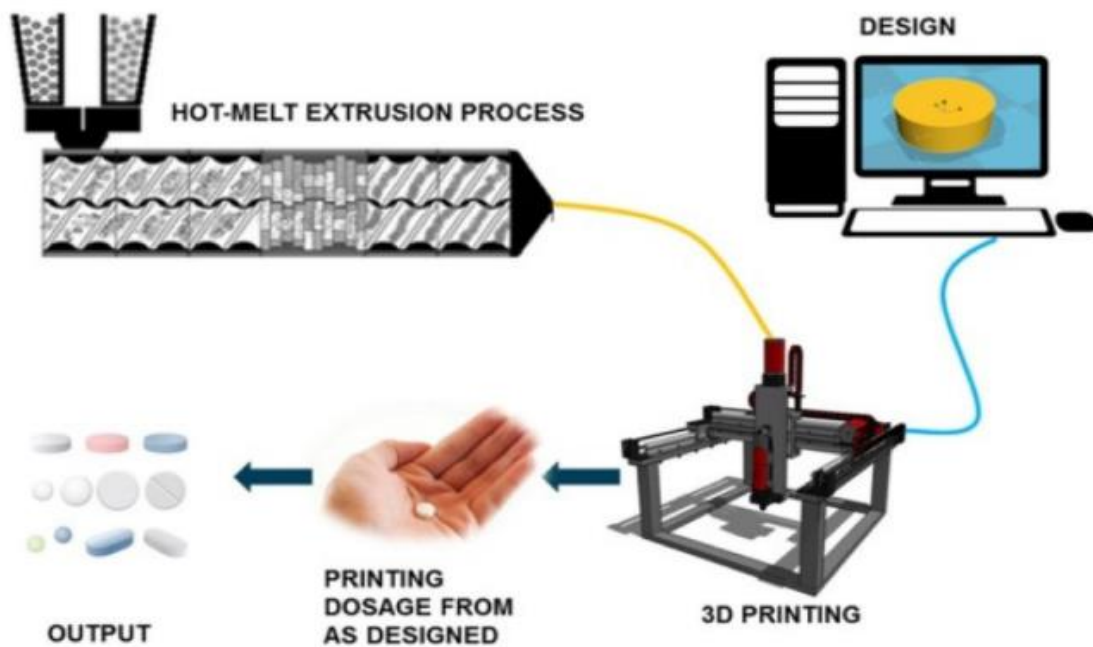
Figure 3:Twin screw extrusion integrated with FDM printing [11]

1.2.2   HME process

The HME process starts from feeding the physical mixture (P.M) in the feeder (Gravimetric, Volumetric), then transferring it to the barrel which contains the screw(s) and different zones that can be heated separately from each other [12].

Next, the P.M melts in the barrel due to the screw shear stress and the barrel temperature which is usually 15-60°C above the melting point of semi-crystalline polymers and glass transition temperature of amorphous ones [12].

Finally, the melt conveyed towards the die which may have different shapes. In our case, it is a cylinder with 1.75±0.05 mm diameter, where constant pressure forces the material out [12].

The screws contain two types of elements, as shown in Figure 4. The conveying elements; that transfer the materials to the die and kneading ones that ensure the mixing, softening and partial melting of the materials inside the barrel [12].

The screws have to be identical in diameter to move correctly and smaller than the barrel diameter to establish a specific small clearance between the external wall and the screw tip [12],[13],[14].
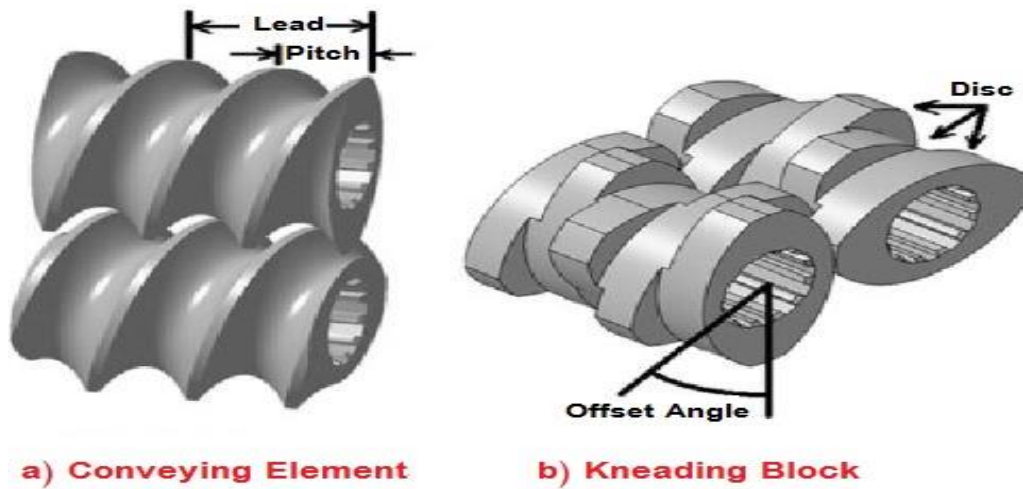
Figure 4: Screw elements; a) Conveying element, b) Kneading block [12]

In the HME process many parameters should be taken into consideration and must be optimized, these parameters are:

(a) formulation (ingredients and concentrations)

(b) extruder configuration (screw configuration, die geometry)

(c) barrel set- temperature profile

(d) throughput

(e) screw speed

These parameters can be divided into input parameters and output parameters, as shown in Figure 5.

Input parameters that can be adjusted by the operator such as the feeding rate, process temperature, screw speed. Output parameters such as the torque value, the pressure profile, melt temperature profile, residence time distribution, and dispersion quality. Unluckily, not all these outputs can be directly measured. For example, the molten temperature, homogeneity since the probes cannot penetrate the mass to measure its temperature and there is nothing to measure the dispersion quality [12], [13], [15].
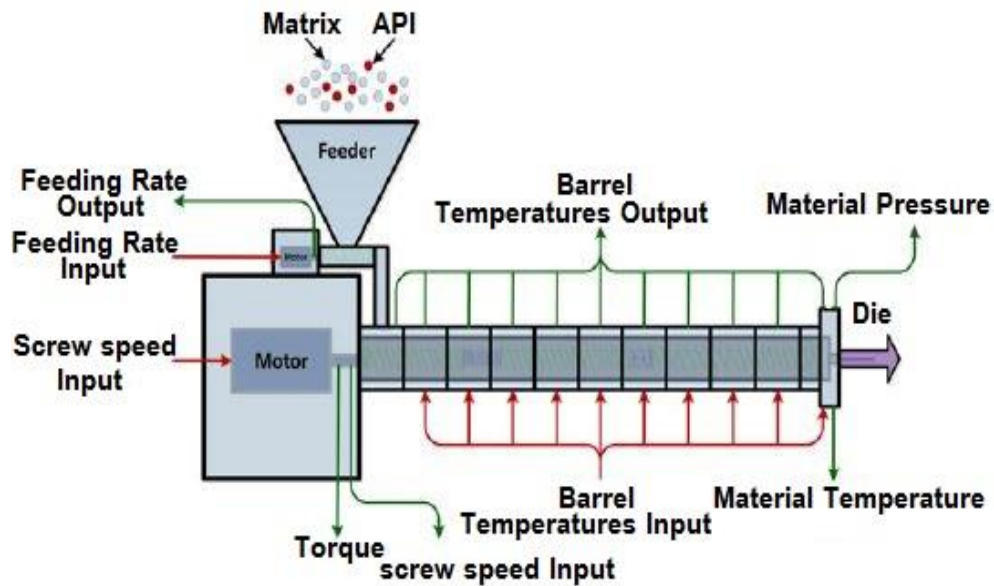
Figure 5: HME scheme with input (highlighted in red) and output (highlighted in green) parameters [12]

1.2.3   Single and Twin-screw extruders

There are two different types of extruders available depending on the number of screws in the barrel: single and twin-screw extruders.

Single-screw extruders (SSEs): These contain one rotating screw with a feeding zone, compression zone, and the melting zone used to melt polymers, as shown in Figure 6 [16].

It is the most widely used extrusion system in the world, its screw dimension plays an important role in the extrusion process, since if once the screws are reduced less than 18mm, it becomes weak and less reliable. However, to overcome this issue a vertical screw used instead of horizontal one [17].
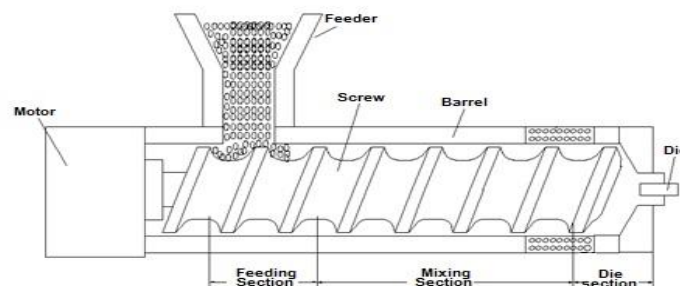
Figure 6:Single screw extruder [16]

Twin-screw extruders (TSEs): which contains two rotating screws (co-rotating or counter-rotating), it is used to melt and mix polymers and APIs, as shown in Figure7.

TSEs are better compared with SSEs because they have easier material feeding, improve mixing (distributive or dispersive mixing), less tendency to overheat (less heating and residence time), superior control of parameters of operation and higher process flexibility [16],[18].
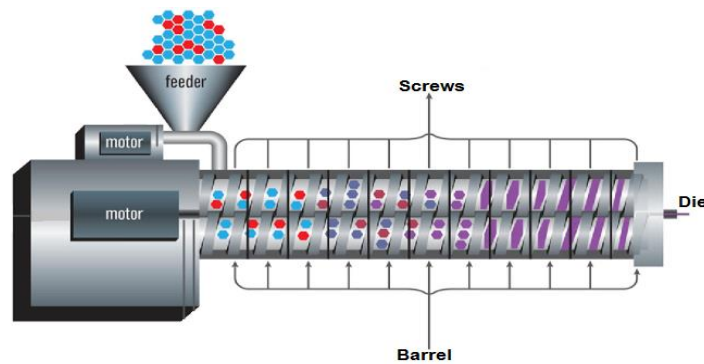
Figure 7: Twin screw extruder [16]

Single and Twin-screw extruders have different advantages and disadvantages. Table1, summarize the main points.

Table 1: Advantages and Disadvantages of Single and Twin-screw extruders [6]

	Advantages	Disadvantages
Single Screw Extruder	▪ Mechanical simplicity	▪ The high tendency of overheating
	▪ Low maintenance	▪ Not suitable for heat-sensitive materials
	▪ Low cost	▪ Poor mixing
Twin Screw Extruder	• Easier material feeding	• High input energy
	• High kneading and dispersing Capa® 6506 city	• Not suitable for shear sensitive materials
	• Lower tendency to overheat	
	• Higher process productivity and flexibility	
	• Better control process parameters	
	• Enhanced mixing	

1.2.4 Advantages and Disadvantages of Hot Melt Extrusion

Amongst the industrial pharmaceutical operations, the interest of using HME nowadays raised due to different reasons. One of those signs is that the HME is a continuous manufacturing process. Vary operational steps can be done through it, for instance, melting, mixing, shaping, and homogenizing. Moreover, it minimizes the material lost, enhances the throughput and reduces the input energy [12],[13].

HME can increase the quality of the product since it provides an efficient process of production. Mainly it is used in pharmaceutical industries to manufacture solid dispersions. Where the API dispersed into the matrices of the polymers. Besides, it is used to increase the water-insoluble drugs` bioavailability. Which is a real challenge in the pharmaceutical industry, by controlling the drug release. Besides, it is used to produce solid solutions and thin films as well as to mask the taste of bitter APIs [16].

Furthermore, HME is preferred because it is an environment-friendly process. It is solvent-free compared with traditional techniques such as spray drying and roll spinning that need organic liquids to produce solid dispersions. Those organic solvents can cause pollution while they are being disposed of [6]. Other advantages can be, short time of production, increasing the efficiency of drug delivery, higher process efficiency and the ability to produce novel and new formulation [19].

Different solid dosage forms can be produced through HME, including but not limited to, pellets, tablets, caplets, solid suspensions and solutions with poorly water-soluble APIs [20]. Where the API dissolves in the matrix of the polymer. Thus, the matrix acts as a binder, drug solubilizer and stabilizer or/and drug release excipient. However, this matrix must be a suitable carrier and carefully selected based on the miscibility, stability, drug-polymer interaction and the final dosage form function [12],[21].

William et al mentioned that HME boosts the solubility of the drug and the rate of dissolution. Also, a solid solution prepared by HME has better thermodynamic stability compared with those manufactured by solvent evaporation and spray drying technologies [8].

On the other side, there are some obstacles to HME. Since HME needs high input energy, that required for the barrel temperature and shear force of the extruder. This high temperature can cause mechanical degradation to some polymers and thermal degradation to APIs. Upon that some thermolabile substances cannot be used [6], [8], [16],[22].

Considering stability issues, dosage forms produced by HME depend on the final product's physical state. The API, polymers, and excipients' physical state. As well as, the filaments packaging and storage.

Chemical and physical stability must be done. Since degradation should not happen and the crystalline state should stay crystalline where the amorphous should not be recrystallized over the long term [16]. X-ray diffraction (XRD), Differential Scanning Calorimeter (DSC), FTIR and electronic scanning microscope can be used to characterization the filaments and tablets[23].

1.3 3D printing

1.3.1   Introduction

Through back, for hundred years "Batch manufacturing" used to produce tablets dosage forms in pharmaceuticals; which is a long process that needs multi-steps such as mixing, milling, sieving, wet or dry granulation, tablet compression, coating, long-term stability study as well as large scale equipment, as shown in Figure 8 [24],[25],[26].
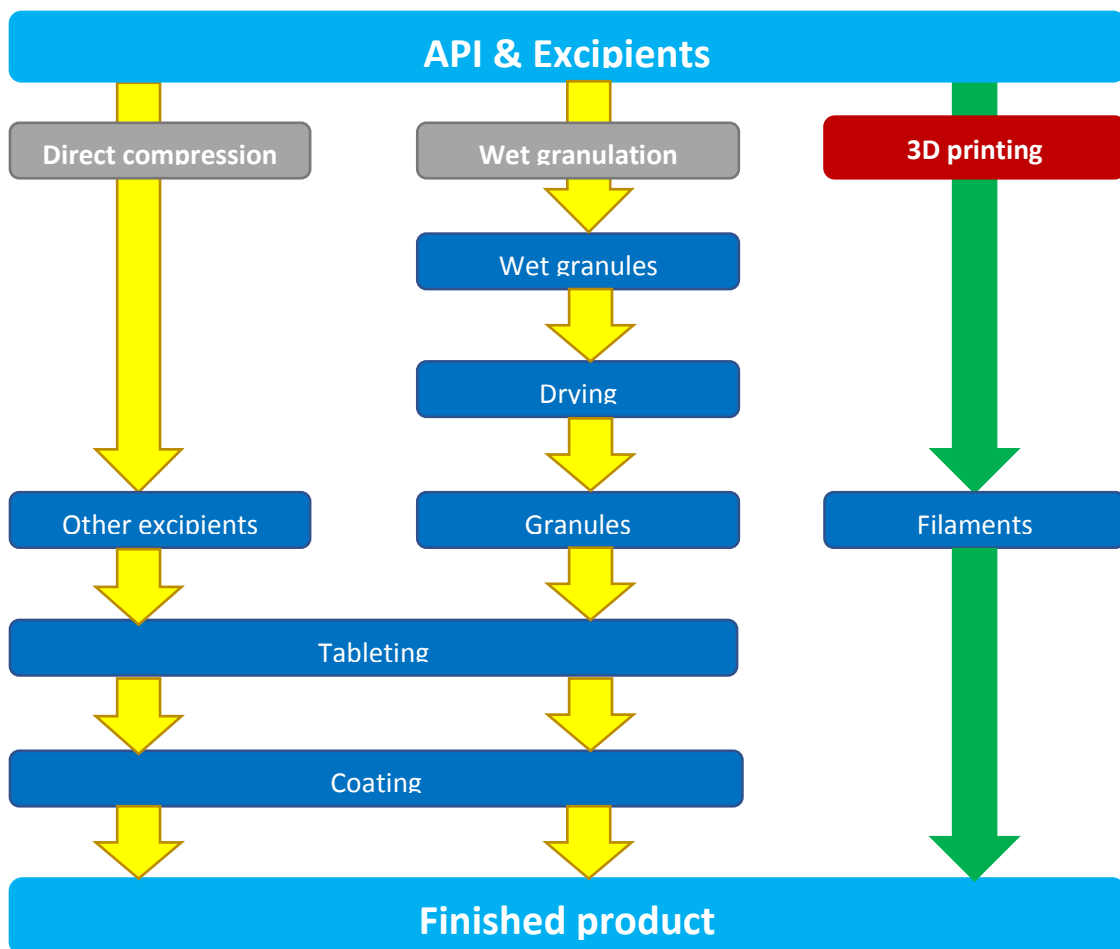
Figure 8: Tablet manufacturing processes

Recently, the pharmaceutical industry moves a step forward for a more fast, continuous and cost-efficient method of drug manufacturing by using new advanced technologies to increase the quality of the product and deal with many of the implicit causes of results and shortage of drugs [27].

One of these technologies is Three-Dimensional Printing (3DP) that diminish the manufacturing steps and display agitate steps toward changing the process of manufacturing to offer personalized medicines [24]. Researchers try to use it for novel drug formulation to produce tablets of satisfying regulatory tests and matching the release and standards of commercial ones [28].

3D printing is an additive manufacturing and rapid prototyping method in which materials deposit in layers to produce the 3D object by using a computer-aided design (CAD) file that later converted to slices to cut the design into thin cross-sections till building the layers later [29]. This technology gives the designing and manufacturing processes new flexibility especially of complex compounds with high precious and accuracy that can be used in programmable and personalized medicine [30],[31].

In the last few decades, 3D printing caused a revolution in different human activities sectors which leads the pharmaceutical industry to join the fourth industrial revolution [32]. It is an extremely automated and clean process [33]. Meanwhile different solid dosage forms can be built with adjustable densities and diffusivities,

complex internal geometries, multiple drugs, and excipients at the point of care which is a unique aspect[30],[34]. With its development, it is turned into a solid freeform fabrication (FFF) technology which increases the research efforts toward manufacturing personalized solid oral dosage forms [29],[30].

1.3.2   3D printing History

In the middle of the 1980s, a Japanese doctor called Charles Hull was considered as a pioneer in 3D printing technology [29]. He sophisticated, patented, and traded the first device for building 3D objects and the STL file that linked with present CAD software. This technique is called Stereolithography (SL); in which a laser moves across a liquid resin surface and cures surface until the desired layer obtained [34].

In the same year, the Massachusetts Institute of Technology (MIT) worked on developing another additive manufacturing technique called "inkjet printing". Later on, in 1992 Fused Deposition Modelling 3D printing was patented by Scott Crump, co-founder of Stratasys [34].

This technique fabricates objects through depositing layers of solidifying materials until the desired shape is obtained. However, as shown in Figure 9, trails didn`t stop until laminated objects manufacturing (LOM) technology developed in 1996 by cubic technologies; which form shapes by staking adjusted layers from predefined material sheets by welding or adhesion [34].

1984

First patent application for stereolithograhy

1986

First patent registration for sterrolithography

1988

| Selective laser sintering | Fused deposition modeling |

1992

First patent registration for Fused Deposition Modeling

1996

Free solid form fabrication of drug delivery devices

2015

First FDA approval 3D printed tablet -Spritam
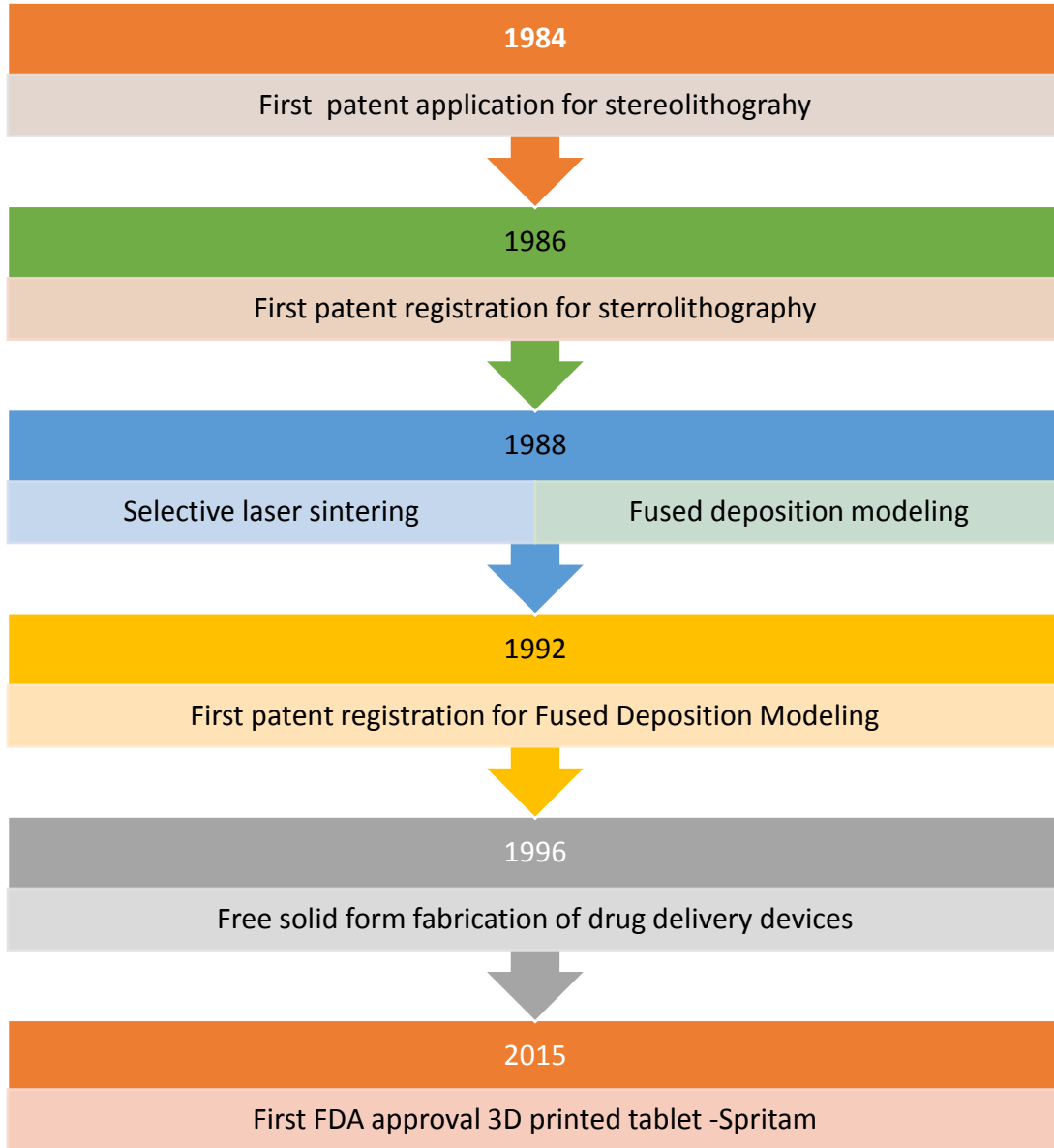
Figure 9:History of 3D printing technologies

1.3.3   3D printing technologies

There are many techniques used for 3D printing, they are classified as shown in Figure

10 according to (1) Powder solidification, (2) Liquid solidification and (3) Extrusion.
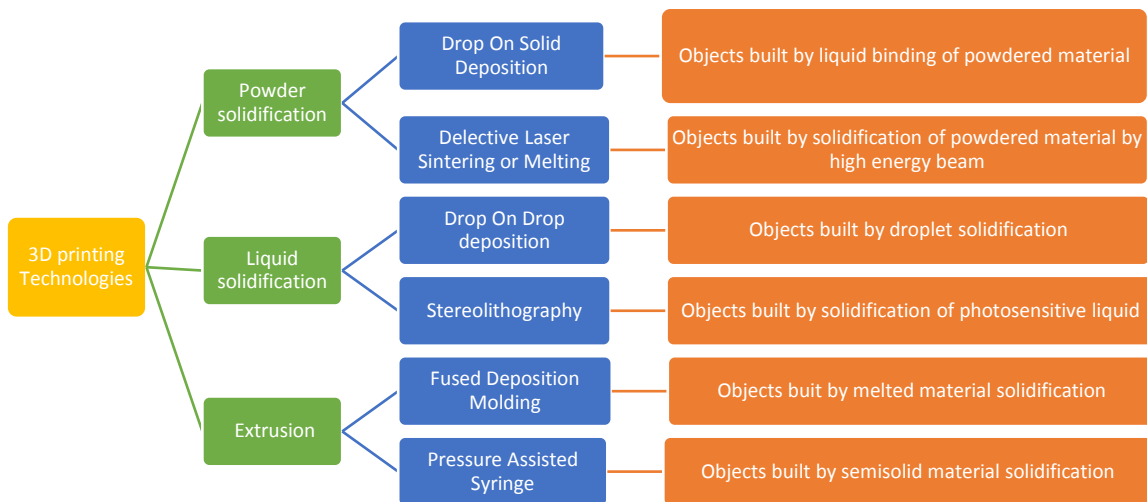
Figure 10: 3D printing technologies

In powder solidification there are two methods used; (a) Drop on Solid deposition:

where a powder bed is used and a continuous flow of liquid deposit on to bend it and

form the desired object. (b) Selective Laser Melting: where a powder bed is used as a

thin layer and the laser beam sinters the powders and binds them in layers [31], as

shown in Figure 11.
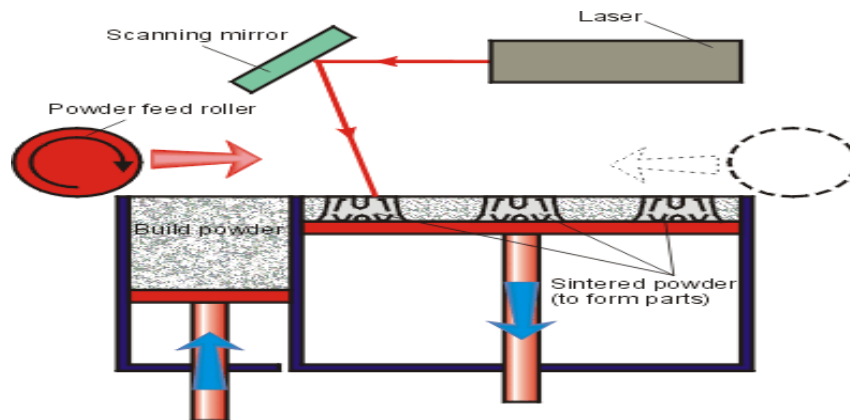
Figure 11:Selective Laser melting [31]

In Liquid solidification there are also two methods used; (a) Drop on Drop deposition: where drops shoot one by one from a nozzle to produce the desired shape, as shown in Figure 12. (b) Stereolithography: where photosensitive materials used and a UV beam scan them to cause gelation and then the desired shape, as shown in Figure 13 [31].
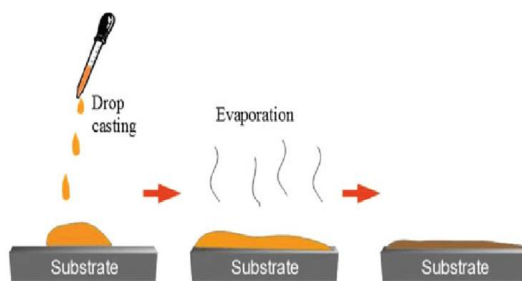
Figure 12: Drop on Drop deposition [31]
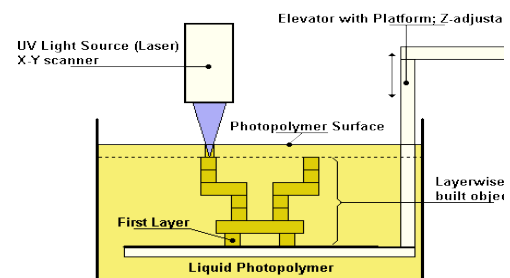
Figure 13: Stereolithography[31]

Upon the extrusion technology, there are also two methods used; (a)Pressure assisted syringe: where a viscous material can deposit by using an extruder that uses pressurized air piston, as shown in Fig 14. (b) Fused Deposition Modelling, that is used

in this research, where a thermoplastic filament extruded through a high-temperature nozzle, then objects formed layer by layer according to predesigned geometry, as shown in Figure 15. Furthermore, this technology discussed in detail in the next section [31].
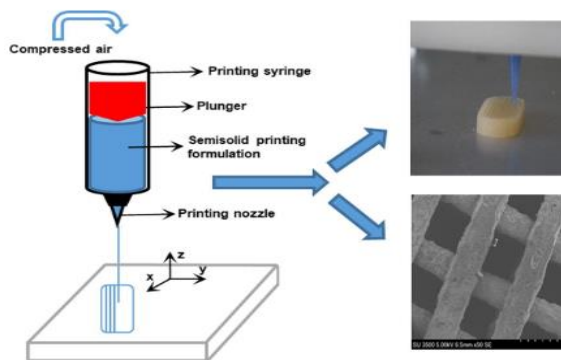
Figure 14: Pressure assisted syringe [31]   Figure 15: Fused Deposition Modeling [31]
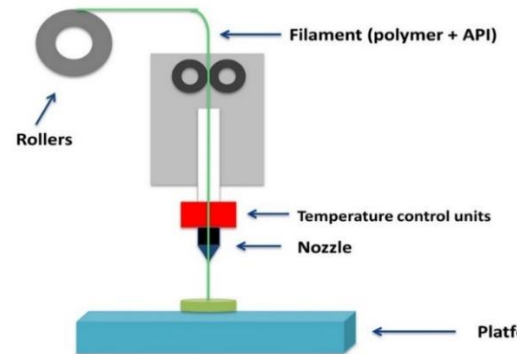
1.3.4   Fused Deposition modeling

FDM is one of the 3DP techniques, where thermoplastic filaments with appropriate thermal, mechanical, and rheological properties enter the preheated nozzle through counter-rotating wheels. Once the filament gets inside the liquefier it melts and with the help from the yet solid part, which acts as a piston, the molten gets out from the nozzle. The nozzle moves in the Z-direction from bottom to top and the molten deposits layer by layer on the printer bed according to a predesigned CAD file [31],[35],[36].

FDM is widely used and has many advantages over other 3DP techniques such as good mechanical strength, high resolution, low cost and it is solvent free [37]. Furthermore, it has some challenges like a limited range of APIs and thermoplastic polymers. This limitation in using the polymer is due to their mechanical properties (See section 1.6: Mechanical properties)[31].

FDM printer consists of the following parts;

(1) Feeder and it is used to pull the filament from the spool to the nozzle, it contains a motor(s) to move the counter-rotating wheels.

The rate of feeding can be changed as a variable parameter to be a unique value for each polymer. The filaments should have good mechanical properties to pass between the wheels since brittle ones broken between the wheels and flexible ones bend on the wheel, as shown in Figure 16 [35],[38].
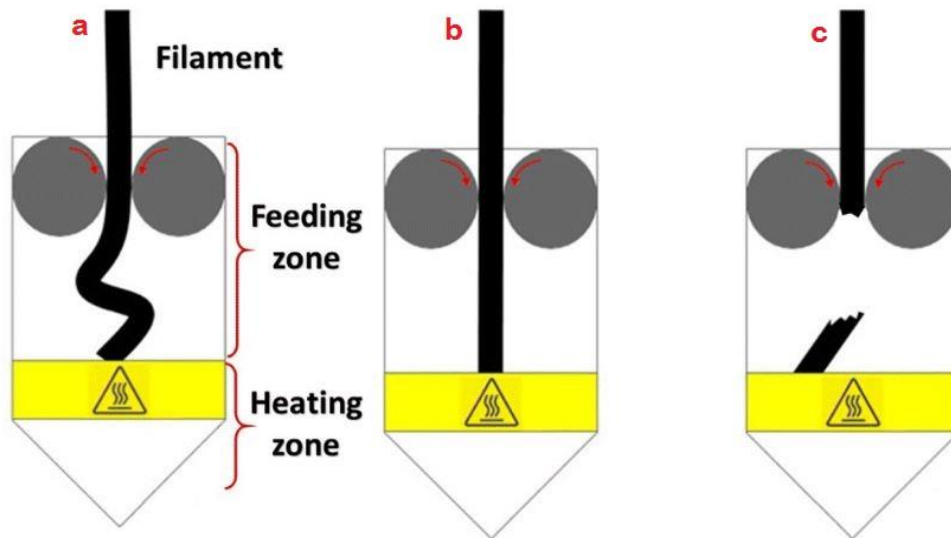
Figure 16: Filaments in FDM printing, (a) flexible filament that bend, (b) filament with good mechanical properties, and (c) brittle filament that broken between the wheels

(2) Liquefier, where filaments melt according to a predetermined temperature for each polymer.

(3) Nozzle with its tip, where the molten gets out from the printing head to the bed. This nozzle connected to a thermo-sensor to read the temperature and show it on the monitoring screen, as well as thermo-heater to heat the nozzle.

The printing temperature should be above the T_g of the amorphous or semi-crystalline polymers and above T_m of the crystalline ones to soften the filament [39]. The temperature must be precisely and sensitively controlled since overheating can lead to viscosity change of polymer which later affects the drug release and stability as well[39].

(4) Fan(s), to adjust the temperature and help in the solidification process, the speed of the fan also can be adjusted upon the polymer type and layer(s) height.

(5) Bed or platform, where the molten deposit and solidify. The bed contains thermo-sensor to read the bed temperature and thermo-heater to heat the bed and enhance the adhesion for some polymers.

In fact, 3D printer may contain one or more feeder(s), liquefier(s) and nozzle(s). As a result, two or more different polymers can be used at the same time, or the same polymer with different characterizations.

The processing parameters can affect the FDM final product. Those parameters can be the infill density, infill pattern, nozzle temperature, nozzle diameter, bed temperature, layer height, number of perimeters, number of solid layers, number of tops and bottom layers, infill/ perimeters overlap percentage and printing speed. Thus, they should be adjusted upon the type of the polymers and API(s) used.

The main goal in FDM technology in the pharmaceutical industry is to get the desired drug dissolution rate and release profile. So, a filament with good mechanical properties and rheological ones can be feedable and printable then associate in achieving that goal. The robust filament is the key factor to obtain a successful printing, it should hold the pressure that done from the wheels to be pushed into the

nozzle, also the molten should have optimal viscosity that can pass through the nozzle (see section 1.5: Adequate mechanical properties for FDM) [39],[40].

The diameter of the filament is also significant since the wrong size can cause plug or slow feeding rates. some hygroscopic polymers may rise a large diameter of the polymer that causes it to make it not pass through the nozzle and printer mechanism[39].

To be sure, various quality control (QC) tests applied to the filaments such as; tensile strength, thermal behavior, drug content, dimensions, and organoleptic characteristics. Moreover, drug release should be evaluated using dissolution or Franz diffusion cells [32],[37],[41].

Ordinarily, polymers used in FDM should be thermoplastic with appropriate thermal, rheological, and mechanical properties. Moreover, they should be non-volatile, non-aerosolized and thermally stable [42].

Polylactic acid or polylactide (PLA), polyvinyl alcohol (PVA) and acrylonitrile butadiene styrene (ABS) are examples of common polymers used in FDM researches and studies [43],[44],[29]. The first two polymers are common in pharmaceutical but the ABS is not used because it is not biodegradable[45].

However, different studies performed to investigate other polymers in FDM such as polycaprolactone (PCL), Eudragit EPO, Kollicoat IR, polycarbonate (PC), polyphenyl-sulfone (PPSF), high-density polyethylene (HDPE) and polyetherimide (PEI) [46].

For example, GGioumouxouzis et al used PLA and PVA with mannitol and hydrochlorothiazide to study the dissolution profile of the hollow cylinder dosage form[47]. PVA used as a model polymer in Skowyra, et al research to produce extended-release tablets of prednisolone [48]. Also in Zhao, et al study to print high stable and strength tables with convex drug release profile [49].

Moreover, PVA used in different studies for Goyanes, et al (a) To print controlled release tablet dosage form [50]. (b) To print 3D tablets with multi drugs and paracetamol/ caffeine used as a model drug [51]. (c) To evaluate the geometry and surface area to surface ratio effect on the release profile [52]. While ABS used in Hwang, et al studies where ABS mixed with iron and copper particles to check the effect of metals on thermo-mechanical properties [40],[35]

This technology helps in formulating and manufacturing various innovative dosage forms and products with different releases profiles. It can be used to produce immediate-release tablets by using hydrophilic polymers or implement the Solid Dispersion method and sustained release by using hydrophobic polymers. In addition,

combining different APIs with dual drug release, that can raise patient's compliance with complex dosing regimens [34].

Like other conventional technologies, FDM products must offer physical and chemical stability at manufacturing, packaging, and storage for months and ideally years. Printing at the same point of care for solid dosage form is a great Capacity that allows flexibility and uniform individualized dose strength. As a result, this increases the therapeutic effect on patients [34].

1.3.5   3D printing in Pharmaceutics

Spritam is the brand name of Levetiracetam, which is used to treat epilepsy [53]. It was the first drug manufactured through 3D powder-liquid printing technology by Aprecia pharmaceutical company and approved by the Food and Drug Administration (FDA) in 2015, as shown in Figures 17&18. It shows an instantaneous disintegration of the Active Pharmaceutical Ingredient (API)[54],[43], [29].

It was manufactured by using Aprecia`s ZipDose® technology based on the drop on solid technique, and it was available in the market in 2016. The pharmacological efficiency measured and it was equal to levetiracetam manufactured by traditional process, but with a fast release profile, since this technology can improve the solubilization time which reduced because of the porous and soluble matrix composition [45].

Upon manufacturing, to produce the matrix tablet; the antiepileptic API (100mg) and the necessary excipients form the first layer, then the liquid binder deposited to obtain perfect aggregation and integration between all the desired layers. In the end, the final orodispersible tablet obtained and dissolved in a few seconds with a minimum amount of water [45], [55].

This innovation is done, to keep up with the demand for novel drug delivery systems and the advancement of 3D printing as well as in demand for rapid action and patient

compliance among pediatric and geriatric. However, this drug is expensive now because the manufacturing company patented it. Due to this reason, the cost is higher than levetiracetam which prepared by the conventional manufacturing process. As a result, the cost highly depends on the patent expiration date [29].

This step encourages researchers to go forward and manufacture 3D printing customized and complex dosage forms [34]. As well as making the concept of manufacturing personalized medicine in pharmacies and hospitals very futuristic [29].

Figure 17: Spritam 3DP tablets

Figure 18: Spritam, first FDA 3DP drug

1.3.6 Drugs manufactured by FDM technology

After the release of Spritam in the market, research in developing different dosage forms by using a 3D printer increased. Scientists tried many experiments by using different 3D printing techniques, APIs, and Polymers to obtain different formulas and geometries to check their characteristics and properties as in vivo or invitro.

The below table (Table 2), presents earlier studies in tablets manufacturing by using Fused deposition modeling techniques so many results achieved from single tablets, bilayer tablets (by changing the API, or different release profiles) as well as capsules shells.

Table 2: Drugs manufactured by FDM technology

#	Dosage form	API	Brief	Reference(s)
1.	Tablet, IR/ER bilayer	Guaifenesin	IR and ER bilayer tablets obtained with lower hardness, friability, and faster release profiles compared with commercial tablets.	[28] [56]
2.	Tablet, SR	Captropril (CAP), Nifedipine (NIF), Glipizide (GLI)	The individual formulation prepared and zero-order release obtained from Captopril while	[57] [56]

			Nifedipine and Glipizide showed the first-order release.	
3.	Tablet, IR/SR	Pravastatin, Atenolol, Ramipril, Aspirin, Hydrochlorothi-azide	IR release profiles obtained for aspirin and hydrochlorothiazide, while the remainder showed SR release.	[58] [56]
4.	Tablet	Fluorescein	0.29% was the drug load in PVA filament, the release inversely proportion with the infill percentage.	[50] [56]
5.	Tablet, MR	5-ASA, 4-ASA	0.06% of the drug load obtained, and 50% of the drug degraded during manufacturing.	[1], [29], [31], [32], [34], [41], [51], [52], [56]–[61]
6.	Tablet, ER	Prednisolone (2 – 10mg)	Amorphous API used; 1.9% drug loaded in PVA filament 88.7-107% theoretical dose strength achieved.	[1], [29]–[32], [34], [35], [37], [41], [43],

				[46], [49], [51], [52], [56]–[62]
7.	Tablet	Acetaminophen	Effect of surface area, surface area to volume ratio, and tablet weight on the dissolution of varying geometries. Higher surface area to volume ratios exhibited faster release rates. Constant weights showed less variability in release indicating erosion-mediate release from the PVA matrix.	[56] [52]
8.	Tablet, IR and MR	Acetaminophen Caffeine	Bilayer tablet produced (as the size of capsule 4) with PVA filament and 100% infill and it produces ease swallowing characteristics.	[56] [51]

1.3.7   3D printing Regulations

Efficacy, safety, and quality of the drug are the main important goals in pharmaceutical Industries. Unfortunately, until now there are no clear regulations regarding 3D printing drugs.

That is due to variability in 3DP technologies, it is impossible to give one rule for all printing techniques and methods, so every single method needs a unique regulatory. As a result, there is no valid regulation upon drug design, manufacturing process, and quality control tests. Moreover, there are still many questions that must be answered, regulatory and legal issues that must be addressed regarding that new manufacturing process [32],[56].

In order, there is a strong need for those regulations, the scientific community needs to work more on the regulatory issues to ensure the efficiency of the drugs and safety of the patients. Upon that the FDA is working on understating this technology through its research centers in science and engineering and solid mechanics laboratories [31],[53],[60].

In controversy, regardless of the fast growth in the 3D printing field, FDA approved guidance for 3D printing medical devices in abbreviated pathways. It includes pathways in emergency use and pathways in compassionate exemption use. Those pathways especially the emergency one save a newborn baby life who was suffering

from tracheobronchomalacia by approving the anatomically specific tracheal splint device [56].

Despite all the regulatory obstacles that are related to 3DP medicine, the FDA released Spritam® (levetiracetam) the first 3DP drug in August 2015, while there are still many drugs under research [53],[56].

1.4 Individualized medicine

Pharmacogenetics, metabolomics and pharmacogenomics developments increase the needs of individualized medicine [29],[63]. Individualized medicine is moving from "one fits all" idea, to specialized the health care to individuals by connecting diagnostics and treatments with genetics and emerging technologies like proteomics and metabolomics analysis, as well as the phenotypic response and pathophysiology to obtain the best therapeutic results and diseases management [24], [29], [60], [62].

Individualized medicine is important because several drugs have been assured to have higher efficiencies in certain genetics differences, while they are harmful to others, For example, millions of side effects leading to 10,000 deaths in the USA [60]. Moreover, not all patients respond similarly to the same drugs, as shown in Table 3. Thus, this variation can shift the traditional manufacturing method backward and use individualized medicine instead [45].

Table 3: patients responses rates

Disease Category	% therapy response
Analgesics for pain (Cox-2 inhibitors)	80%
Asthma	60%
Cardiac Arrhythmias	60%
Schizophrenia	60%
Migraine (acute)	52%
Migraine (prophylaxis)	50%
Rheumatoid Arthritis	50%
Osteoporosis	48%
HCV	47%
Alzheimer's diseases	30%
Oncology	25%

Where individualized medicine supports the formulation of therapeutic efficacy and safety, for example, the drug dose can be modified according to the patient`s weight, sex, height, age, genomic profile, and lifestyle, as shown in Figure 19 [37], [53].
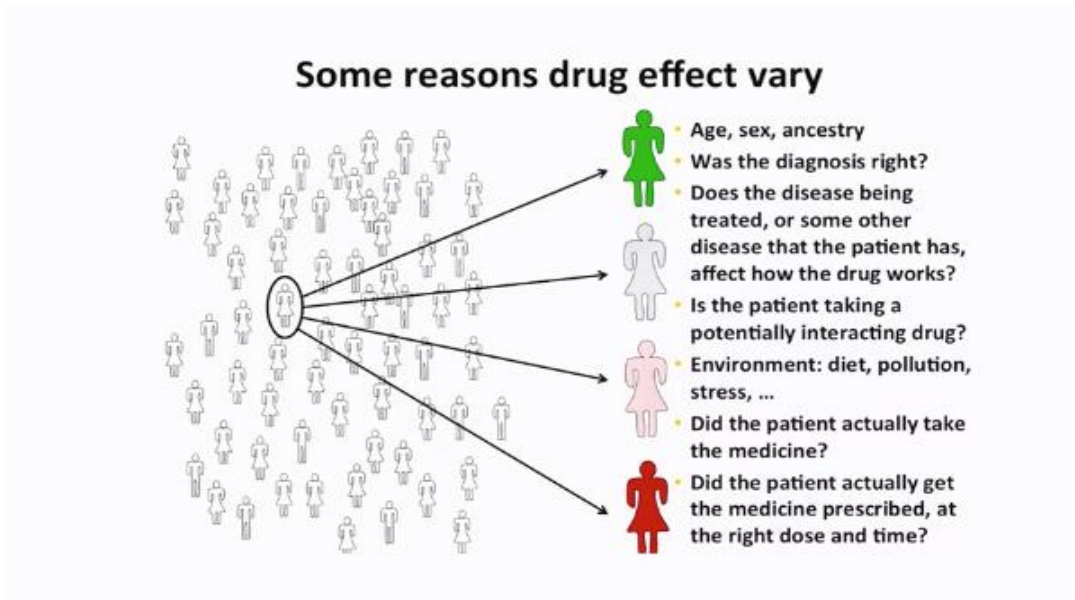
Figure 19: Reasons for drug effect varies

3D printing technology opens a new era and brings us to step forward in this field; since it allows the production of customized medicine that tailored the patients' needs. It allows forming precious doses in different shapes, sizes as well as textures which is a bit difficult to do in the conventional methods in less cost, excipients and operation space while taking into consideration accessibility of biocompatible, biodegradable, physical and chemical substances [29].

This technology helps the formulation of different dose strengths upon the patient needs, also it can produce drugs at the point of care and get accurate and personalized treatment regime such as multiple active ingredients in a single tablet or multi-layered one additionally complex drug release profiles tablets [28], [34], [37].

3D printing can be useful in manufacturing orphan drugs, essentially in pediatric patients which not only the dose is significant but also the shape, color and taste of

the drug play an important role in the care process [49], [53], [64]. These features affect acceptability from the patient especially in terms of swallowing difficulties. Knowing that until now there is no valid regulation referencing manufacturing process, designing and quality testing [53].

The 4th industrial revolution leads the pharmaceutical industry to produce safety and efficacy drug-loaded filaments in a large scale, and transform the filaments in individualized medicine upon the prescription by the digital pharmacies since the dose can be controlled by modifying the printing settings, as shown in Figure 20 [32], [53].
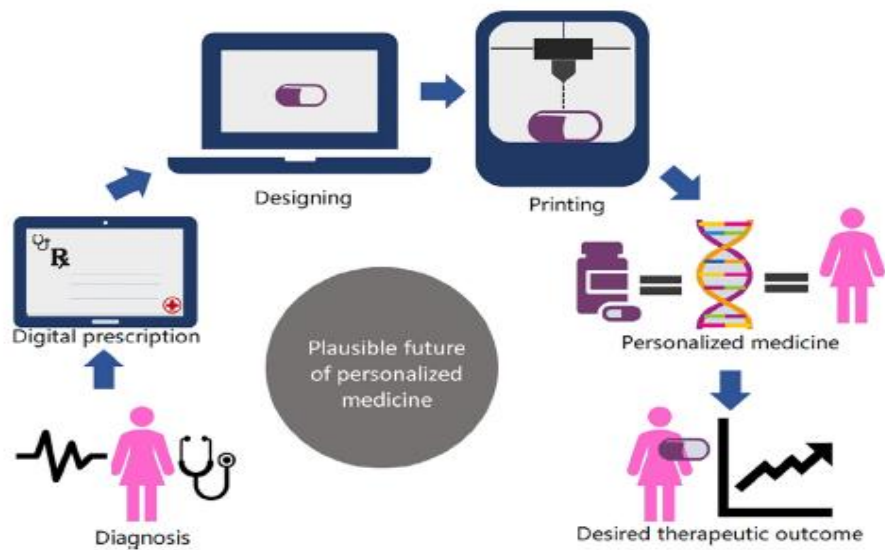
Figure 20: The future of personalized medicine [53]

1.4.1 Individualized medicine and 3D printing

Since Filaments can be manufactured as an intermediate product by hot-melt extrusion at the pharmaceutical companies and 3D printer can be easy to operate and portable, personalized medicine can be simply produced at local hospitals and pharmacies. 3D printers can be easily installed in hospitals and pharmacies since they just need network and power sources to operate [32].

Mainly the printers could be connected by one or more computers that have interfaces in the central control room. The doctor sends the prescription to the pharmacy administration authorized person then it will be sent to the pharmacist to review after that it's sent to the printer to print the desired dose for the patient, as shown in Figure 21 [32].
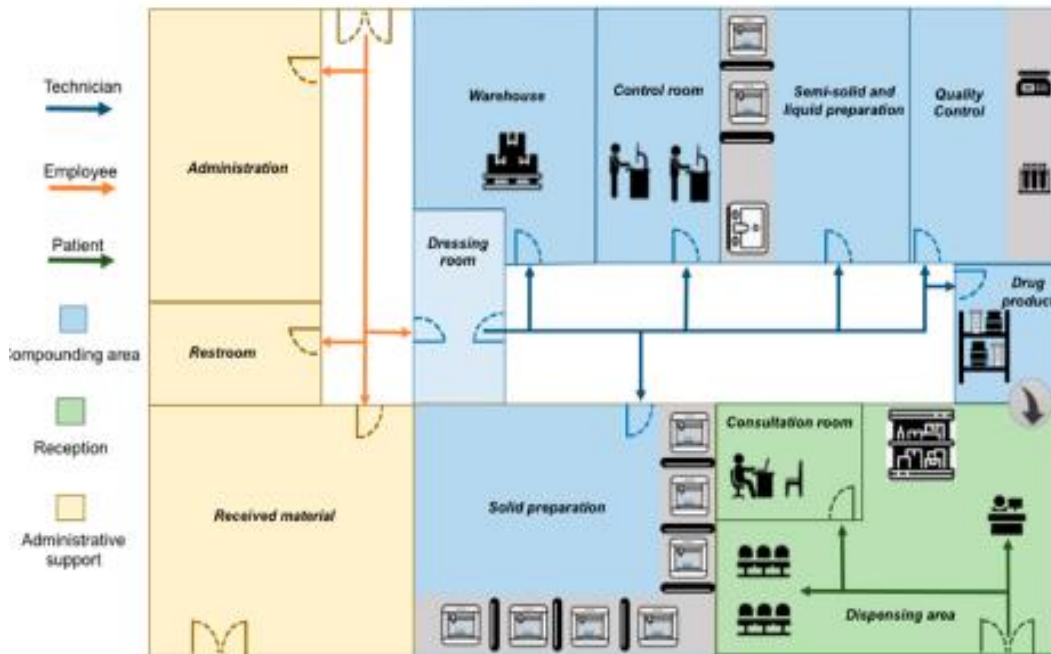
Figure 21: Digital Pharmacy Layout [32]

The success of this idea depends on the technicians, who should be educated, trained, and qualified with access to the materials area and can deal and set the parameters of the printer for each dose such as the infill, speed, temperature, tablet geometry. Also, the intermediate filaments should be safe and validated to the process specifications also stored in a suitable place. And the printing preparation and spool attachment should be adjusted to ensure the right dose. Moreover, the drug should be packaged and labeled before transferred to the patient. Finally, the printer must be cleaned and validated after each use [32].

1.5 Adequate properties for fused deposition modeling

FDM is one of the 3DP techniques, where the filament is supplied into the feeder, then passed to the heating nozzle through the counter-rotating pulling wheels, as shown in Figure 22. There, the filament liquefies and gets out from the heated nozzle to the bed/platform and solidifies. While the nozzle moves in the z-axis to build the layers one by one upon the CAD file [36] [35].
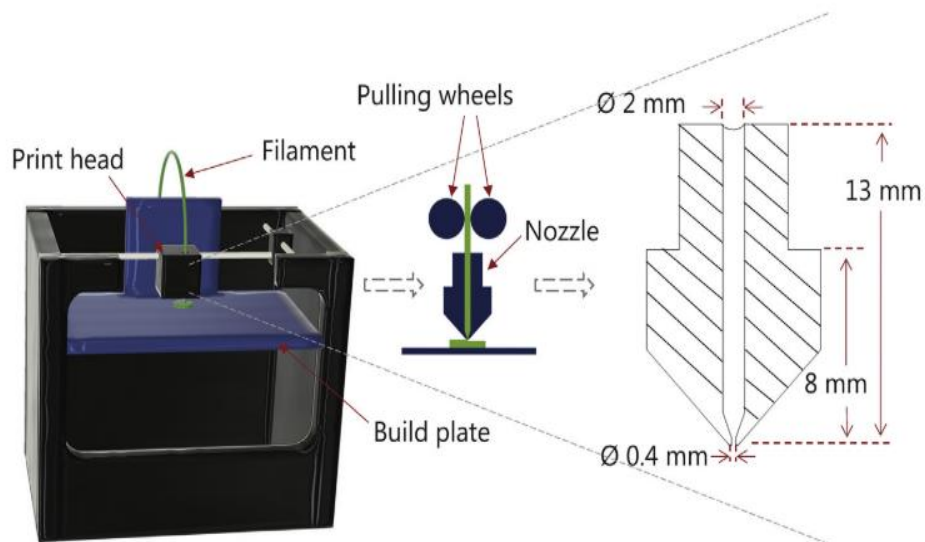
Figure 22: FDM Technology [35][36][36][36]

In FDM printing, different facts of matters must be taken into consideration; such as the filament diameter (1.75 mm), suitable thermal attributes, good mechanical, and rheological properties to be feedable and printable, as shown in Figure 23. Moreover, for the final product characterization, the drug distribution, porosity, weight,

dissolution, and mechanical properties as well. Since, those properties help to get accurate the dose, weight, shape, and surface area [35][48].
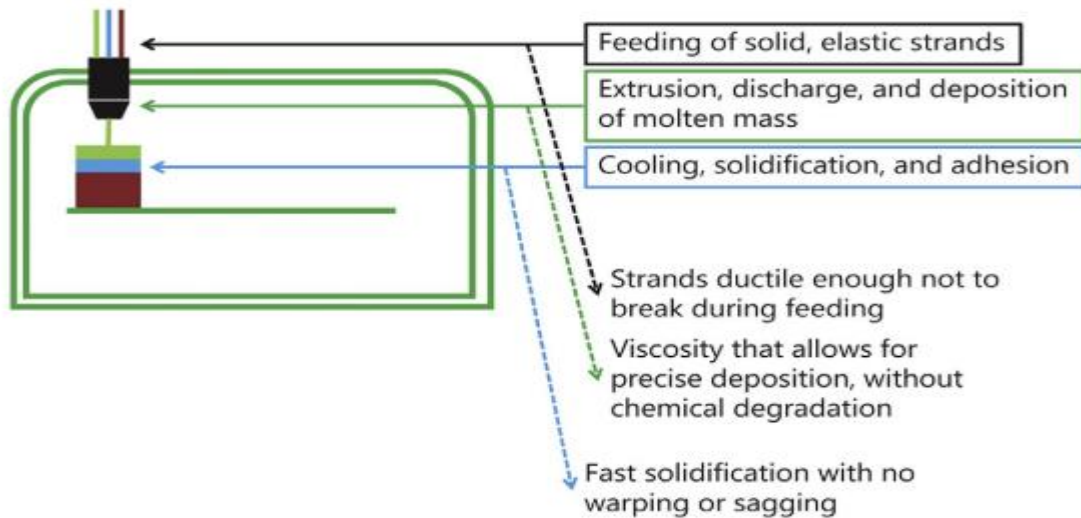
Figure 23: Key parameters to consider during FDM [35]

Regards the materials and formulation; understanding the raw materials' thermal, rheological, and mechanical properties is also important to connect these properties with the printing process parameters. For example, the nozzle temperature, bed temperature and the shear rate in the printer nozzle. Also, to understand the underlying issues of poor printability and to design enable straight forward dosage forms [35],[65].

Recently, Fuenmayor et al. have published a study focusing on the relationship of feedstock filament properties and the FDM printing outcome, as well as polymers with different pharmaceutical grades blends to obtain optimized printing results [35].

Setting up the right properties to match the process requirements and final product properties is a bit complicated. Since specific polymers used in pharmaceutical dosage forms especially in FDM regard the thermal, mechanical, and rheological properties. Sometimes mixing polymers may offer good solutions as well [66],[67].

The drug can coexist in the polymer as amorphous and crystalline. Some APIs can act as plasticizers which reduce the brittleness (e.g. enhance the ductility, the deformation beyond the elastic region), and decreasing the viscosity and glass transition temperature (T_g) of the polymers, therefore enhancing the mechanical properties of the filaments [35],[67].

Also, the amount of the drug plays an important role in FDM, since with high content of the crystalline drug, the filament may become too fragile to withstand the tension, bending, and compression in the feeding system. Moreover, large particles can block the printer nozzle and affect the filament flow [35].

Upon the filament preparation, as a rule, the first criteria in choosing the FDM polymers is to be thermoplastic. This means that the polymer can reversibly solidify and liquefy upon cooling and heating. Those polymers may be amorphous or crystalline in the first case the processing temperature must be above T_g, in the second one it should be above T_m. Moreover, the distribution of drug content

uniformity, constant thickness, and adequate mechanical properties can be prerequisites for effective printing [35].

Related to the feeding issues, this process depends on the unmolten filament that acts as a piston to push the liquified molt through the nozzle. Therefore, the dimension of the filaments is remarkable, also the stiffness to avert buckling. The filament must be sufficiently ductile to allocate some bending in the system and hard enough to pass through the wheels [35].

Despite the fact, some polymers can be extrudable, but the filament brittleness can be one of the FDM challenges. Since those filaments can`t be enough ductile to pass the withstand bending force in the printing process and they broke between the pulling wheels. As a result, some plasticizers, or copolymers used to enhance the mechanical properties and make the filaments feedable and printable. To predict the mechanical properties of the polymers before printing the Texture analyzer used [35].

Deposition and solidification can be the last step in 3D printing. While the z-axis moves the object formed layer by layer on the bed. There should be enough distance between the nozzle and the object. During the liquefaction, the suitable viscosity of the materials, continuous depositing without variation in thickness, avoid materials agglomeration and air bubbles should be achieved to ensure the steady flow. In some cases, diameter variation and die swelling (expansion of the filament after getting out

from the die) can lead to fluctuations in the layer thickness thus leading to surface area and dose variation in the final dosage form [35].

Upon solidification, it should be fast to avoid the elephant leg compensation and structure collapsing during the printing process. Cooling can happen in two different ways. The first one is from conducting the bed with the deposited layers and the second one is between the air and deposited layers. Where the heat conduction regulates by the melt density, bonding between layers, thermal conductivity and specific heat Capacity [35],[68], [69].

The process parameters such as printing speed, bed, and process temperature relay on the rheological and thermal properties of filaments. Because of the higher temperature limited by the APIs, polymers, and excipients degradation temperature. So, the idea is to balance between having suitable flow and good adhesion between the layers to avoid superfluous heating [35].

To highlight the rheological properties, the shear viscosity is important in FDM. It depends on internal factors like molecular weight, molecular weight distribution, the structure of the molecule and the drug solid form (solid dispersion, molecularly dispersed, or both) and external ones such as shear rate and temperature. The shear rate depends on the printing speed and liquefier dimensions. Moreover, the melt flow

rate (melt index) can be used as an inspection tool to assess the melt viscosity of the feedstock materials[35].

Not suitable rheological properties can lead to fail the printing process and avoid the filament to pass to the liquefier by making it flat. Flat filaments cannot pass the wheel because they have a smaller thickness in one dimension and they may be wide so not suitable to fit into the liquefier. To overcome those issues there is a need to raise the processing temperature [35].

Regards the thermal properties, they affect the process parameters such as the process and bed temperatures that are needed for layers adhesion. Mainly, those parameters adjusted based on the T_g of the polymer(s) used as well as the T_g of the physical mixture. Since some drugs have plasticizing effects that can lead to lower T_g of the physical mixture. Upon that, DSC used to measure the T_g and evaluate the temperature of printing [35].

1.6 Mechanical properties

Convenient mechanical properties are important in the feeding process, their characterization helps in evaluating the feasibility of the filaments to be printed. The tensile test used to indicate the mechanical attributes of the filaments as if they are ductile or brittle. In this test, filaments stretched at constant speed whilst the deformation and required force for the deformation are observed over time performing the stress-strain curve [70].

Stress term expresses the internal force of the neighboring particles exerted on each other on an area, as shown in equation 1 [70].

$$\delta = \frac{F}{A}$$

Equation 1: Stress equation

Where, σ = Stress (N/mm^2), F= Force (N), A = cross-sectional area (mm^2).

Strain term expresses the fractional change in length and it is not a physical quantity. In other words, a strain is a difference between the final length and initial one divided on the initial length, as shown in equation 2 [70].

$$\varepsilon = \frac{\Delta L}{L_o}$$

Equation 2: Strain Equation

Where, ε =strain (%), ΔL = final length(L) − initial length(L_o) (mm), L_o= initial length(mm)

From the stress-strain curve, different variables can be obtained. Figure 24, can be used as a model to simplify the idea. The first section of the curve is the elasticity which means that after the unloading the deformation disappeared. In other words, the atoms stretched and returned to their original length after the force removed. The slope of this part equals the elastic modulus or young's modulus and quantifies the material stiffness. Larger slope indicates to larger stiffness [70],[35].

Then, the second section is the plastic deformation where the deformation is preserved after the unloading. Thus, comprise irreversible atomic-level breaking of bonds. Ductility can be identified as the Capacity of the material to deform plastically before it is broken. When the ductility is low the filament called brittle. Which means that it fractures immediately after it reaches the elastic limit [70].
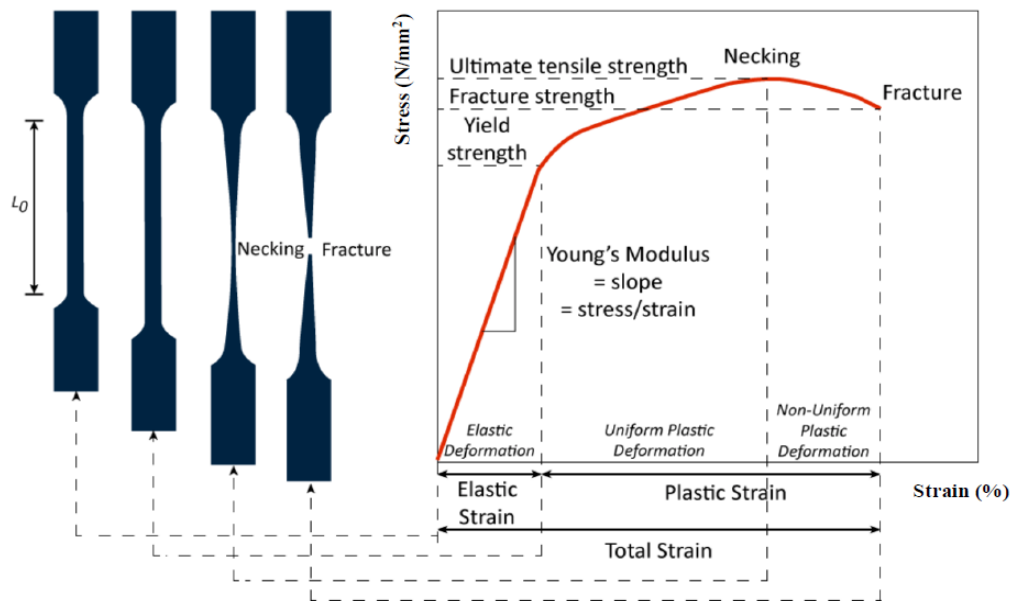
Figure 24: Stress-Strain curve f a typical metal with an elastic and plastic sections, presenting young`s modulus (N/mm², yield strength (N/mm²), ultimate tensile strength(N/mm²), fracture strength(N/mm²) and necking. [70]

For some materials, there may be a deviation from the above curve. The stress-strain curve of those kinds of materials shown in Figure 25 present obvious yield points with upper and lower yield strength. Those materials are completely elastic before the stress reaches the upper yield strength then suddenly plastic deformation happens [70].
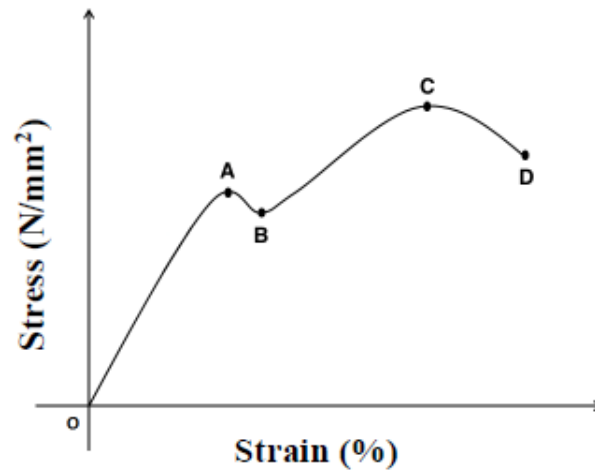
Figure 25: stress-strain curve present and upper (A) and lower (B) yield strength (N/mm²), the ultimate tensile strength(N/mm²) (C) and fracture strength (N/mm²) (D) [70]

While the elongation resume, the stress reaches its maximum value (the ultimate tensile strength) then the sample begins to neck. Necking indicates reducing the cross-section in some weak parts in the filament [35].

The tensile test finished when the filament was broken. The energy needed to break the filament called toughness and it equals the area under the curve in the stress-strain curve up to fracture strength, as shown in equation 3[70].

$$Ut = \int_0^{\varepsilon f} \sigma d\varepsilon$$

Equation 3: Toughness Equation

Where, Ut = toughness (10^6 J/m³), εf = strain at fracture strength (%), σ = stress (N/mm²) ε = strain (%).

Polymers can act in various ways, so they can present different patterns in stress-strain curves, as shown in Figure26. Some polymers present a clear yield point (curves 2&3). Whereas others the stress monotonically increases until a fracture happens without presenting an obvious yield point (curve 4). Upon brittle filaments, they are elastic until fracture with no plastic deformation (curve1) [70].
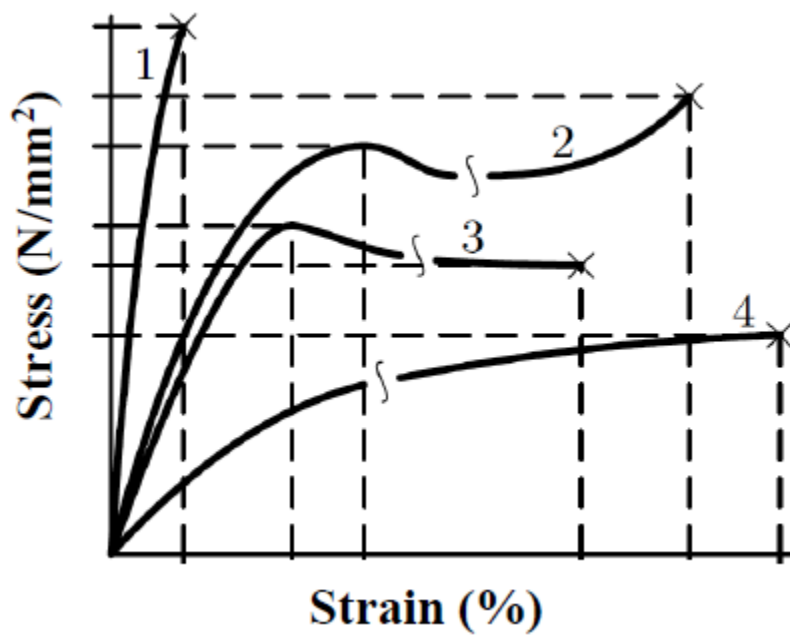
Figure 26: Different stress-strain curves of polymers, curve 1 present the brittle filaments, while curves 2,3 &4 present the filaments with elastic and plastic behavior elongation [70]

1.7 Differential scanning calorimetry

Differential scanning calorimetry (DSC) is a thermal analysis technique used to measure the difference in the heat flow rate between a reference and a sample in a function of temperature and time, as shown in Figure 27. The heat that is absorbed from the sample results in endothermic reaction (e.g. glass transition, melting, evaporation) whereas the heat that released from the sample results in exothermic reaction (e.g. crystallization). Through using the DSC, the glass transition, melting point and melt enthalpy can be detected [71].
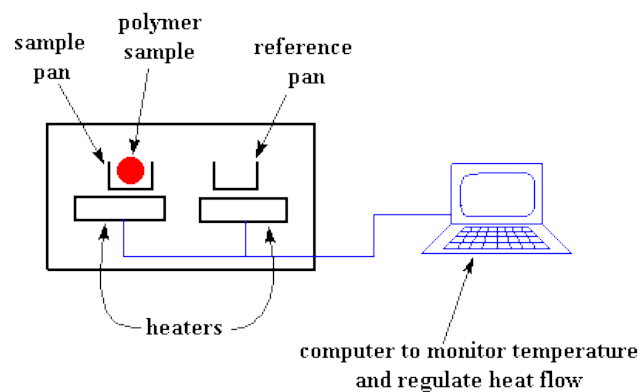
Figure 27: Differential scanning calorimetry principle

DSC is used to evaluate the crystallinity content in solid dosage forms. Since the drug can be amorphous or crystalline and these phases affect the drug properties. In the amorphous phase, the molecules are not arranged in a specific way. Thus, those types of drugs have a fast dissolution rate but they have problems in drug stability. because they may recrystallize. On the other side the crystalline drugs the molecules arranged

and their dissolution rate is slow compared with amorphous ones since they require more energy to break up the crystalline lattice but they are more stable in storage [72], [73].

The crystallinity percentage can be calculated as follows using the melting enthalpy:

$$Xc = \frac{\Delta H1}{f \Delta H2} * 100$$

Equation 4: crystallinity percentage equation

Where; Xc = Crystallinity (%), $\Delta H1$= melt enthalpy of PM, filament, tablet (J/g), $\Delta H2$= melt enthalpy of pure API (J/g), f = fraction of the drug in the formulation

To determine the melting enthalpy, the T_{max} of the DSC cycle must be higher than the T_m of the drug. However, it should not be above the T_d of the drug since that damages the equipment.

1.8 Polymers used in this research

1.8.1 Capa® 6506

Polycaprolactone (PCL) is a linear semi-crystalline polyester, as shown in Figure 28. It is flexible, non-toxic, and hydrophobic. The crystallinity of PCL increased by increasing the molecular weight. Since PCL molecular weight vary between 3000 to 80000g/mol [74].
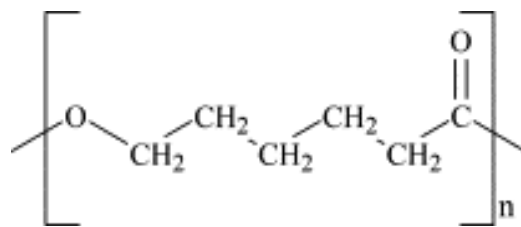
Figure 28: Polycaprolactone structure [74], [75]

PCL has a glass transition (T_g) of -60°C and a low melting point in a range of 55-60°C. As well as, low tensile strength (nearly 23MPa). On the other side, it has an extremely high elongation at breakage (>700%). These properties allow it to be used in tissue engineering, drug delivery system and wounds dressing [74], [75].

Recently, PCL had used in different FDM studies. For instance, in A. Goyanes et al. research to figure out the possibility of printing personalized antiacne patches [44]. And in J. Aho et al. to explain the effect of rheological, thermal and mechanical properties of the physical mixture characteristics on the printing properties while indomethacin used as a model drug [35]. Also, in Lin et al. to manufacture subdermal

implants using Ethinylestradiol as a model drug [1]. Also, in Berck, R.C.R. et al. study of polymeric nano capsules manufactured from PCL and Eudragit RL100 [45]. In this study PCL was used for sustained release layer.

1.8.2 Ateva® 1850A

Ethylene-vinyl acetate (EVA) is a copolymer of ethylene and vinyl acetate, as shown in Figure 29. EVA is a hydrophobic, biocompatible, non-toxic and FDA approved thermoplastic copolymer. The VA percentage can be between 0 to 40% and upon this percentage, the copolymer characteristics vary. Increasing the VA content resulting in higher adhesion, polarity, flexibility, impact resistance, compatibility, and polarity. On the other hand, increasing the VA content leads to decrease stiffness, crystallinity, melting point and softening of the copolymer [76],[77].
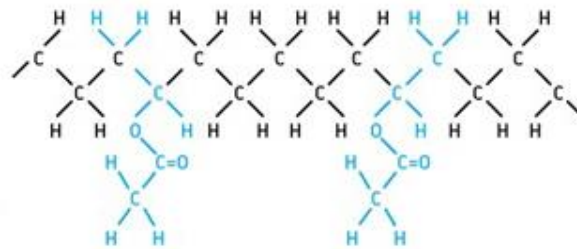
Figure 29: EVA Chemical structure[76]

EVA shows complex crystalline and amorphous phase regimes, with not less than two transitional temperatures in its amorphous phase. EVA T_g can be from -35 to -25°C and its independent of VA percentage. Also, other groups identify another T_g at

-110°C. Consistently, EVA has high material diffusion and flexibility even at low temperatures [78],[79]–[82].

EVA used in FDM studies especially in medical devices. Genina et al. used it as a drug carrier to produce subcutaneous rods and T-shape intrauterine system whereas indomethacin was the model drug [6], [30], [77].

1.8.3 Eudragit ® E PO

Eudragit is a Basic Butylated Methacrylate Copolymer, as shown in Figure 30. It has different grades Eudragit E100, Eudragit 12.5 and Eudragit EPO. Eudragit EPO is a solid substance obtained from Eudragit E100. It has an average molecular weight of 47000g/mol [83].

Eudragit is a semi-crystalline hydrophilic copolymer. It is used in immediate-release formulation due to the presence of a dimethyl aminoethyl group which ionizes and lets the polymer dissolve in acidic PH. Besides, it can form Hydrogen bonds so it can be used in solid dispersion formulations. It has a T_g at 52°C and T_m in a range from 130 to 135°C and T_d at 250°C [84].
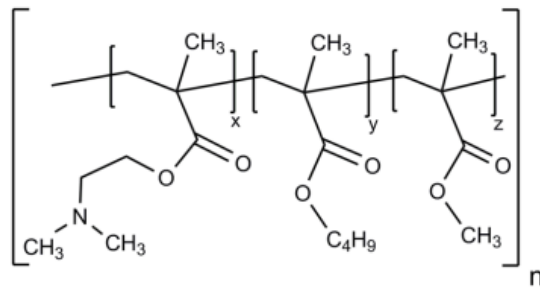
Figure 30: Eudragit EPO structure [83]

Eudragit E used in FDM studies. For example, M. Sadia et al. used it as a drug carrier to make channeled tablets with accelerated release profiles by using hydrochlorothiazide (BCS class IV) as a model drug [29],[85]. Also, in another M. Sadia et al. study to study the suitable pharmaceutical excipients in immediate-release tablets. Thus, Eudragit EPO used as a drug carrier and four drugs used as model ones. The drugs are theophylline, captopril, prednisolone, and 5-ASA [86].

1.8.4   kollidon ® 12 PF

Kollidon is a commercial name of Polyvinylpyrrolidone (PVP) which has different soluble and insoluble grades, shown in Figure 31. Kollidon can be used in immediate release and sustained release formulation upon its grades [87]. In this work PVP K12 used.
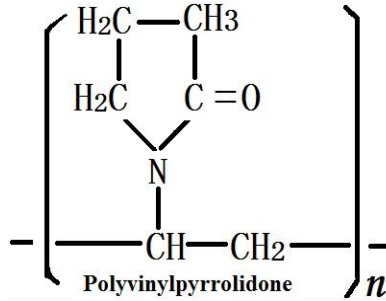
Figure 31: PVP structure

Kollidon filaments are brittle, thus it can`t be used alone to produce 3D tablets. But they are printable once they mixed with other polymers or palletizers. Kollidon used in FDM studies.

PVP K12 used with different polymers by many researchers. For example, Kempin et al. Study used five different polymers (Polaxamer 407, PEG20000, PEG 6000, PVP K12, kollidon VA64) to produce immediate-release tablets with fast release while pantoprazole was the model drug [6],[88].

1.8.5   Klucel^{TM} ELF Pharm and Klucel^{TM} EF Pharm

Hydroxypropyl cellulose (HPC), are nonionic water-soluble polymers used in an immediate-release formulation, as shown in Figure 32. The mechanism of drug release from HPC polymers can be by erosion or swelling [89]. They are used to enhance the solubility of poorly soluble drugs (class II). However, the solubilization rate depends on the molecular weight. Klucel EF and ELF molecular weights are 80,000 and 40,000 Dalton respectively [90].

Klucel filaments are flexible even without plasticizer. Their Klucel EF has a T_g at 0°C while Klucel ELF has two T_g at 0°C and 120°C because it has a beta transition[91][92].
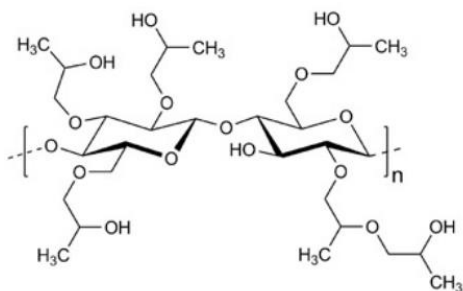
Figure 32: Klucel HPC chemical structure

Klucel EF, used in Zhang et al. research to study the possibility of coupling HME with FDM to manufacture controlled-release tablets while Paracetamol (BCS I) used as a model drug [11]. On the other side and until now, there are no publications regards Klucel ELF with FDM technology.

1.8.6   Kollicoat® IR

Kollicoat IR is an engrafted copolymer of polyvinyl alcohol and polyethylene glycol (PVA: PEG, 3:1), as shown in Figure 33. This molecule is hydrophilic and used in immediate-release tablets. It is a highly flexible polymer due to the linkage between PVA and PEG and can act as a plasticizer as well, thus it can get through the mechanical stress throughout manufacturing and storage steps. It has a molecular weight of 45000 mol/g and low viscosity compared with HMPC [93].
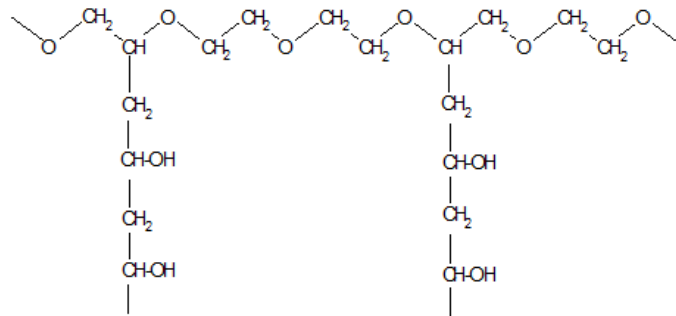
Figure 33: Kollicoat IR structure

Kollicoat IR is a water-soluble polymer and non- ionic which means that its solubility is stable in the GI. Its viscosity increases by increasing the polymer concentration. On the other hand, its viscosity is lower than cellulose derivatives molecules [94]. It has a T_g at 45°C, while its T_m = 208°C and T= 200°C [95].

It is a "Peroxide free" thus it is used as a binder for APIs that are sensitive to oxidation degradation[93]. Kollicoat IR used in N.G. Solanki et al. to distinguish the best amorphous polymers in FDM and kollicoat IR released in less than 60 min in PH whereas haloperidol used as a drug-polymer [6], [61]. Also, it was used in A. Melocchi et al study to produce suitable filaments for FDM printing and it was successfully produced [96].

1.8.7 POLYOX^{TM}

Polyethylene oxide (PEO) is a crystalline hydrophilic polymer, as shown in Figure 34. It has a melting point in the range of −23 to 63°C depending on its molecular weight [97]. Generally, it is used in the immediate-release formulation. PEO (MWT 100K) named N10 used in this study.
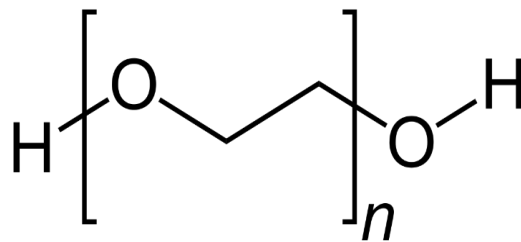
Figure 34: Polyethylene oxide chemical structure [97]

PEO used in Melocchi et al works to produce appropriate filaments for FDM from different polymers with different pharmaceutical grades and physio-chemical properties [96]. Moreover, it was used in Nasereddin et al, a screening study to predetermine the filaments feedability for FDM printing while using paracetamol as a model drug and it was feedable and printable [38].

1.9 API used in this research

In this research, Metoprolol Tartrate (MPT) used as a model drug to formulate bilayer tablets in that the immediate release used as an initial dose and sustained as a maintenance one [98]. By using Eudragit EPO and PEO as hydrophilic polymers and polycaprolactone (CAPA® 6506) as a hydrophobic one.

Metoprolol is a beta-blocker that works by blocking the action of certain natural chemicals in the human body. As a result, it reduces the blood pressure, heart rate and strain on the heart. It is used to treat hypertension to lower the high blood pressure which helps to prevent strokes, kidney problems, and heart attacks [99].

Metoprolol Tartrate, its structure shown in Figure 35, is a white crystalline powder, has a molecular weight of 684.8g/mol and a molecular formula of $C_{34}H_{56}N_2O_{12}$. It has a melting point of 120°C and pK_a 9.68 and 14.02 and it has high water solubility and permeability (BCS class I) also it is well absorbed over a large part of the gastrointestinal tract [100].

Metoprolol has a low bioavailability (20-50%), and short biological half-life (4-5) hours. Its usual dose is 25mg three times a day. This requires a high frequency of administration that might cause oscillation in the drug concentration in the plasma, it is substantial to produce dosage form with sustained-release effect. There is a serious need to manufacture sustained release bi-layer tablets to decrease the administration

frequency, deliver loading dose in the stomach, increase drug efficacy and

bioavailability and give sustained action [98].
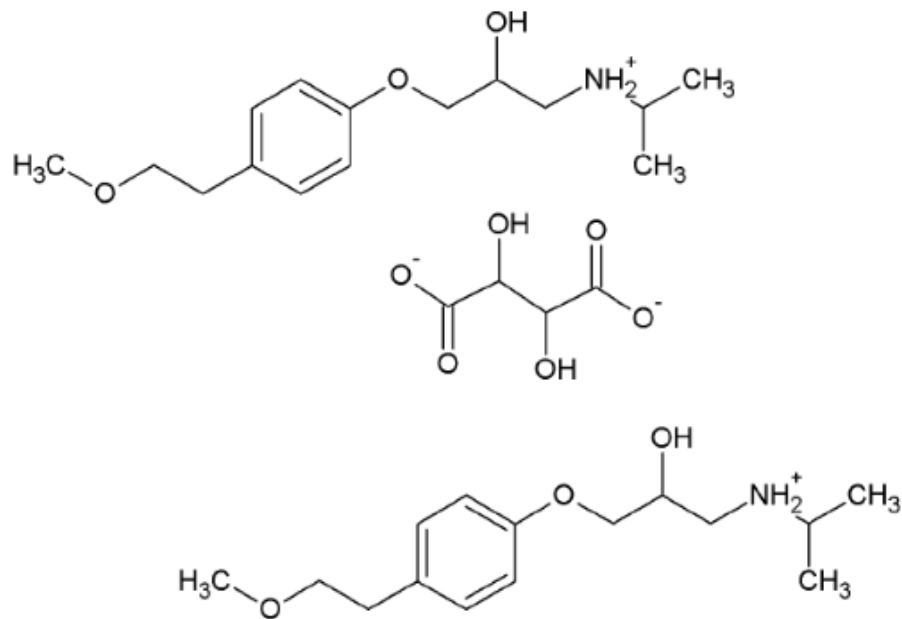
Figure 35: Metoprolol tartrate chemical structure

2. Objectives

1- To manufacture hydrophilic and hydrophobic filaments with good diameter, smooth surface, and morphology, as well as good mechanical, thermal and rheological properties.

2- To manufacture mono sustained and immediate release tablets that had appropriate drug release and dissolution profile.

3- To manufacture bilayer tablets with appropriate drug release and dissolution profile.

4- To compare the dissolution profile and release rate of the mono SR, IR and bilayer tablets that manufactured with FDM technology with the same tablets that manufactured with DC.

3. Materials and Methods

3.1 Materials

Metoprolol Tartrate (MPT) obtained from Polydrug Laboratories (Maharashtra, India), used as a model drug to investigate the drug release profile in hydrophilic and hydrophobic polymers. It is a very water-soluble and permeable API (BCS 1), that has a melting temperature of 120°C and degradation temperature at 160°C [101][102].

Capa® 6506 (Capa® 6506), Ateva® 1850A (EVA), Eudragit ® E PO, kollidon ® 12 PF, and Kollicoat® IR, POLYOX^{TM}, Klucel^{TM} ELF Pharm and Klucel^{TM} EF Pharm purchased from Perstorp (Warrington, United Kingdom), Celanese (Frankfurt, Germany), Evonik (Darmstadt, Germany), BASF (Ludwigshafen, Germany), DOW (Michigan, USA), Ashland (Schaffhausen, Switzerland) respectively.

3.2 Preparation of FDM feedstock material

Physical mixture (P.M) of MPT and different polymers weighted using AG245 analytical balance (Mettler Toledo, New Hampshire, USA), mixed by tumbler mixer (Inversina tumbler mixer from Bioengineering, UK) for 15 min at 25 RPM. Then, Bulk density of the P.M was calculated and P.M transferred to the gravimetric feeder (Brabender Technology, Germany) and extruded by a co-rotating, fully intermeshing twin-screw extruder (prime Eurolab 16, Thermo Fisher, Germany), equipped with a with co-rotating twin screws, that have standard screw configuration with three

mixing zones, four conveying zones and a DD flex wall. As well as, custom-made die

with a diameter of 1.7 mm, as shown in Figure 36.
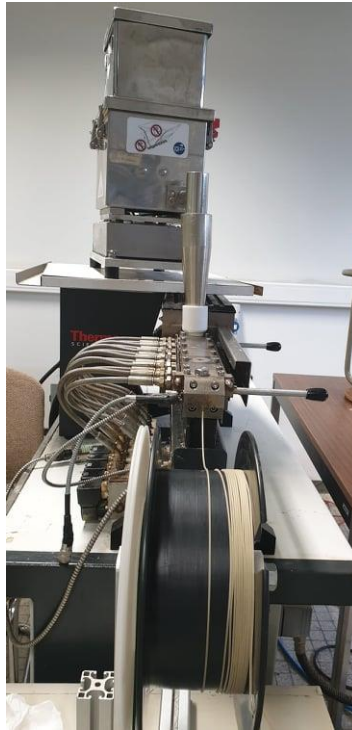
Figure 36: Filaments Extrusion

The feeding rate, screw speed, and barrel temperature were adjusted according to

each formula to not exceed a torque value of 80%.

3.3 Filaments characterization

3.3.1 Filaments dimension

Immediately after extrusion, filament diameter measured every 10 cm using a digital caliper (Bodson, Luik, Belgium), and the obtained diameter was 1.75±0.05mm.

3.3.2 Mechanical testing

TA.XTPlus texture Analyzer (stable microsystems, UK) used to evaluate filament stiffness by using the tensile test with a 30 kg load cell and a TA-243 self-tightening roller grip system, as shown in Figure 37. The initial distance of separation, test speed, and maximum elongation distance were set as 20mm, 3mm/s. A stress-strain diagram was plotted taking into consideration the applied force and filament diameter. Exponent software version 6.1.5.0 (stable microsystems, Godalming, UK) was used for data collection and analysis and all experiments were performed triplicate.
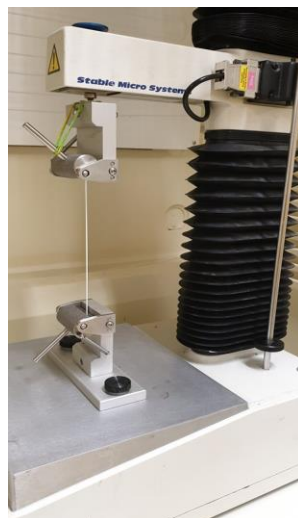
Figure 37:Mechanical properties, Tensile test

3.4 Tablets printing

The filament feeding performance (feeding efficiency) for filaments with good mechanical attributes (constant diameter and acceptable surface smoothness) was tested by using the 3D printer (Prusa I3, Prague, Czech Republic), as shown in Figure 38.
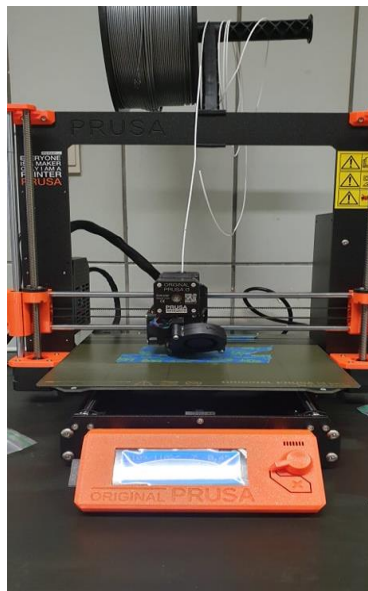
Figure 38:Tablets printing

MPT: Capa® 6506 (40:60%, w/w) filament used to print SR mono tablets with a diameter and thickness of 10.0 and 2.5 mm, respectively. And printing parameters as mentioned in table 4. Due to the filament`s good ductility, hence 10 tablets were printed together at each printing run.

Table 4: SR mono tablet (MPT: Capa® 6506 40:60%, w/w) printing parameters

Filament used ➔ MPT:Capa® 6506 (40:60%, w/w)	
Processing temperature	110°C
Bed temperature	20°C
Infill percentage	100%
Infill pattern	Concentric
Number of perimeters	3
Perimerters/infill overlap percentage	160%
Elephant foot compensation	0.6 mm
Solid infill every	2 layers
Number of top and bottom solid layers	5
The pattern of top and bottom solid layers	Concentric
Perimeters printing speed	45 mm/s
Infill printing speed	80 mm/s
Top and bottom solid infill printing speed	40 mm/s
Solid infill printing speed	80 mm/s

While for IR mono tablets two different hydrophilic filaments used, MPT: Klucel EF (25:75%, w/w) and MPT: Eudragit EPO: POLYOX^{TM} (25:52.5:22.5%, w/w). Considering tablets from both formulas, the same diameters, and thicknesses of 10 and 2.5 mm used. And printing parameters as shown in tables 5 and 6.

Table 5: IR mono tablet (MPT: Klucel 25:75%, w/w) printing parameters

Filament used ➔ MPT: Klucel EF (25:75%, w/w)	
Processing temperature	150°C
Bed temperature	20°C
Infill percentage	50%
Infill pattern	Grid
Number of perimeters	5
Perimeters/infill overlap percentage	25%
Elephant foot compensation	0
Solid infill every	0
Number of top and bottom solid layers	3
The pattern of top and bottom solid layers	Concentric

Perimeters printing speed	5 mm/s
Infill printing speed	5 mm/s
Top and bottom solid infill printing speed	5 mm/s
Solid infill printing speed	5 mm/s

Table 6: IR mono tablet (MPT: Eudragit EPO, POLYOX^{TM} 25:52.5:22.5%, w/w) printing parameters

Filament used ➔ MPT: Eudragit EPO: POLYOX^{TM} (25:52.5:22.5%, w/w)	
Processing temperature	120°C
Bed temperature	20°C
Infill percentage	50%
Infill pattern	Grid
Number of perimeters	2
Perimeters/infill overlap percentage	25%
Elephant foot compensation	0
Solid infill every	0
Number of top and bottom solid layers	3

The pattern of top and bottom solid layers	Concentric
Perimeters printing speed	45 mm/s
Infill printing speed	80 mm/s
Top and bottom solid infill printing speed	40 mm/s
Solid infill printing speed	80 mm/s

For bilayer tablets, using MPT: Capa® 6506 (40:60%, w/w) and MPT: Eudragit EPO: POLYOX™ (25:52.5:22.5%, w/w) filaments, each tablet printed separately with a diameter and thicknesses of 10.0 and 5.0 mm respectively. Using the same printing parameters for mono tablets.

All Tablets were designed by Tinkercad® (Autodesk, Inc., USA) and exported as a G-code by Prusa Slicer software v2.1.0 (Prague, Czech Republic).

To configure the printing parameters for SR and IR tablets, various printing trials implemented while changing different parameters. For example, the number of perimeters, infill ratio, perimeters infill overlap percentage, infill pattern and the number of solid layers in the object. During these trials MPT: Capa® 6506 (40:60%, w/w) used as a model filament.

3.5 3D Tablets Characterization

3.5.1   Tablets Dimensions

After printing, the dimensions of each tablet (n=10), as shown in Figure 39, were measured using and a digital caliper (Bodson, Luik, Belgium) and the test rechecked using semi-automatic tablets testing system (SmartTest 50, Allschwill, Switzerland).
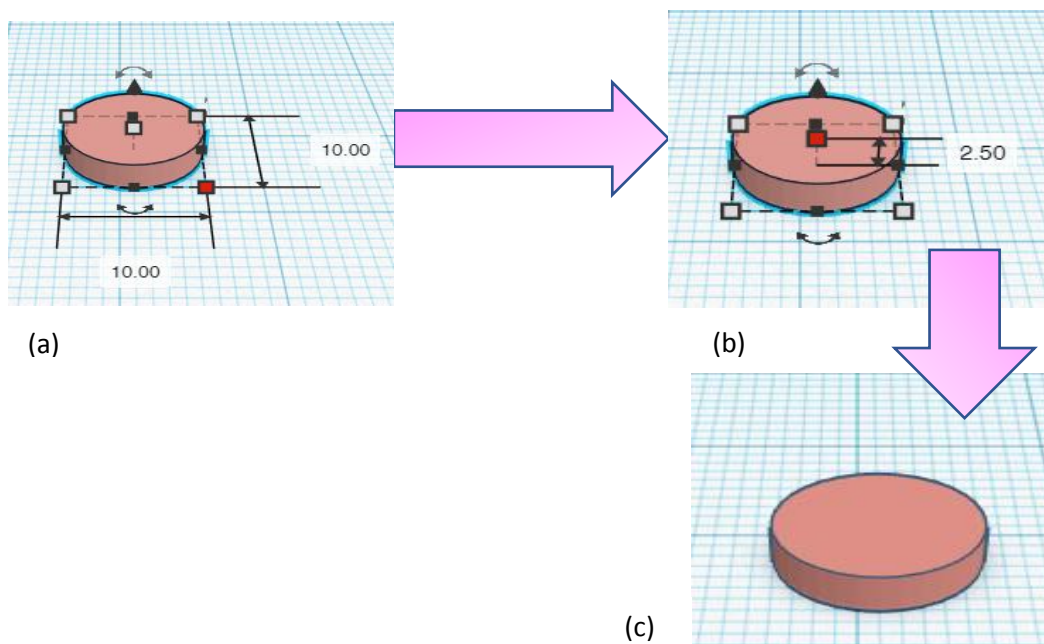
Figure 39: Mono tablets diameter(s) and thickness (a) tablet diameter, (b) tablet thickness, (c) ready tablet for printing

3.5.2   Weight variation and Hardness

SR, IR, and Bilayer tablets weight variation and hardness measured (n=10) using tablets semi-automatic tablets testing system (SmartTest 50, Allschwill, Switzerland). Regards the weight variation acceptance criteria it states that, not more than two tablets should deviate from the average weight by more than the percentage given in

the pharmacopeia (see table 7) and none deviate by more than twice the percentage[103].

Table 7: Weight deviation acceptance criteria [103]

The average weight of tablets	Deviation (%)
Less than 80 mg	±10.0 ±20.0
80mg to 250 mg	±7.5 ±15.5
More than 250 mg	±5.0 ±10.0

3.5.3   Tablets Friability

Friability test for SR, IR, and Bilayer tablets (n=10) operated using (Pharmatest, Hainburg, Germany). Tablets weighted and placed in the friabilator, that operated for 4 minutes at a speed of 25 RPM. Later tablets removed from the apparatus, dedusted and reweighted. Finally, Equation 5 used to calculate the friability percentage [104], [105].

$$\% \, Friability = \frac{Tablets \; initial \; weight - Tablets \; final \; weight}{Tablets \; initial \; weight} * 100$$

Equation 5: Friability Equation

3.5.4   Tablets morphology

Effect of the number of solid layers between infill layers, perimeters number, and overlap percentage of the tablets observed by using Olympus SZX9 Stereo Microscope (Ontario, USA).

3.5.5   Content Uniformity

Content uniformity test for all tablets performed, as shown in Fig 39, by using phosphate buffer PH 6.8 for SR tablets (n=10) and HCl buffer PH 1.2 for IR (n=10). The test ran for all types of tablets for 48 hours. Then samples were withdrawn and analyzed by spectrophotometer (UV-1650PC, Shimadzu Benelux, Antwerp, Belgium) at a wavelength of 222nm.

3.5.6   Differential Scanning Calorimetry

Drug crystallinity was evaluated using a DSC Q2000 (TA Instruments, Leatherhead, UK) equipped with a refrigerated cooling system, as shown in Figure 40. API, physical mixtures, filaments, and 3D printed tablets (sample mass 4-6 mg) were analyzed using non-hermetic T_{zero} pans (TA instruments, Zellik, Belgium) at a heating rate of 10°C/min. The DSC cell was purged using dry nitrogen at a flow rate of 50 mL/min. Single heating run from -20 to 150 °C was performed to analyze the thermal characteristics (T_m and melting enthalpy (ΔH)) of pure components, physical mixtures, filaments, and 3D printed tablet.
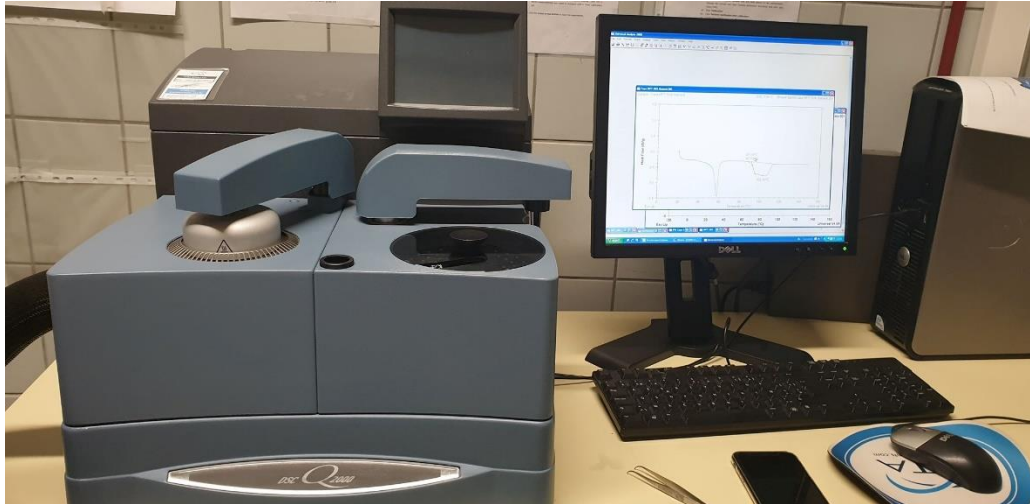
Figure 40: DSC Q2000

3.5.7   Disintegration test

This test applied to check if tablets disintegrates in a prescribed time when they are under specific conditions stated in the USP[106].

3.5.8   In vitro Dissolution

Impact of perimeters number, overlap, and the number of solid layers on the in vitro release kinetics were determined using a VK 7010 dissolution system (Vankel industries, New Jersey, USA), as shown in Figure 41. In house method used, where paddle speed and bath temperature were set at 100 rpm and 37.5± 0.5 °C, respectively.

For sustained-release tablets, dissolution vessels were filled with 900 ml with Phosphate buffer PH 6.8, prepared according to USP buffer solution preparation[107],

and 5ml of samples were withdrawn at predetermined time points (0.5, 1, 2, 4, 6, 8, 12, 16, 20 and 24 hours).

On the other hand, for immediate release tablets, dissolution vessels were filled with 900 ml with HCl buffer PH 1.2, prepared according to USP buffer solution preparation[107]. The samples were withdrawn at predetermined time points (5, 10, 15, 30,45, 60, 90, 120, 150, 180 minutes).

For Bilayer tablets at the beginning dissolution vessels filled with 700ml of 0.1N HCl for 2 hours followed by 200ml of 0.2M tribasic phosphate for 22 hours, according to USP Method A. Samples withdrawn at predetermined points as following (5,10,30, 60, 90, 120, 240, 360, 720, 960, 1440 min). All samples diluted and analyzed with a spectrophotometer (UV-1650PC, Shimadzu Benelux, Antwerp, Belgium) at a wavelength of 222nm.

Figure 41: VK 7010 dissolution system

Calibrations curve of MPT in Acid and Base buffers shown below in Figures 42 and 43.
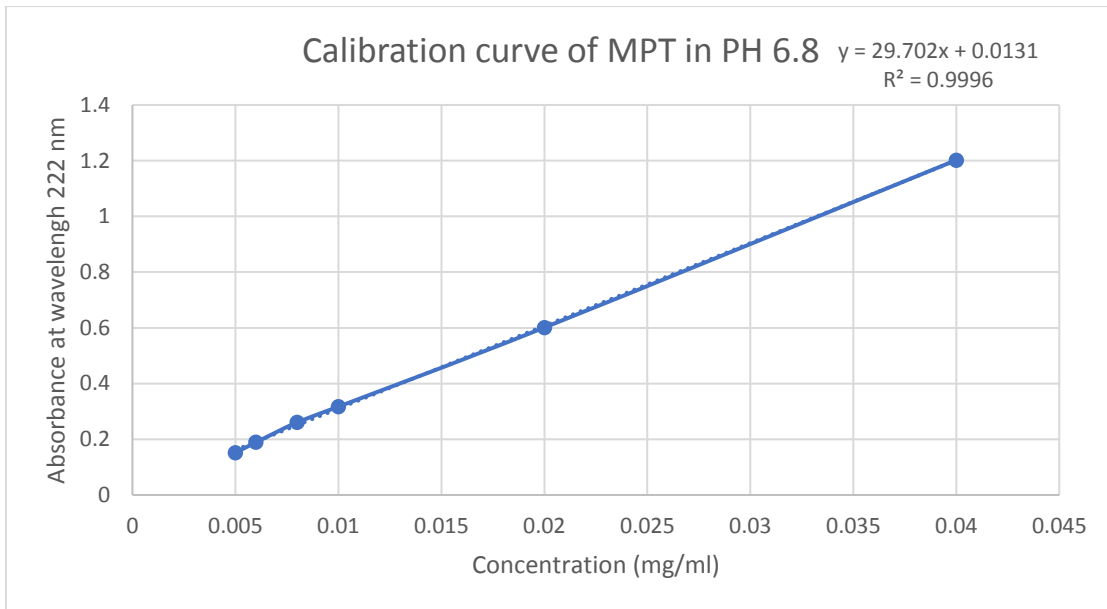
Figure 43: Calibration curve of MPT in PH 6.8
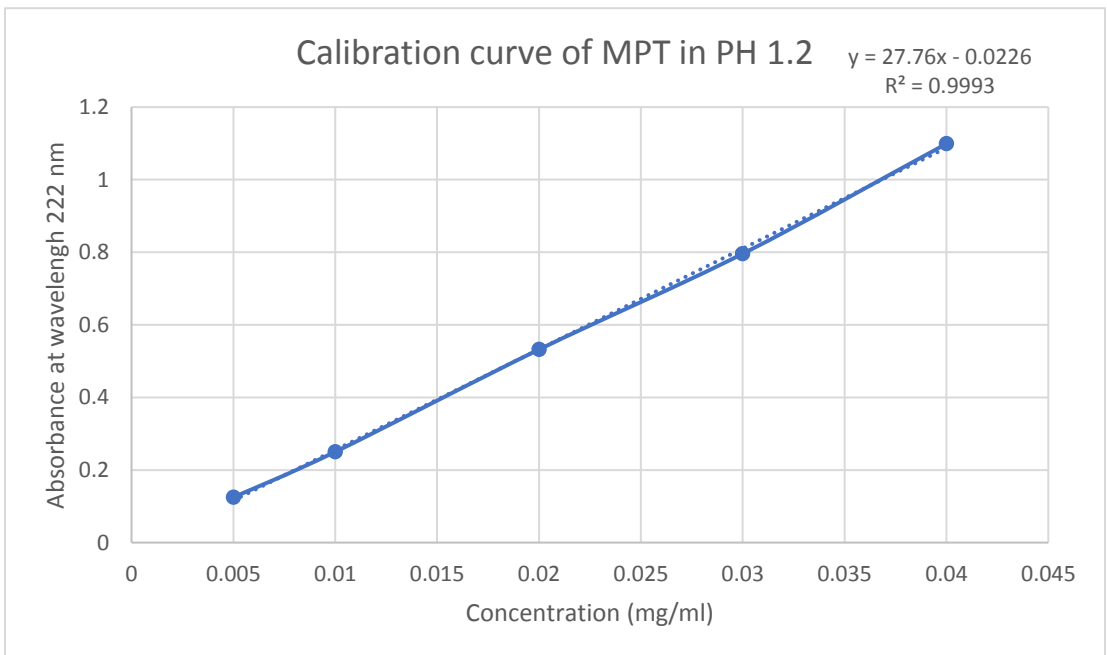
Figure 42: Calibration curve of MPT in PH 1.2

3.5.9 Dissolution kinetics

To study the kinetics of MPT release in all the printed formulation, attained data analyzed using KinetDS3 software and fitted in zero, first orders, Higushi, Hixon-Crowell and Korsmeyer-Peppas models [108].

Zero-order: the drug release is independent on the concentration and it is expressed in this equation:

$$Qt = Q_{o} + K_{o}t$$

Equation 6: Zero-order equation

Where; Qt: drug dissolved amount, Q_{o}: initial drug amount, K_{o}: constant, t: time in hours.

In First order: The drug release depends on the drug concentration.

$$Log\ Qt = Log\ Q_{o} + \frac{kt}{2.303}$$

Equation 7: First order equation

Where; Qt: drug dissolved amount, Q_{o}: initial drug amount, K_{o}: constant, t: time in hours.

Hixson-Crowell model: the drug release depends on the tablet`s surface area and diameter.

$$\sqrt[3]{Q_{o}} - \sqrt[3]{Qt} = K_{HC}.$$

Equation 8: Hixson - Crowell equation

Where; Qt: drug dissolved amount, Q_0: initial drug amount, K_0: constant, t: time in hours.

Higuchi model: where the drug release plotted versus the square root of time. And it assumes that the tablet dissolution performs diffusion mechanism.

$$Qt = K_H\sqrt{t}$$

Equation 9: Higuchi equation

Where; Qt: drug dissolved amount, K_0: constant, t: time in hours.

Korsmeyer-Peppas release model: it describes the drug release from polymeric systems.

$$F = K\,t^n$$

Equation 10: Korsmeyer - Peppas equation

Where F: drug fraction, K: constant, t: time in hours, n: diffusion exponent.

3.6 Direct compression and tablets dissolution

The same physical mixture formula MPT: Capa® 6506 (40:60%, w/w) and MPT: Eudragit EPO: POLYOX™ (25:52.5:22.5%, w/w/w) blended and compressed using Styl`One compression machine (Medel pharm, Lyon, France) and B FF 10mm punch (Medel pharm, Lyon, France).

Not long afterward, in vitro dissolution implemented for the obtained tablets using the same dissolution medium, peddle speed, sample volume and time as used for tablets manufactured by FDM.

4. Work Methodology

The Methodology of this work summarized in Figure 44. Where the physical mixture fed into the extruder, the extrusion temperature must be below 150°C to avoid API degradation, because MPT degradation temperature is at 155°C. Regards sustained-release formulations it should be below 120°C to avoid solid dispersion since the melting temperature for MPT is 120°C.

The extruder torque must not exceed 80%, to ensure the good rotation of the motor and screws thus achieving good homogenous mixing. The formula should be modified if it does not pass the above rules. Otherwise, the mechanical properties calculated using the texture analyzer.

If the filaments have weak mechanical properties they should be reformulated. Else, they should be fed into the 3D printer. The printing temperature also should be below 150°C for all formulas and below 120°C for sustained release formulas, for the same reasons that mentioned above.

When the filaments have poor rheological properties hence temperature should be increased above 120°C for SR and/or 150°C for IR filaments. The formula should be rejected and reformulated. Differently, tablets printed below the limited temperatures.

Then, QC tests for tablets should be done such as weight variation, tablets` dimensions, hardness, friability, content uniformity. whenever, the tablets fail the tests, the formula or the parameters must be modified. Otherwise, tablets should be transferred to the in vitro dissolution test.

Supposing the tablets fail the dissolution test or results poor release rate and weak release profile, printing parameters should be changed such as the infill ratio, perimeters/infill overlap percentage, number of perimeters ...etc. Otherwise, the final product obtained.

API and Thermoplastic Polymer

Mariana Musallam | March 3, 2020

Preparation of FDM feedstock material

HME

Extrusion Temp > 150 °C   Extrusion Temp ≤ 150 °C

Modify Formula

Torque > 80%   Torque ≤ 80%

Do Extrusion

Poor mechanical properties   Good mechanical properities

Printing Temp > 150 °C   Printing Temp ≤ 150 °C

3D Print

QC Tests

Change Parameters

Fail   Pass

In Vitro Dissolution

Poor release rate and release profile   Good release rate and release profile

Final Product

Figure 44: Work Methodology

5. Results and discussion

5.1 Extrusion and 3D printing

To prepare sustained-release tablets, two hydrophobic polymers used, polycaprolactone with different drug loads MPT: Capa® 6506 (50:50%, w/w) and MPT: Capa® 6506 (40:60%, w/w) and Ethylene vinyl acetate with higher drug load MPT: EVA 1850 (50:50%, w/w) but this one was still under research and no further tests applied to it due to lack of time.

For immediate release tablets, it was more complicated because generally hydrophilic polymers were brittle. Thus, different formulations done. In the beginning, Metoprolol tartrate loaded in the following polymers (Kollicoat IR, Eudragit EPO, Kollidon K12, POLYOX™, and Klucel ELF) in a ratio of 25% for MPT and 75% for the polymers. However, all the previous filaments were brittle. Then MPT: Klucel EF (25:75%, w/w) extruded and it was printable, but because of dissolution issues (see in-vitro dissolution section), more formulas tested.

Pore former added such as POLYOX™ and copolymers used such as mixing Eudragit EPO with Klucel EF and POLYOX™. All formulas and extrusion details presented in Table 8 below.

Later, because MPT: Klucel EF (25:75%, w/w) was a printable, dissolution test implemented and all filaments were successfully extruded below 150°C, that

temperature had been chosen because the MPT degradation temperature is 155°C and without exceeding the torque value of 80%.

Whereas, torque can be defined as the force that the motor needs to rotate the screws. And there was a variation in the torque values due to different formulas that act various resistance on the screw where high resistance generates high torque value[109].

Different variables affect the torque considering the (a) die temperature, where increasing the die temperature leads to decreasing the molt viscosity thus decrease the torque. (b) moisture content, where increasing the moisture content leads to low melt viscosity thus decrease the torque value. (c) screw speed, where increasing the screw speeds leads to generate more energy so increasing the temperature that leading to decreased viscosity thus decreasing the torque value. On the other hand, (d) mass flow rate, where increasing the mass flow rate leading to increase the barrel of the extruder so more shear needed to compensate the molten resulting to increase the torque value [110].

Moreover, the Smooth surface of the filament is highly needed for adequate feeding. In this work all the filaments have a smooth surface, no shark skinning observed even with 50% drug load.

Table 8: Extruded formulas and extrusion parameters for different formulations

Formulation (% w/w)		Feeding rate (kg/h)	Temperature °C						Screw speed (rpm)	Torque value (%)
			1	2	3	4	5	Die		
SR	MPT: Capa® 6506 (50:50%, w/w)	0.3	60	80	80	80	80	/	100	50
	MPT: Capa® 6506 (40:60%, w/w)	0.3	60	80	80	80	80	/	100	47
	MPT: Ateva 1850 (50:50%, w/w)	0.3	60	80	80	80	80	80	100	20
IR	MPT: Eudragit EPO (25/75%, w/w)	0.25	70	100	100	100	100	80	100	37
	MPT: Kollidon K12 (25:75%, w/w)	0.3	100	125	125	125	125	60	100	28
	MPT: Klucel ELF (25:75%, w/w)	0.3	100	115	115	115	115	90	100	26
	MPT: Kollicoat IR (25:75%, w/w)	0.2	140	150	150	150	150	115	150	18
	MPT: POLYOX™ (25:75%, w/w)	0.25	100	120	120	120	120	120	150	22
	MPT: Klucel EF (25:75%, w/w)	0.25	80	115	115	115	115	50	100	26

MPT: Klucel EF: POLYOX™ (25:65:10%, w/w/w)	0.25	100	125	125	125	125	100	100	24
MPT: Eudragit EPO: POLYOX™ (25:52.5:22.5%, w/w/w)	0.25	90	120	120	120	120	100	120	30

5.2 Filament characterization

5.2.1 Filaments dimensions

As mentioned before, the FDM filament diameter should be 1.75±0.05 mm to be feedable and printable [37]. In this work, all the filaments' diameter is measured directly after extrusion with a digital caliper. The mean value and standard deviation are shown in Table 9.

Notable die swelling was observed while extruding Klucel EF and Klucel ELF. Where die swelling is a phenomenon where the cross-section area of the filament increases after leaving the die [96],[111].

This happened due to polymer relaxation after high shear and stress inside the barrel. The increase in die swelling depends on the polymer itself such as the polymer molecular weight and melt elasticity and external factors as well such as the temperature, shear rate, shear stress and die geometry [96],[111].

To decrease the die swelling problem, barrel temperature increased, screw speed decreased, collecting roller speed increased and heated die used. Since using heated die through extrusion decreases thermoplastic polymers swelling [112]. Nevertheless, filaments were not extruded with a diameter below 1.80 mm.

Table 9: Filaments diameters

Formulation (% w/w)	Diameter (mm)
ABS	1.75±0.03
MPT: CAPA® 6506 (50:50%, w/w)	1.78±0.11
MPT: CAPA® 6506 (40:60%, w/w)	1.74±0.01
MPT: Eudragit (25:75%, w/w)	1.74±0.03
MPT: Kollidon K 12 (25:75%, w/w)	1.78±0.1
MPT: Kollicoat IR (25:75%, w/w)	1.71±0.05
MPT: Klucel ELF (25:75%, w/w)	1.81±0.02
MPT: Klucel EF (25:75%, w/w)	1.81±0.06
MPT: POLYOX™ (25:75%, w/w)	1.78±0.04
MPT: Klucel EF: POLYOX™ (25:65:10%, w/w)	1.75±0.01
MPT: Eudragit EPO: POLYOX™ (25:52.5:22.5%, w/w/w)	1.72±0.04
MPT: Klucel EF: Eudragit EPO (25:40:35%, w/w/w)	1.77±0.02

5.2.2 Mechanical properties

Tensile test applied and stress-strain curves plotted. Stiffness (N/mm^2), breaking strength (N/mm^2), ultimate tensile strength (N/mm^2) and toughness (N/mm^2) calculated by using the mean of these curves and results obtained (see Table 8).

Starting from the sustained release formulation MPT: Capa® 6506 (50:50%, w/w) filament was not printable, because it was brittle and broken between the feeding gears.

And that was proven from the stress-strain curve and calculations. MPT: Capa® 6506 (50:50%, w/w) filament had smaller stiffness, breaking strength values, and low toughness compared with ABS that is a commercial filament used in FDM technology (see Figure 45).
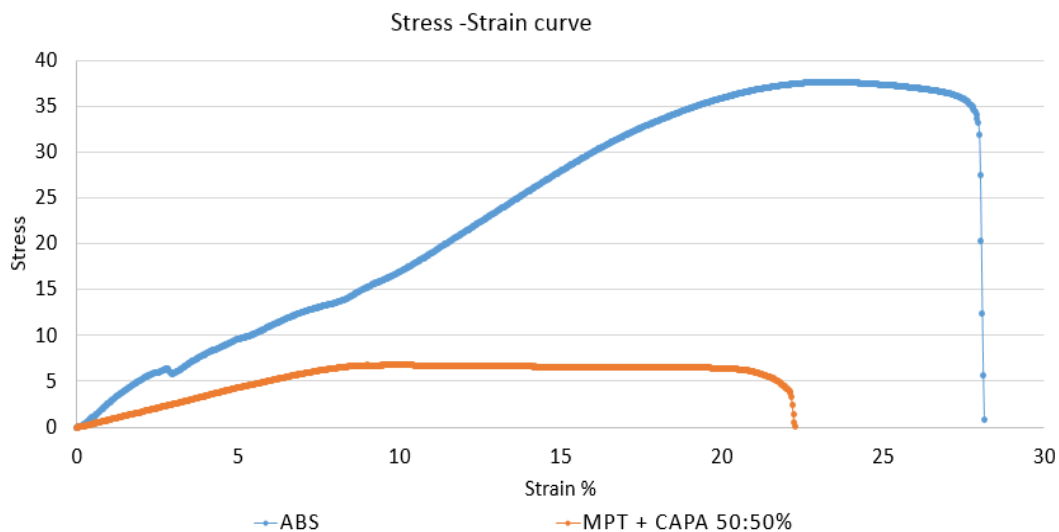
Figure 45: stress-strain curve ABS, and MPT: Capa (50:50%, w/w)

Consequently, filament with lower drug load extruded, MPT: Capa® 6506 (40:60%, w/w), and stress-strain curve plotted, as shown in Figure 46. Higher Stiffness, ultimate tensile strength, stain percentage and toughness values resulted compared with MPT: Capa® 6506 (50:50%, w/w) (see table 10). That happened due the "plasticization effect of the drug on the polymer" [38].

High value in ultimate tensile strength (700N/mm^2), indicated to a ductile filament. Where ductility defined that the filament can undergo notable plastic deformation before rupture [113].

In this case the filament ductility and the high toughness value led to printable filament. Because the filament had enough energy to pass the feeding gears without breaking.

Until now, no previous publication indicated Metoprolol Tartrate and Polycaprolactone filaments used in FDM. On the other hand, Polycaprolactone is used in two researches with different drug loads.

Hollander et al used Polycaprolactone with (5%, 15%, 30%) drug load of indomethacin in their work, to manufacture T-shape of intra urine system [114]. Also, Aho et al used polycaprolactone with (10%,30%,50%) drug load of indomethacin in their work, to study the effect of thermal, mechanical and rheological properties of the materials on FDM technology [35].
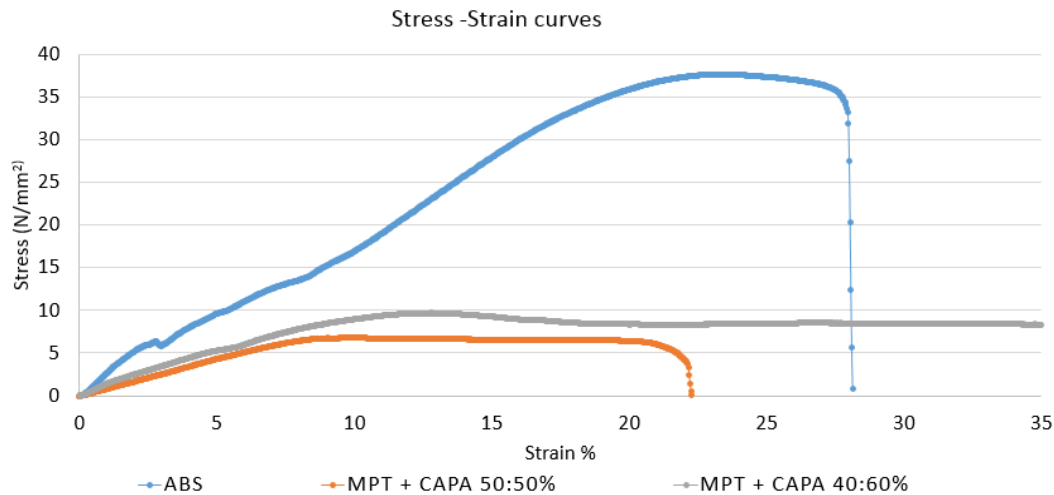
Figure 46: stress-strain curve ABS, MPT: Capa® 6506 (50:50%, w/w) and MPT: Capa® 6506 (40:60%, w/w)

For immediate release formulation, the process was harder since most of the hydrophilic filaments were brittle.

Different hydrophilic polymers used (Eudragit EPO, Kollidon K12, Kollicoat IR, Klucel ELF, and POLYOX™) with the same drug load which was 25%. All of them were brittle and broken between the feeding gears.

From the flexibility profile of those filaments obtained from stress-strain curves it was found that MPT: Eudragit EPO (25:75%, w/w) and MPT: Kollidon K12 (25:75%, w/w) were suddenly fracture directly after the elastic region showed no bending neither plastic deformation (see figure 47). Moreover, they had short breaking distance and low toughness value thus they were not feedable.

Eudragit EPO used in Nasereddin et al research when they study the effect of mechanical properties on the feedability process. As a result, Eudragit EPO (100%) filament was fractured between the feeding gears in the head of the printer and did not pass to the nozzle. Moreover, it showed a sharp brittle curve that the filament broke after the maximum force applied [38].

In addition, Sadia et al studied the effect of different excipients on Eudragit EPO for producing immediate release tablets by FDM. And from that study it was found that Eudragit EPO was brittle filament, thus different ratio of plasticizers and fillers used. After trials it was found that Eudragit EPO: TEC: TCP: drug (46.75:3.25:37.5:12.5%, w/w/w/w) was a feedable and printable formula. Where TEC was Triethyl citrate and TCP was tricalcium phosphate, while the drugs were captopril, prednisolone, Theophylline, and 5-ASA [86].

Regarding Kollidon K12, it was a brittle filament (see figure 47) due to its low molecular weight, that facilitated short interlinkage between the chains of the polymer, led to short tensile strength [115].

Kollidon K12 used in Kempin et al research, when they studied the development of gastro resistant tablet by using dual extrusion method. While 10% pantoprazole sodium used as a model drug. It was found that the filament was brittle thus 15% Triethyl citrate (TEC) added in the formula to improve the feeding and printing

properties [116]. Also in Kollamaram et al research Kollidon K12 mixed with Kollidon VA64 and other excipients such as PEG and mannitol to improve the mechanical properties while they tried to manufacture Ramipril immediate release tablets [6],[115].

Upon MPT: POLYOX^{TM} (25:75%, w/w) it was brittle and fractured between the feeding gears on the head of the printer. That was proven from its flexibility profile, it had plastic deformation but it also had short breaking distance and low toughness (see figure 47).

POLYOX^{TM} used in Melocchi et al study to investigate the effect of polymers grade on extrusion and FDM process and it was extrudable and printable [96]. Also, it was used with Soluplus, PEG 4000 and Tween 80 in Alhijjaj el at research to improve the drug release of FDM oral dosage forms where felodipine was used as a model drug [67].

Regards MPT: Klucel ELF (25:75%, w/w) was brittle because it had lower stiffness value compared with other filaments, as shown in Figure 47. Zhang et al mentioned that stiffness is one of the significant indicators for printable filament [11]. Besides, to short breaking distance, where Verstaete et al and Zhang et al mentioned that filaments with short breaking distance are brittle[11], [37].

Until today, no previous publications cited that MPT: Klucel ELF or Klucel ELF filaments used in FDM previous researches. However, more investigation is needed, perhaps

more modifications in the printing properties may lead to different results since the filament is not that weak compared with other filaments that is used (see figure 47).

Regards MPT: Kollicoat IR was very brittle and weak filament so it was broken on the roller before implementing the test. Kempin et al mentioned in their study of manufacturing immediate release tablets of thermolabile drugs by using FDM technology where Pantoprazole sodium (5%) used as a model drug, that Kollicoat IR was brittle thus not printable [88]. While it was printable when it was used with 10% Haloperidol in Solanki et al study that worked to screen drug release polymers [6], [61].
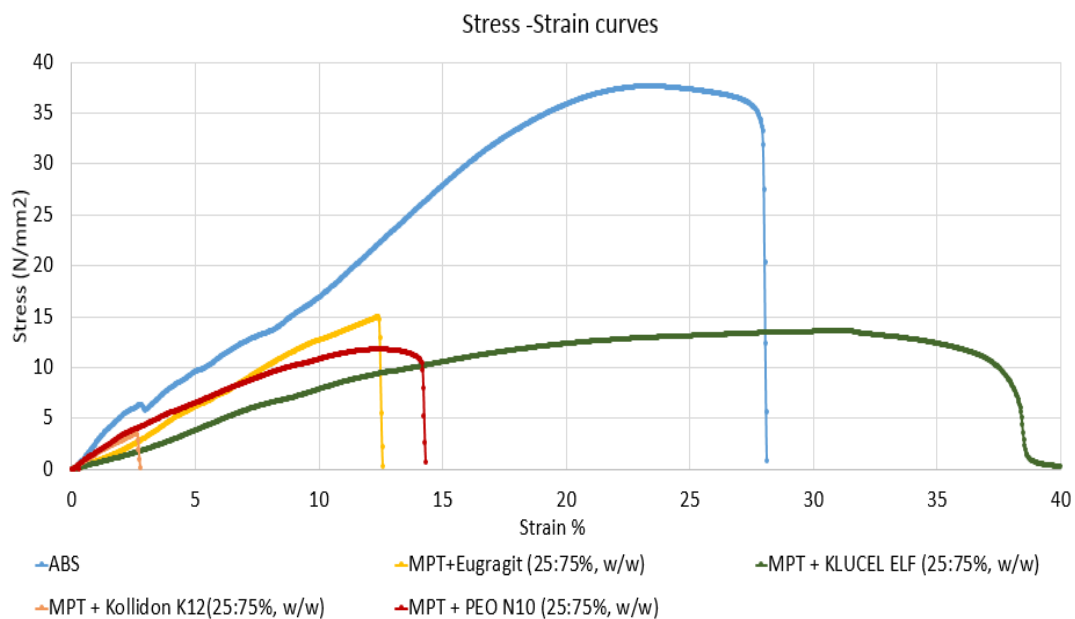
Figure 47: stress-strain curves for ABS, MPT: Eudragit EPO (25:75%, w/w), (MPT: Kollidon K12 (25:75%, w/w) , MPT:POLYOX^TM (25:75%, w/w) and MPT: Klucel ELF (25:75%, w/w)

After that, MPT: Klucel EF (25:75%, w/w) prepared and this was feedable and printable filament. It was printed at low speed (see Table 5).

Its Flexibility profile compared with Klucel ELF presented in Figure 48. However, it was not printed easily and continuously. The printing process paused many times because the filament broken inside the feeding gears and under-extrusion layers resulted. Where under-extrusion mixed 30% paracetamol and 35% HPMC E5 and also when it was mixed with 30% paracetamol and 45.5% HPMC E5 [11].
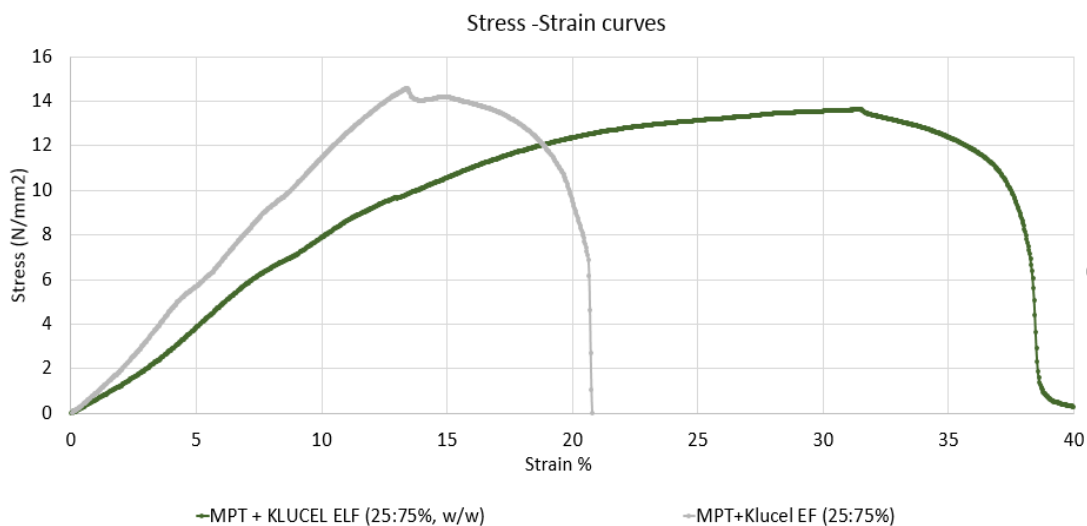
Figure 48: stress-strain curves for MPT: Klucel EF (25:75%, w/w) and MPT: ELF (25:75%, w/w)

After MPT: Klucel EF (25:75%, w/w) passed the printing stage, in vitro dissolution implemented and the tablets failed the test. Thus, PEO added to the formula to enhance the dissolution. Because PEO is a pore former [117]. MPT: Klucel EF: Polyox^{TM} (25:65:10%, w/w/w) was brittle, thus not feedable and printable.

Then because Eudragit EPO is the most hydrophilic polymer, it decided to be used [84]. Thus, it was used with Klucel EF as a co-polymer to enhance the mechanical properties of the filament. As cited in literature Eudragit EPO is brittle filament while Klucel EF is flexible filament and neither of them are feedable and/or printable [11], [38]. However, MPT: Klucel EF: Eudragit (25:40:35%, w/w) was also brittle thus, had broken inside the printer`s head.

On the other hand, MPT: Eudragit EPO: POLYOX^{TM} (25:52.5:22.5%, w/w/w) was an adequate filament. It was feedable and printable. That was proven from its flexibility profile, as shown in Figure 49. It had higher Stiffness, breaking strength, Ultimate tensile strength, and toughness values thus this formula enhanced the mechanical properties of the filament and made it feedable and printable.
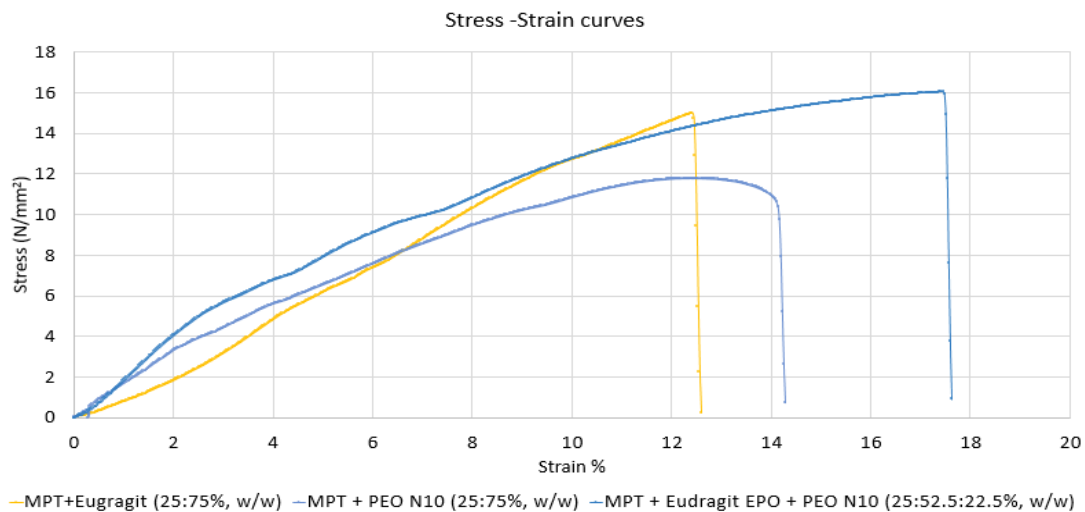
Figure 49: stress-strain curves of MPT: Eudragit (25:75%, w/w), MPT: POLYOX^{TM} (25:75%, w/w) and MPT: Eudragit EPO: POLYOX^{TM} (25:52.5:22.5%, w/w/w)

As mentioned above, filaments should have adequate mechanical properties. In this work, most of the filaments were broken between the gears in the FDM printer since they were brittle. On the other side, three filaments successfully forwarded towards the nozzle and those had good mechanical properties.

Table 10 present the formulas with their mechanical properties that resulted from stress-strain curves after applying tensile test using texture analyzer.

Table 10: Formulations and their mechanical properties

	Formula	Stiffness (N/m)	Ultimate tensile strength (N/mm²)	Strain at breakage (%)	Toughness (J/mm³)
1.	ABS	1.65±0.39	38.88±1.05	29.84±2.16	1736.51±319.97
2.	MPT: CAPA® 6506 (50:50%, w/w)	1.2377±0.313	6.94±0.24	30.60±7.84	223.47±49.63
3.	MPT: CAPA® 6506 (40:60%, w/w)	1.065±0.07	9.86±0.17	700±0.00	61687.41±1601
4.	MPT + Eudragit (25:75%, w/w)	0.87± 0.073	16.01±1.42	14.06±2.08	127.59±42.14
5.	MPT: Kollidon K 12 (25:75%, w/w)	1.52±0.04	3.46± 0.10	3.68±1.32	7.06±2.17
6.	MPT: PEO (25:75%, w/w)	1.58±0.16	12.28±0.43	15.28±0.83	129.80±8.55
7.	MPT: Kollicoat IR (25:75%, w/w)	Very brittle and weak, broken while it was in the probe, it`s mechanical properties can`t be measured			
8.	MPT: Klucel ELF (25:75%, w/w)	0.82±0.06	13.86±0.43	45.12±6.38	398.27±39.11
9.	MPT: Klucel EF (25:75%, w/w)	0.96±0.34	15.50±2.24	28.09±8.59	264.48±121.73
10.	MPT: Eudragit: PEO (25:52.5:22.5%, w/w)	1.80±0.30	15.97±0.606	17.22±2.44	188.85±37.63

5.3 FDM printing

The Printing temperature should be above the T_g or T_m of the polymer [35]. Also, it should be higher than the HME processing temperature to ensure appropriate flowability. Due to screw absence and thus less shear stress as well as short residence time than HME. On the other side, it should be as low as possible to avoid the thermal degradation of the API or/and polymer(s). In this research, all printing temperatures were below the degradation temperature of each substance.

The printer bed temperature may be heated or cooled to ensure good adhesion and solidification for some polymers. But in this work, there was no need to do that and all tablets were solidified and had good adhesion when they are printed at the room temperature 20-25°C.

The printing speed also can be increased or decreased to get a better printing process especially with polymers with low ductility. In this work, the printing speed lowered while printing MPT: Klucel EF (25:75% w/w) to avoid fast filament breaking between the wheels.

In this work, three formulas (MPT: Capa® 6506 40:60%, w/w), (MPT: Klucel EF 25:75% w/w), and (MPT: Eudragit EPO: POLYOX^{TM} 25:52.5:22.5% w/w) were feedable and printable. Where Feedable indicates that the filaments can pass the counter rotating wheels without breaking or bending. And, printable indicates that the filaments pass

from the printer nozzle to the bed. This happened because those filaments had good mechanical, and rheological properties.

Other filaments such as (MPT: Capa® 6506 50:50% w/w), (MPT: Eudragit 25:75%), (MPT: PVP K12 25:75%), (MPT: Kollicoat IR 25:75% w/w), (MPT : Klucel ELF 25:75% w/w), (MPT: Klucel ELF: Eudragit 25:37.7:37.5% w/w), (MPT: KLUCEL EF: POLYOX^{TM} 25:65:10% w/w), (MPT: POLYOX^{TM} 25:75% w/w), (MPT: Klucel EF: Eudragit EPO 25:40:35% w/w) were brittle thus broke between the wheels. And this was proven in the mechanical properties section. To reduce the filament brittleness, suitable plasticizers can be added to the formulas. However, this work aimed to find a simple formulation with fewer excipients.

All the filaments had 1.75±0.05 mm diameter except Klucel filaments and that was due to a swelling mechanism (see filaments dimension section). To solve this issue, smaller die in HME or larger nozzle diameter in FDM can be used. However, in this research, they were printed because it was not that large and they passed the wheels to the nozzle.

Table 11 summarized all the formulas extrudability, feedability and printability.

Table 11: Sustained and Immediate release formulas extrudability, feedability and printability

	Formula	Extrudable	Feedable	Printable
SR	MPT + CAPA® 6506 (50:50% w/w)	✓	✗	✗
	MPT +CAPA® 6506 (40:60% w/w)	✓	✓	✓
IR	MPT + Eudragit (25:75%, w/w)	✓	✗	✗
	MPT + Kollidon K12 (25:75%, w/w)	✓	✗	✗
	MPT + Kollicoat IR (25:75%, w/w)	✓	✗	✗
	MPT + POLYOX™ (25:75%, w/w)	✓	✗	✗
	MPT + Klucel ELF (25:75%, w/w)	✓	✗	✗
	MPT+ Klucel EF (25:75%, w/w)	✓	✓	✓
	MPT+ KLUCEL EF + POLYOX™ (25:65:10%, w/w/w)	✓	✗	✗
	MPT + KLUCEL EF + EUDRAGIT (25:40:35%, w/w/w)	✓	✗	✗
	MPT+ Eudragit EPO+ POLYOX™ (25:52.5:22.5%, w/w/w)	✓	✓	✓

5.4 Tablets characteristics

5.4.1 Tablets Dimensions

Tablets roundness, thickness, masses and volumes are shown in Tables 12, 13, and 14. The original dimensions of the sustained release and immediate-release tablets were the same (10.0*10.0*2.55mm) whereas (10.0*10.0*5.0mm) for the bilayer tablets (see figure 50).
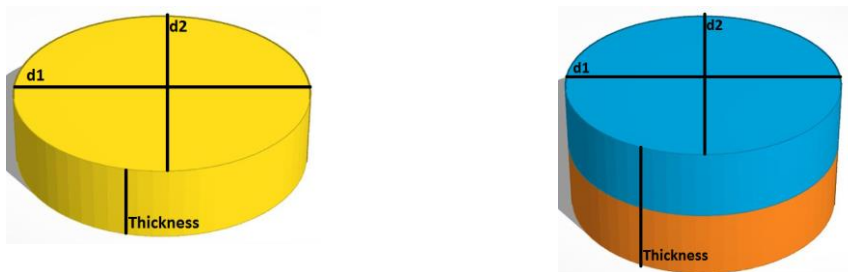
Figure 50: Tablets Dimensions

Table 12: SR tablets diameter 1 (D1), diameter 2 (D2), roundness (R), average diameter (Avg D), thickness(H), average diameter/thickness deviation (Avg D/H div) and tablets volume (V) using MPT: Capa® 6506 (40:60%, w/w) filament

Tablet#	D1 (mm)	D2 (mm)	R	Avg D (mm)	H (mm)	Avg (D/H) div	V (mm³)
1	10.28	10.19	1.00	10.23	2.69	3.80	221.20
2	10.19	10.15	1.00	10.17	2.64	3.85	214.35
3	10.15	10.2	0.99	10.17	2.7	3.77	219.43
4	10.45	10.43	1.00	10.44	2.68	3.89	229.30
5	10.27	10.25	1.00	10.26	2.64	3.87	218.15

6	10.25	10.32	0.99	10.285	2.67	3.85	221.71
7	10.19	10.18	1.00	10.185	2.65	3.84	215.79
8	10.18	10.25	0.99	10.215	2.68	3.81	219.52
9	10.42	10.38	1.00	10.40	2.69	3.87	228.39
10	10.17	10.15	1.00	10.16	2.64	3.85	213.92
Average	10.25	10.25	1.000	10.25	2.67	3.84	220.18
STDEV	0.10	0.09	0.005	0.09	0.02	0.04	5.29
RSD%	1.0	0.95	0.51	0.95	0.88	1.00	2.40

Table 13: IR tablets diameter 1 (D1), diameter 2 (D2), roundness (R), average diameter (Avg D), thickness(H), average diameter/thickness deviation (Avg D/H div) and tablets volume (V) using MPT: Eudragit EPO: POLYOX™ (25:52.5:22.5%, w/w/w) filament

Tablet #	D1 (mm)	D2 (mm)	R	Avg D (mm)	H (mm)	Avg (D/H) div	V (mm³)
1	9.77	9.7	1.00	9.73	2.79	3.49	207.56
2	9.56	9.61	0.99	9.58	2.76	3.47	199.05
3	9.83	9.84	0.99	9.83	2.68	3.67	203.45
4	9.77	9.77	1	9.77	2.77	3.53	207.56
5	9.84	9.83	1.00	9.83	2.8	3.51	212.61
6	9.78	9.78	1	9.78	2.75	3.56	206.48
7	9.6	9.62	0.99	9.61	2.77	3.47	200.81

8	9.77	9.78	0.99	9.775	2.79	3.50	209.27
9	9.84	9.85	0.99	9.845	2.69	3.66	204.67
10	9.79	9.77	1.00	9.78	2.78	3.52	208.73
Average	9.75	9.75	0.999	9.76	2.75	3.54	206.02
STDEV	0.09	0.08	0.003	0.09	0.04	0.07	4.08
RSD%	0.99	0.87	0.31	0.92	1.49	2.03	1.98

Table 14: Bilayer tablets diameter 1 (D1), diameter 2 (D2), roundness (R), average diameter (Avg D), thickness(H), average diameter/thickness deviation (Avg D/H div) and tablets volume (V) using MPT: Capa® 6506 (40:60%, w/w) and MPT: Eudragit EPO: POLYOX^{TM} (25:52.5:22.5%, w/w/w) filament

Tablet #	D1 (mm)	D2 (mm)	R	Avg D (mm)	H (mm)	Avg (D/H) div	V (mm³)
1	9.97	9.93	1.00	9.95	5.7	1.75	442.99
2	10.18	10.16	1.00	10.17	5.22	1.95	423.82
3	10.02	10.1	0.99	10.06	5.56	1.81	441.71
4	10.12	10.08	1.00	10.1	5.56	1.82	445.23
5	10.18	10.18	1	10.18	5.23	1.95	425.47
6	10.17	10.16	1.00	10.16	5.24	1.94	425.03
7	10.18	10.17	1.00	10.17	5.61	1.81	455.93
8	10.18	10.16	1.00	10.17	5.23	1.94	424.63
9	10.13	10.18	0.99	10.15	5.55	1.83	449.29

10	10.18	10.18	1	10.18	5.42	1.88	440.9
Average	10.13	10.13	1.00	10.13	5.43	1.87	437.50
STDEV	0.08	0.08	0.00	0.07	0.19	0.07	11.79
RSD%	0.75	0.77	0.38	0.74	3.44	3.96	2.69

According to SR, IR, and bilayer tablets average diameter, they were (10.25±0.09, 9.76±0.09, 10.13±0.07mm), respectively. Where the original diameter in the CAD file for all the tablets was 10.00 mm. It was noticed that SR tablets' diameter increased due to elephant leg compensation.

Where elephant leg compensation is a term that indicates increasing the first layer dimensions as the weight of the object pushed on it [118]. This phenomenon appears due to a hot bed or slow cooling and solidification of the polymer [118]. In this work, it happened due to the slow solidification of PCL, whilst the bed temperature was adjusted at room temperature (25°C) and that was the lowest temperature the printer can cool.

On the other hand, elephant leg compensation minimized when 10 tablets printed together at the same time. Thus, there was enough time for cooling and solidification. As a result, tablets roundness and thickness were 10.01± 0.08 mm and 2.48±0.03 mm respectively.

Regarding roundness, which calculated according to equation 11, all the tablets were gently round. SR, IR, and bilayer tablets roundness were (1.00±0.00, 0.999±0.003, 1.00±0.00) while the theoretical value is 1. This indicates that FDM printed tablets were adequately circular and this technology is very precise.

$$\Psi = \frac{d1}{d2}$$

Equation 11: Roundness Equation

Where, Ψ= Roundness, d1= diameter 1 (mm), d2: diameter 2 (mm)

Upon the thickness of the SR, IR, and bilayer tablets they were as follows (2.67±0.02, 2.75±0.04, 5.43±0.19mm). Thickness original values were 2.55mm for SR and IR tablets and 5.0mm for bilayer tablets. However, the thickness value that the printer took after the slicing was 4.95 mm as 2.40mm for the SR layer and 2.55mm for the IR layer.

Upon the diameter/ thickness ratio, it was fixed for all tablets in the safe formula with a small standard deviation. D/H deviation for SR, IR, and bilayer (3.80±0.01, 3.54±0.07, 1.87±0.07). The biggest deviation value was for SR tablet and that was due to the polymer used which was polycaprolactone because it had slow cooling and solidification and the measurements should be taken after days due to the volume shrinkage because is the semi-crystalline polymer and the crystalline part shrink and packed more than the amorphous filaments. However, the smallest deviation value

was for bilayer tablets because there was enough time for cooling while changing the filaments since the Prusa printer with one extruder used.

Consider the volume of the tablet, they were for SR, IR, and bilayer (220.18±5.29, 206.02±4.08, 437±11.79 mm³) while the original volume of SR and IR tablets was 200.18 mm³ and for bilayer 392.50 mm³. As observed, there was a significant difference in SR and Bilayer tablets volume and that was due to the slow solidification of polycaprolactone. That occurred due to the crystallization phenomenon considering the crystalline structures are more packed and ordered. Thus they occupied less volume in comparison with amorphous structures [119].

5.4.2   Weight variation and Hardness

Corresponding to the Weight variation of the tablets (from 130 mg to 324mg) in the European Pharmacopeia (EP) and the United States Pharmacopeia (USP), "not more than two of individual tablet mass can deviate more than 7.5% from the average mass and none can deviate more than 15%". In this work, all tablets (n=10) passed the test and none of the tablets exceed the limit as shown in Table 15. Since the average weight and standard deviation of SR, IR, and bilayer tablets are (225.2±3.5, 168.6±6.4, 418.4±8.9mg) where the upper and lower limits are (208.3-242.0, 155.9-181.2, 387.0-449.8 mg) respectively.

Table 15: Weight variation data for SR, IR and bilayer tablets

	SR	IR	Bilayer
Tablet No	Tablet weight (mg)	Tablet weight (mg)	Tablet weight (mg)
1	226.7	170.6	428
2	218.9	160.2	428.1
3	225.3	160.8	400.5
4	227.3	176.1	421.4
5	227.9	171.1	420.5
6	220.6	168.4	421
7	222.1	161.3	415.2
8	225.6	165.6	411.6
9	228.3	177.3	410.3
10	228.9	174.3	427.2
average	225.16	168.57	418.38
Stdev	3.46	6.39	8.98
RSD%	1.54	3.79	2.15
Upper limit	242.05	181.21	449.76
lower limit	208.27	155.93	387.00

It was found that different materials, process, and machine parameters affect the uniformity of the dose. For example, the rheology behavior of the filament, the nozzle temperature, the printing speed and the level of the bed [120]. Furthermore, the printing speed is the most important factor [120].

As shown in table 10, it was noticed that the IR tablets had higher RSD% value compared with SR tablets. In this work, all processes and machine parameters were fixed during the printing process. However, the rheology of the filament was not studied due to time limitations.

Melt flow index (MFI) is a term that describes the facilitate flow of the thermoplastic material in ten minutes at a fixed processing temperature and it expresses the rheology behavior of the material [121].

From observation, it was found that the MFI rate of MPT: Eudragit EPO: POLYOX^{TM} (25:52.5:22.5%, w/w/w) filament was lower than MPT: Capa® 6506 (40:60%, w/w) filament. This was corresponding to less branching or/ and high molecular weight of the polymers[122]. This issue can be modified after measuring the MFI of the filaments then choosing the appropriate nozzle diameter [120].

Despite that, all the printed tablets were within the upper and lower limits of the weight variation test and all the results accepted. This leads to taking into

consideration all the material, process and machine parameters while printing individualized medicine.

Regards hardness tests, hardness can be defined as the "breaking force of a tablet" [123]. Materials deformation can be elastic, plastic and brittle fracture [124]. In this work, tablets were not broken using the hardness tester and that was due to the plastic deformation of the tablets. Instead, an Indentation hardness test should be applied which defined as "resistance of the material to plastic deformation" [124]. Indentation hardness can be determined by dividing the impact energy over the volume of indentation [124].

5.4.3   Tablets Friability

Shock and friction are the main forces that lead to tablets breaking, chipping, and capping. Thus a friability test was done to determine the ability of tablets packaging, handling, and shipping [125]. Tablets pass the friability if they are not cracked, broken, or cleaved and the weight loss was not greater than the estimates targeted value. Otherwise, the test should be repeated twice and the average weight loss of three trails should not exceed 1.0% [126].

In this work, all the SR, IR, and bilayer tablets pass the friability test (see table 16). The tensile strength of the tablet plays an important role in the friability test. Because

tablets which passed the friability test should have tensile strength ≥2Mpa [127].

Tensile strength calculated through the following equation (see equation 12) [128].

$$T = \frac{2*9.8*H}{\pi*Ld*Lt}$$

Equation 12: Tensile strength Equation

Where, T: tensile strength (Pa/mm^2), H: Hardness (Pa), L_d: Tablet diameter(mm), L_t: Tablet thickness(mm)

The tensile strength cannot be calculated because the tablets were ductile (present plastic deformation then fracture). Thus, they were not broken in the hardness test, at a constant speed of 0.35mm/s with a force up to 800 N.

Generally, 3D printed tablets are more intact than tablets produced by traditional methods because of the thermoplastic polymers that yield ductility. In his work, it was noticed that mono tablets have approximately zero weight loss, but the friability percentage for bilayer tablets was larger than mono tablets.

That was happened due to the interfacial adhesion between the two polymers, where adhesion can be defined as the intermolecular and interatomic interaction between two surfaces [129]. Poor adhesion leads to brittle tablets, whereas the interfacial adhesion increases when the two polymers have the same properties as hydrophilicity [129], [130]. Polar functional groups can achieve good adhesion [131]. And adhesion can be estimated by torsion and shear tension tests [132].

Table 16: Tablets Friability

Formulation	Friability (%)
SR tablet using MPT: Capa® 6506 (40:60%, w/w) filament	0.00000%
IR tablets using MPT: Eudragit EPO: POLYOX^{TM} (25:52.5:22.5%, w/w/w) filament	0.00001%
Bilayer tablets using MPT: Capa® 6506 (40:60% w/w) and MPT: Eudragit EPO: POLYOX^{TM} (25:52.5:22.5%, w/w/w) filaments	0.00014%

5.4.4   Tablets Morphology

To study the effect of printing parameters on the invitro dissolution profile and rate, three major parameters selected.

In the beginning, the effect of adding a solid layer between the infill effect studied (see Figure 51). The (a) and (c) photos present the tablet without adding solid layers, where (a) is the model in Prusa slicer software for the printed tablet and (c) is the printed tablet under the microscope.

The lack of a solid layer created a hole in the center of the tablet and tablet infill. Upon that solid layer added as shown in pictures (b), (d) and (e). Where (b) is the tablet on Prusa slicer software while (d) is the printed tablet that had a solid layer between every 1 infill layer and (e) is the printed tablet that had a solid layer every 2 infill layers. From this, it was observed that adding a solid layer can minimize the holes and channels in the tablet and that was proved when a solid layer every 2-infill layer added.

(a): No solid layer	(b): Solid layer
(c): No solid layer	(d): Solid layer every 1 layer	(e): Solid layer every 2 layers
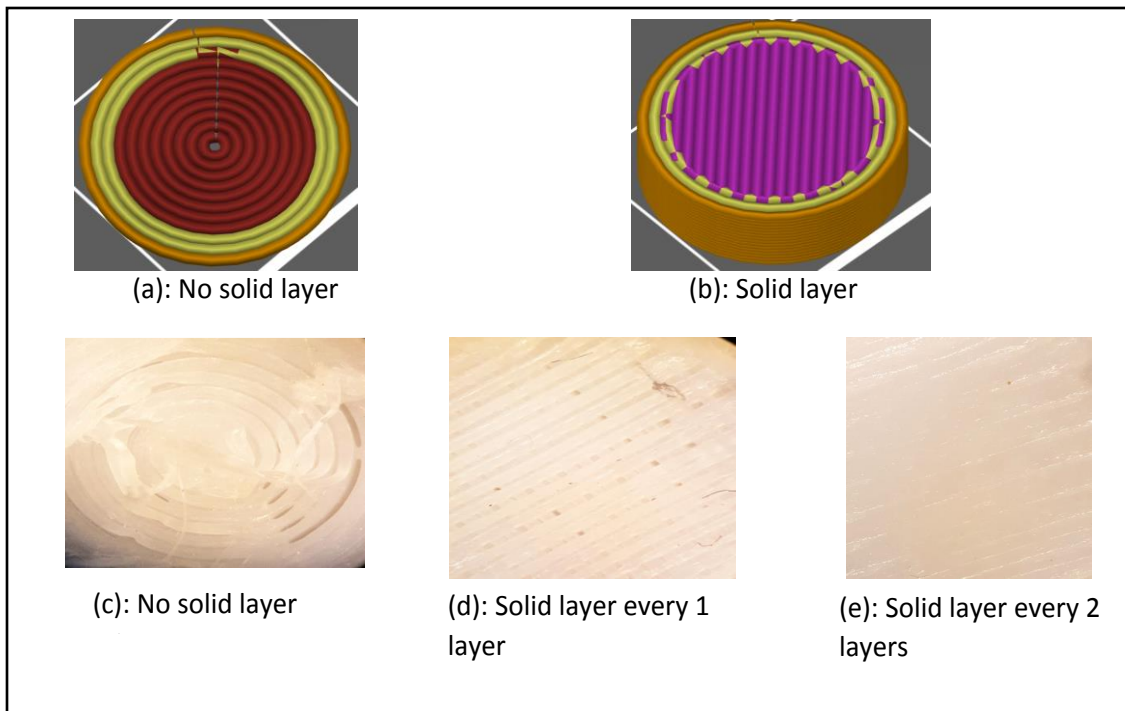
Figure 51: Effect of Solid layer under the microscope

Then, the effect of the number of perimeters studied. Thus, Tablets with one, three and five perimeters designed and sliced as shown in Figure 52 pictures (a), (b) and (c) respectively. The designed tablet printed as in pictures (d), (e), and (f). From the

resulting tablets it was observed that one perimeter is not enough since the infill

passed it and the tablet became weak (see pictures (a) and (d)). When three

perimeters used the tablet became stronger and neat (see pictures (b) and (e)).

Whereas, when five perimeters used a gap between the outer perimeters noticed and

the inner perimeters passed the infill (see pictures (c) and (f)).

(a): One perimeter	(b): Three perimeter	(c): Five perimeter
(d): One perimeter	(e): Three perimeter	(f): Five perimeter
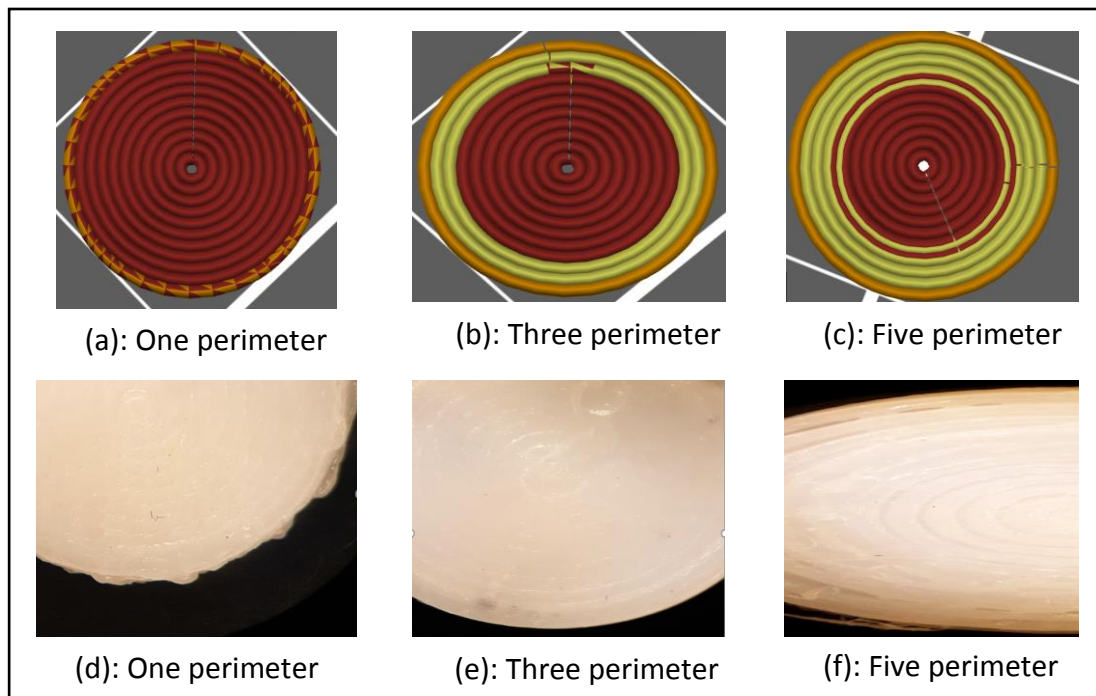
Figure 52: Effect of number of perimeters

The effect of perimeters/infill overlap percentage studied. Three tablets with (25%,

160%, and 200%) perimeters/infill overlap percentage designed and sliced as shown

in Figure 53 pictures (a), (b) and (c) respectively. From the printed tablets it was

observed that tablets with a 25% overlap percentage contained pores and channels

(see pictures (a) and (d)). While tablets with 160% overlap contained no pores or

channels and the tablet is neater and more circular (see pictures (b) and (e)). While in

contrast, tablets with 250% overlap percentage showed a rough surface due to gentle overlap between the perimeters and infill, as a result, the infill passes the perimeters (see pictures (c) and (f)).

| (a): 25% overlap | (b): 160% overlap | (c): 250% overlap |
| (d): 25% overlap | (e): 160% overlap | (f): 250% overlap |
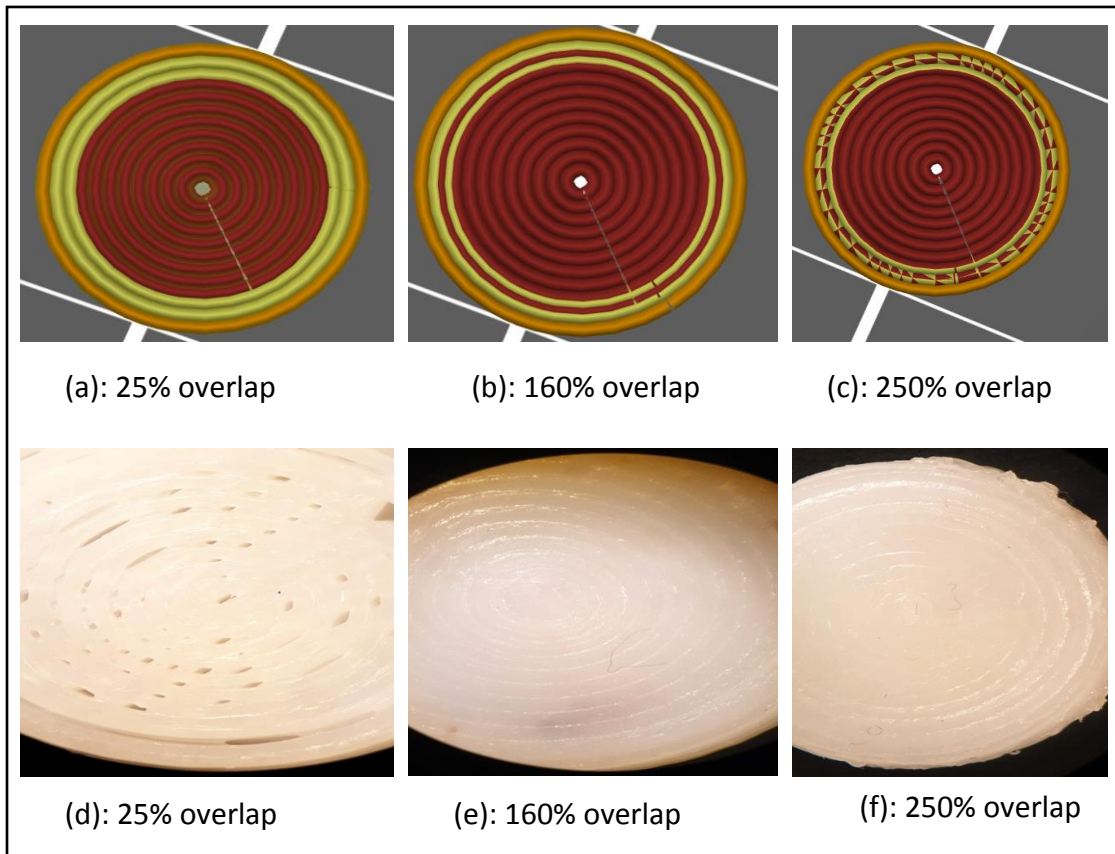
Figure 53: Effect of perimeters/infill overlap percentage

5.4.5 Content uniformity

Based on European pharmacopeia and USP test A, "the preparation complies with the test if each tablet content is between 85 and 115% of the average content. The preparation fails if more than one individual tablet is outside these limits or if one individual content outside limits of 75 -125% of the average content"[103].

In this work content uniformity done for the two printed formulations MPT: Capa® 6506 (40:60%, w/w) and MPT: Eudragit EPO: POLYOX™ (25:52.5:22.5%, w/w) respectively for n=10. All tablets pass the test as shown in Table 17 since all tablets show content uniformity between 85-115% and none of the tablets was outside the limit of 75-125%.

Table 17: SR and IR tablets content uniformity results

Formulation	Content uniformity percentage
SR tablets using MPT: Capa® 6506 (40:60%, w/w) filament	93.1± 2.1 %
IR tablets using MPT: Eudragit EPO: POLYOX™ (25:52.5:22.5%, w/w/w) filament	114.6 ± 0.7 %

However, for more accurate results L1 and L2 should be calculated. L1 and L2 are the limits for uniformity of the dose criteria they are calculated as; Average of the uniformity of the dose from weight variation and assay test, this is called the

acceptance value (L). (L) should be ≤15 for 10 tablets and that is L1. If the accepted value is > 15, the test should be repeated with 30 tablets and the accepted value (L1) should be ≤15. Moreover, the allowed deviation range should be $(1-(0.01)(L2))M \leq$ each unit dose $\leq (1+(0.01)(L2))M$ where L2=25 and M identified as following [103]

If 98.5% $\leq \bar{X} \leq$ 101.5%, then M= $\bar{X}$

If $\bar{X}$ < 95.8%, then M= 95.8%

If $\bar{X}$ > 101.5%, then M= 101.5%

Nevertheless, the results from content uniformity are within the range, but there was a loss in the sustained release formulation and exceed in immediate-release one. Different factors affected the uniformity of the dose and led to this variation.

Those factors can be linked with the blended materials, process, and machine parameters. Such as the material particle size, surface energy, surface area and loss on dry (LOD) value. Also, the blending speed, time because low speed and short blending time leads to inhomogeneity, while fast speed and long bending time lead to overmixing that induce segregation and de-mixing.

Moreover, the volume of the physical mixture inside the blender is important because too large quantity leads to avoid mixing, while small quantity leads to a distribution of the particles thus poor mixing [133]. As well as, the type of mixer that is used and different systematic and random errors.

In this work, all the previous reasons might affect the results plus in the SR formulation, there was a loss from the material when it was blended and transferred from the blender to the extruder. Moreover, the API used in the formulation was not pure (see DSC section). However, in IR formulation there was more than 100% API in the tablets and that was due Eudragit that used in the formula which is sticky and dusty powder thus most of it lost in the feeder and extruder.

Results from this work support Katstra et al. work who stated solid dosage forms manufactured by 3D printing technology demonstrate better content uniformity compared with traditional technologies [59],[134].

5.4.6 Differential Scanning Calorimetry

The solid-state of the oral solid dosage form indicates an important factor for the finished product. The dissolution rate of amorphous drugs faster than crystalline ones because they need less energy to break the bonds. Neither the less, the stability of crystalline drugs is higher compared with amorphous ones [72],[135].

Despite the slow dissolution rate in crystalline solids, which is not recommended in an immediate-release formulation, researchers tried to keep the crystallinity percentage as high as possible in all formulations to avoid stability problems [135].

To determine the melting enthalpy of the drug, the maximum temperature should be above the T_m, T_g of the substance. For all formulas, the cycle starts at -20°C and ends

at 150°C. because the T_g, T_m, and T_d of the used materials are as shown in Table 18 whereas the results found in Table 19.

Table 18: Theoretical Tg, Tm, and Td for substances used in DSC

Substance	T_g (°C)	T_m (°C)	T_d (°C)
MPT	1.2	120	155
CAPA® 6506	-60	60	NA
Eudragit EPO	57	NA	250
POLYOX™	NA	66-75	197

Table 19: DSC results for pure MPT, physical mixtures, filaments and tablets for both SR and IR

	Melting point (°C)	Enthalpy (Jol/g)	Crystallinity %
MPT powder	114.76	92.11	
MPT: CAPA® 6506 (40:60%, w/w) P.M	115.91	35.68	96.84%
MPT: CAPA® 6506 (40:60%, w/w) Filament	112.49	35.70	96.89%
MPT: CAPA® 6506 (40:60%, w/w) Tablet	95.42	34.94	94.83%

MPT: Eudragit EPO: POLYOX^TM (25:52.5:22.5%, w/w) Filament	110.82	2.271	9.86%
MPT: Eudragit EPO: POLYOX^TM (25:52.5:22.5%, w/w) Tablet	117.98	1.541	6.69%

The melting point and enthalpy of Metoprolol tartrate were 114.76°C and 92.11 Jol/g, respectively (see table 19). Where T_m and ΔH values reported in the literature for MPT were 120°C and 100 Jol/g [102],[136].

In this work, even though the analysis repeated three times, it was observed that MPT used was not completely pure, because the obtained peak was not sharp and there was a shift in the T_m and enthalpy as well. Since impurities could shift the melting point to a lower value.

Two reasons could be behind this issue; the first one the raw material was not pure and the second one there was degradation in MPT because it is a photosensitive product. To determine that, DSC should be done for the original raw material. Figure 54 presented the DSC curve for Metoprolol tartrate.
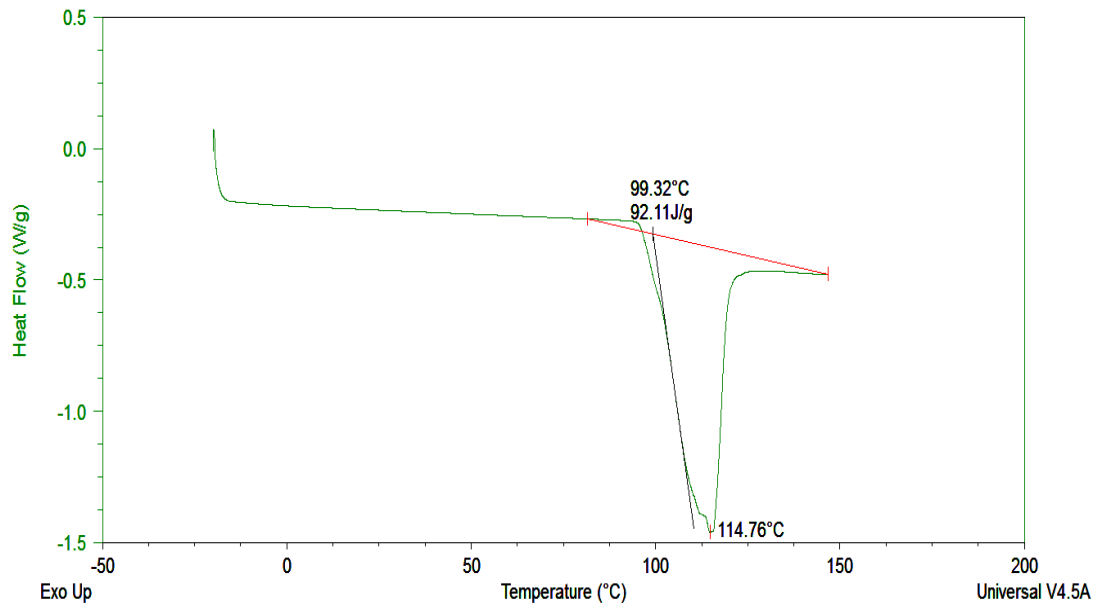
Figure 54: DSC for MPT

Upon MPT: Capa® 6506 (40:60%, w/w) physical mixture, it was observed that there was a loss on crystallinity (see Table19). The crystallinity percentage was 96.84%. There should not be a loss in crystallinity in the physical mixture because it was not faced with temperature. However, that loss might be due to API fraction during heating in the DSC apparatus[137]. Figure 55 presented the DSC curve for MPT: Capa® 6506 (40:60%, w/w) physical mixture.
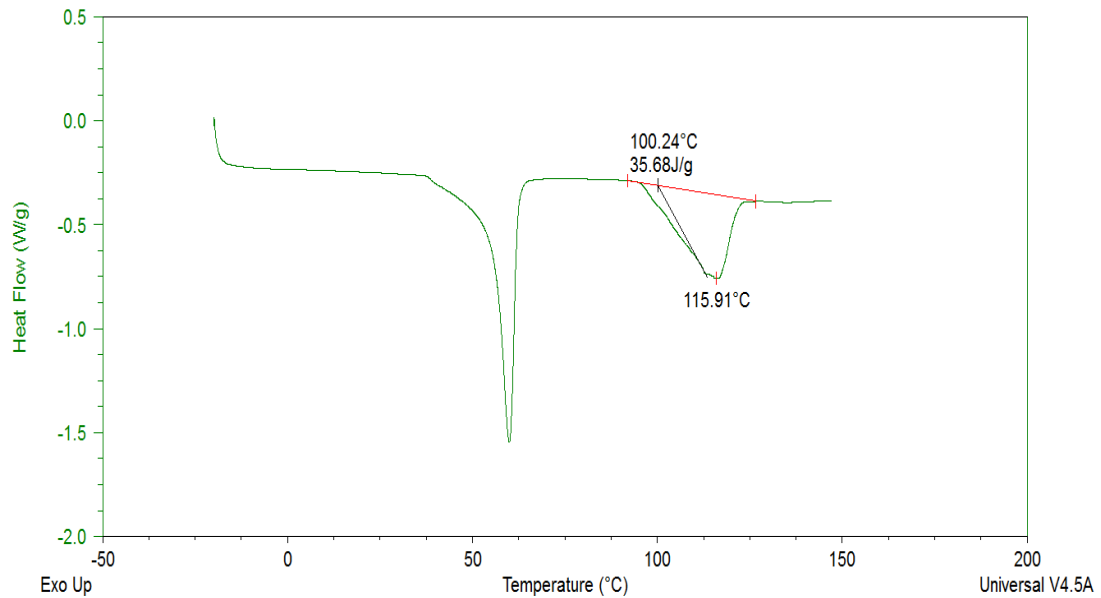
Figure 55: DSC for MPT: Capa® 6506 (40:60%, w/w) Physical mixture

After that, DSC had done for MPT: Capa® 6506 (40:60%, w/w) filaments, due to heat used in HME. The crystallinity percentage was 96.89% (see table 19). It was observed that there was no loss in crystallinity since there was no critical difference between the enthalpy value of the P.M and filaments.

That happened because the extrusion processing temperature had done below the MPT melting point. On the other side, a shift in the melting point happened and a wide peak obtained due to impurities. Figure 56 presented the DSC curve for MPT: Capa® 6506 (40:60%, w/w) filaments.
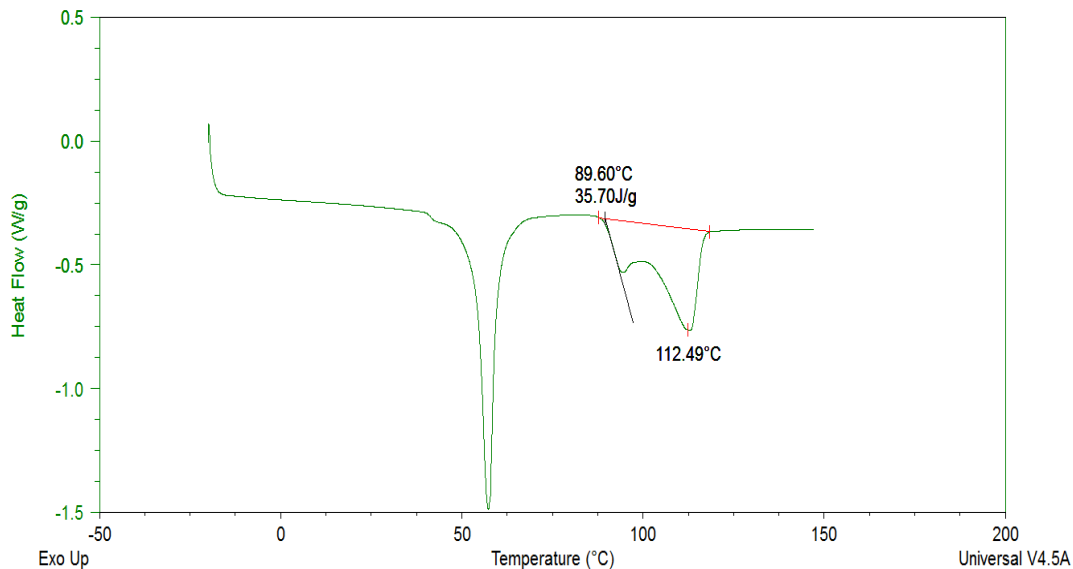
Figure 56:DSC for (MPT: Capa® 6506 40:60%, w/w) Filaments

Later, DSC had done for MPT: Capa® 6506 (40:60%, w/w) tablet, due to heat used in the FDM process. The crystallinity percentage was 94.83% (see table 19). It was observed that there was a small amount of loss in crystallinity but it was not critical. Since the difference between the enthalpy value of the P.M, filament, and tablets is 2.07% and 2.11% respectively.

That loss happened due to the printing temperature used in the FDM. It was 110°C and it was around the T_m of the pure MPT that is used in this work which was 114.76°C. Moreover, there was a significant shift in the T_m due to the impurities. Figure 57 presented the DSC curve for MPT: Capa® 6506 (40:60%, w/w) filaments.
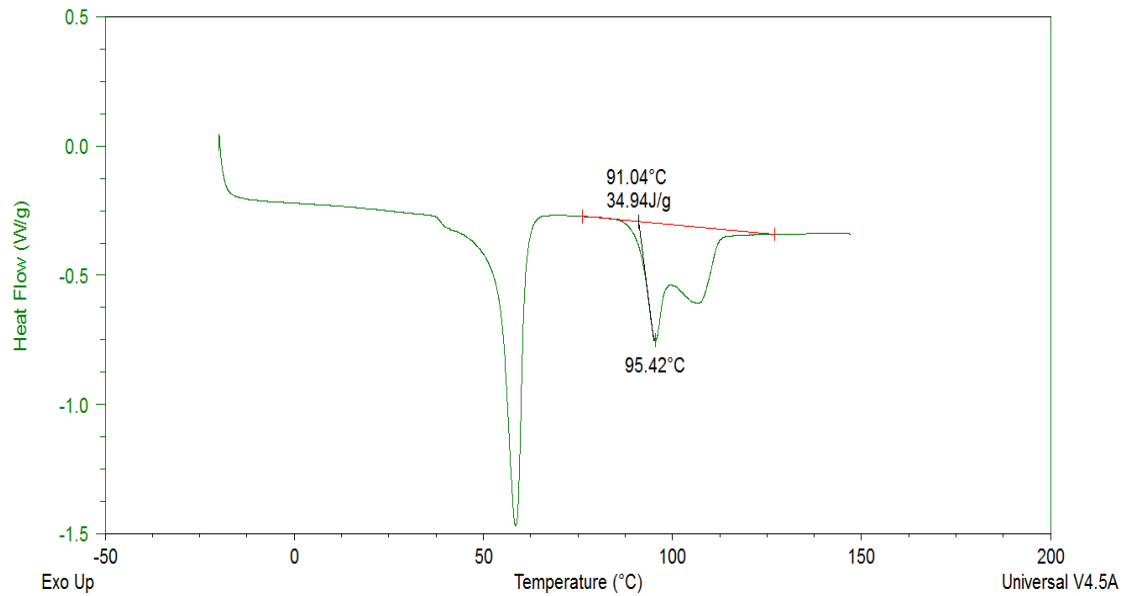
Figure 57: DSC for (MPT: Capa® 6506 40:60%, w/w) Tablet

The below Figure 58 showed the pure MPT, (MPT: Capa® 6506 40:60%, w/w) physical

mixture, filament, and tablet for comparison.
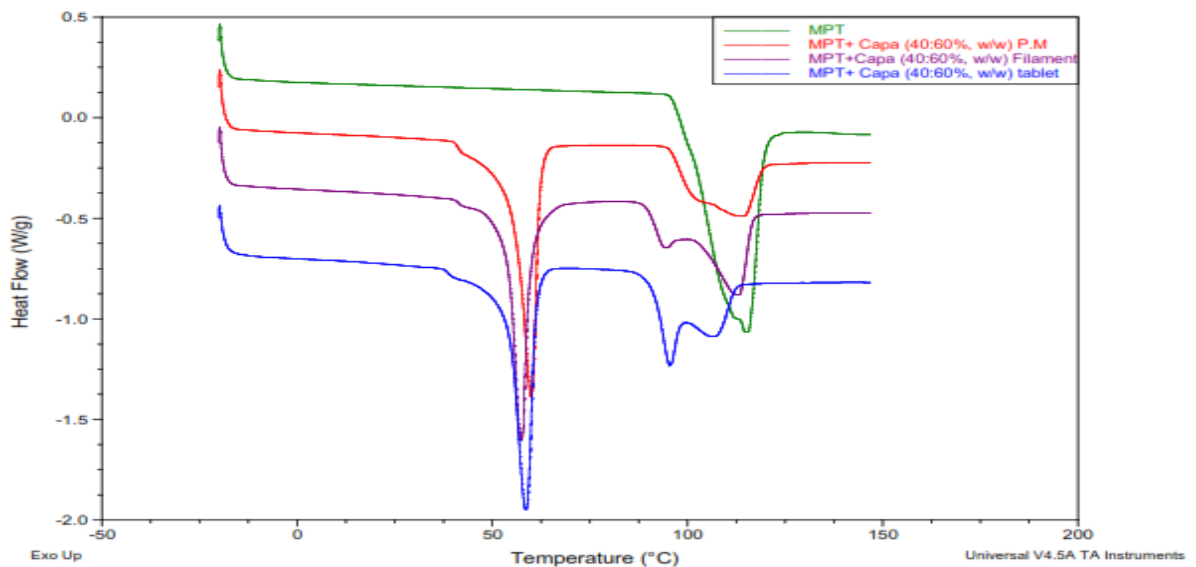
Figure 58: DSC curves for MPT powder, MPT: Capa® 6506 (40:60%, w/w) filaments and tablets

Besides, DSC had done for Immediate release formulation. MPT: Eudragit EPO: POLYOX™ (25:52.5:22.5%, w/w/w) filaments and tablets crystallinity calculated (see table 19). It was observed that the crystallinity percentage decreased below 10%. Because the extrusion processing temperature and printing temperature were above the T_m of Metoprolol Tartrate >120°C. Thus, solid dispersion occurred, where solid dispersion means that the API spread between the matrix of the polymer, and that led to an increase in the solubility, thus the in-vitro release rate and bioavailability [137].

Figures 59 and 60 presented the DSC curves for IR formulations. While Figure 61 presented Pure MPT, MPT: Eudragit EPO: POLYOX™ (25:52.5:22.5%, w/w/w) filaments and tablets DSC curves for comparison.
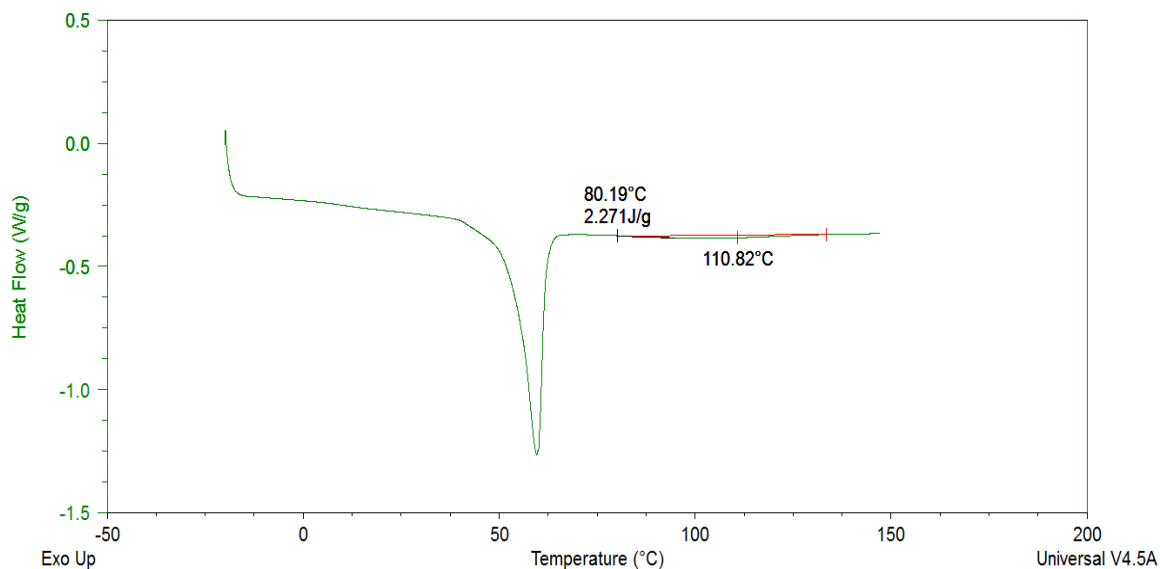
Figure 59:DSC for MPT:Eudragit EPO: POLYOX™ (25:52.5:22.5%, w/w) Filament
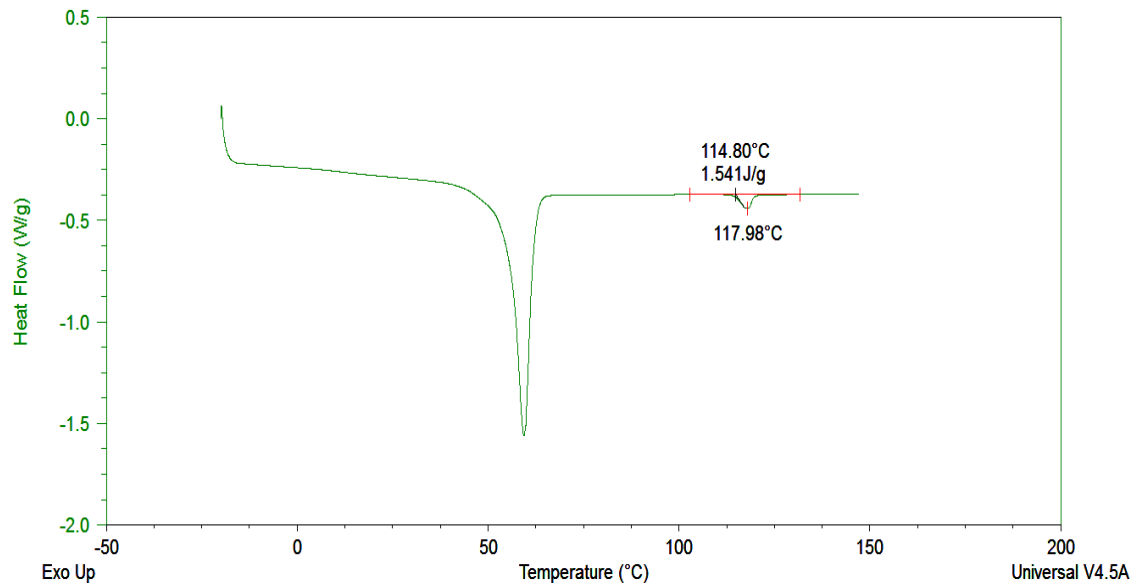
Figure 60: DSC for (MPT: Eudragit EPO: POLYOX^{TM} 25:52.5:22.2%, w/w) Tablet
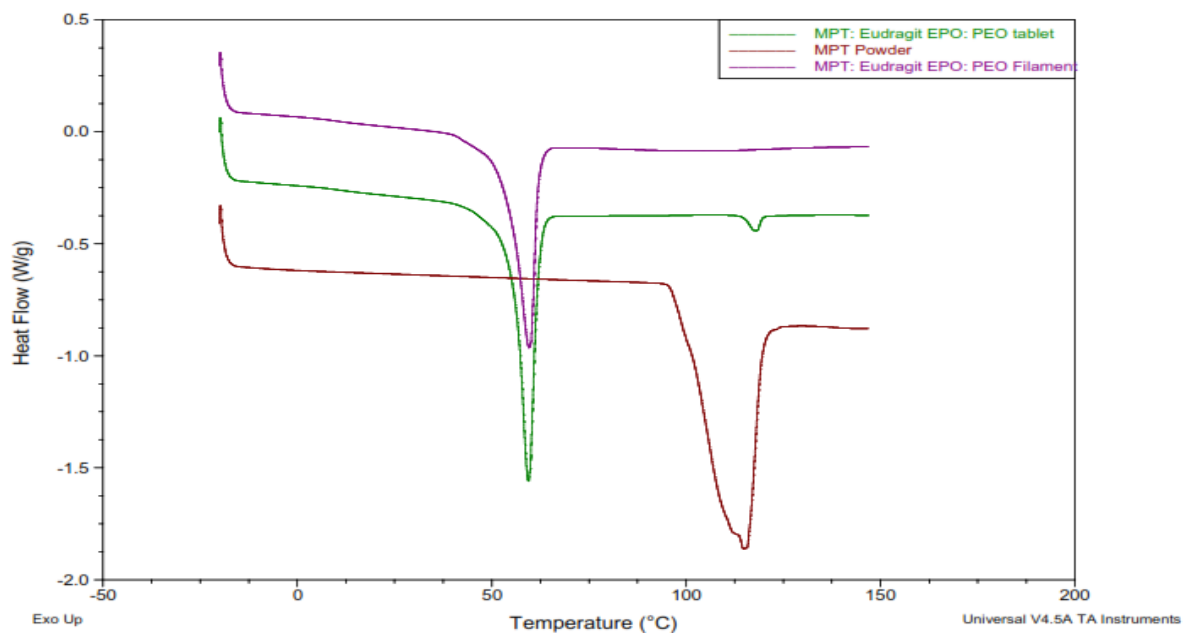
Figure 61: DSC curves for MPT powder, MPT: Eudragit EPO: POLYOX^{TM} (25:52.5:22.5%, w/w) filaments and

Tablets

5.4.7 Disintegration test

Disintegration test performed for IR formulation tablets (MPT: Eudragit EPO: Polyox N10 25:52.5:22.5%, w/w/w) and it was found that all the tablets (n=6) disintegrated in less than 10 min.

5.4.8 In Vitro Dissolution

In vitro dissolution performed to study the drug release rate and release profile for sustained release, immediate release, and bilayer tablets.

To achieve desired drug release profiles for Metoprolol Tartrate, different printing trials implemented using (MPT: Capa® 6506 40:60%, w/w) as a model filament to study the effect of printing parameters on the drug release. Figure 63 presented the best curve for SR formulation (see table 4 for printing parameters). This curve was semi linear and the drug released within 94.11% within 24 hours. Where the tablets stay in their original shape and dimensions before and after the dissolution test, no swelling or disintegration happened (as shown in figure 62).

Figure 62: MPT: Capa (40:60%, w/w), before and after dissolution
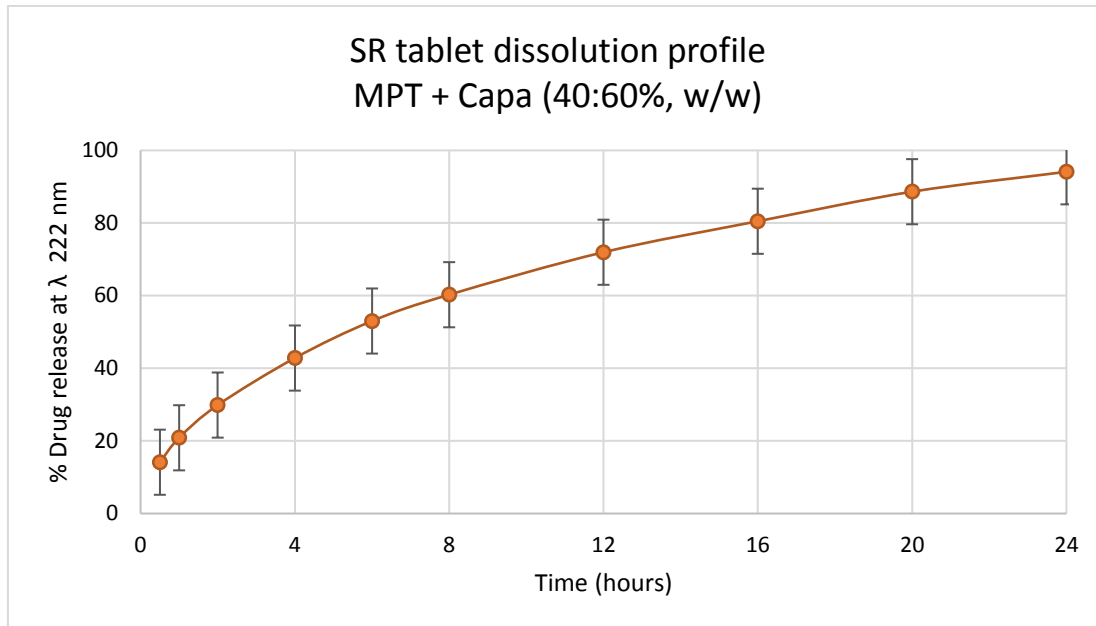
Figure 63: SR MPT: Capa® 6506 (40:60% w/w) Tablet dissolution profile, (n=3)

It was a challenge to use MPT for sustained release formulation since it is a class 1 drug that has high solubility and permeability. Ordinarily, metoprolol succinate used for sustained release formulations because metoprolol tartrate biological life is 4-5 hours, so multiple doses should be taken through the day [98], [138].

To get the best release rate and profile different printing parameters modified, printed tablets observed under the microscope (see tablet morphology section) and then dissolution test implemented to study the effect of the number of perimeters, adding solid layer and perimeters/infill overlap percentage.

Number Perimeter effect: it was observed in figure 64 that an increasing number of perimeters decreasing the dissolution rate. As tablets with three perimeters were

slower in dissolution than those which had 2 two perimeters. However, increasing

the number of perimeters more than three led to the opposite effect. Since with an

increasing number of perimeters, creating more space between them as observed

under the microscope (see tablets morphology section).

Differences factor (f1) and similarity factor (f2) applied. "Dissolution profiles consider

similar and bioequivalence if f1 is between 0 to 15 and f2 is between 50-100". F1 and

f2 can be calculated using the following equations;

$$f_1 = \left\{ \frac{\sum_{t=1}^{n} |R_t - T_t|}{\sum_{t=1}^{n} R_t} \right\} X100$$

$$f_2 = 50 \log \left\{ \left(1 + \frac{1}{n} \sum_{i=1}^{n} (R_t - T_t)^2 \right)^{-0.5} X100 \right\}$$

Equation 13: differences factor (f1) and similarity factor (f2) equations

Where, "n is the number of time points, Rt is the dissolution value of reference

product at time t and Tt is the dissolution value for the test product at time t".

It was found that tablets with 3 walls were similar and bioequivalence to tablets with

2 walls, and tablets with 2 walls were similar and bioequivalence to tablets with 5

walls (see table 20). Also, there was overlap in the error bars of the curves.

MPT + Capa (40:60% ,w/w)
Effect of number of walls on the drug release
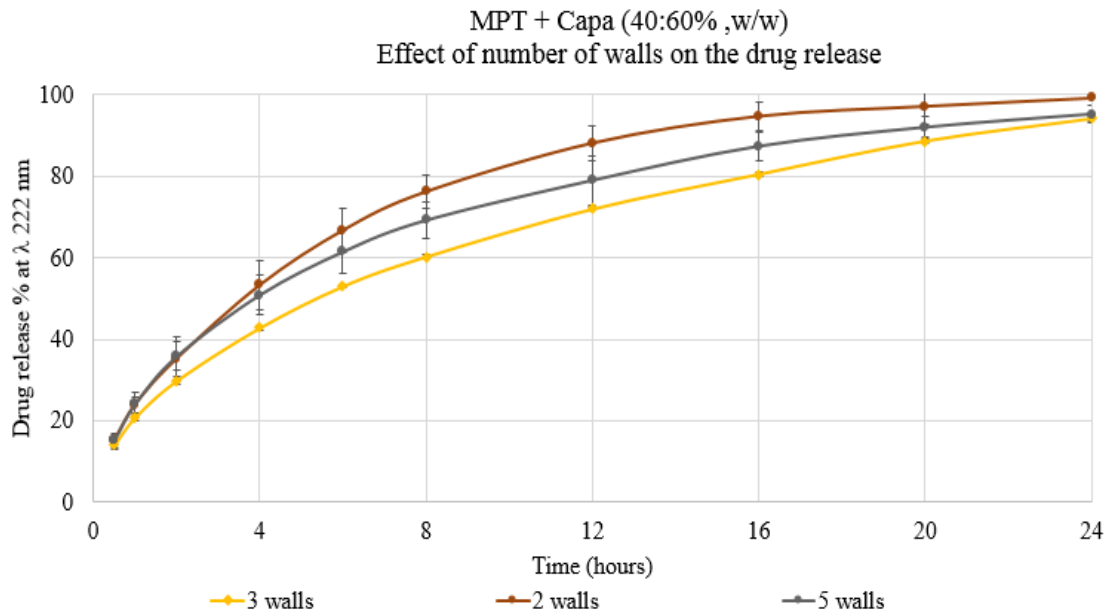
Figure 64: Number of perimeters effect on dissolution, (n=3)

The number of solid layers effect: it was observed in figure 65 that an increasing number of solid layers led to a decrease the rate of dissolution. And from f1 and f2 it was observed that they were not similar and bioequivalence (see table 20).
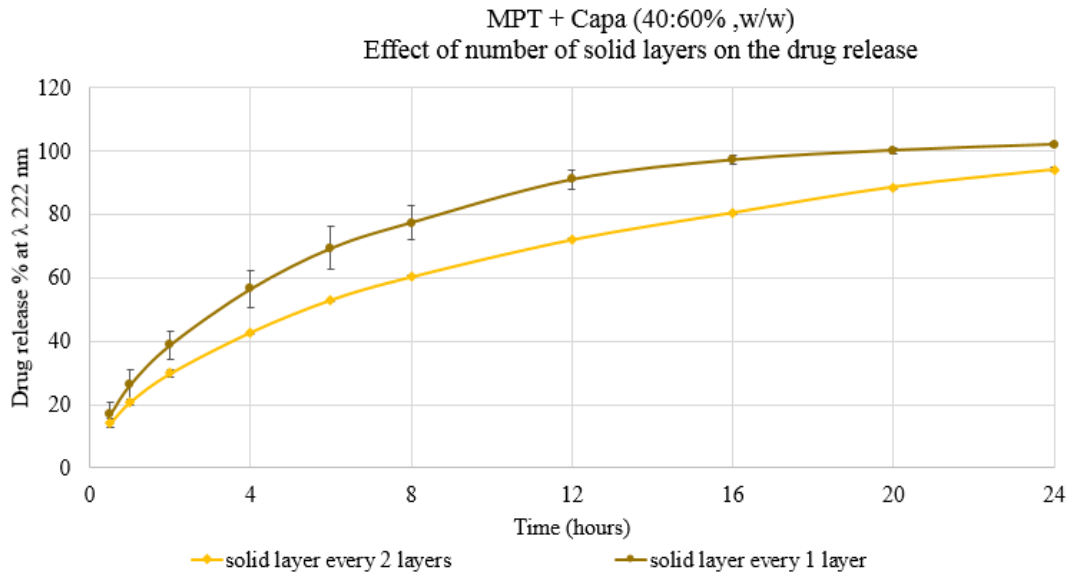
Figure 65: Number of solid layers effect on dissolution, (n=3)

<u>Overlap percentage effect:</u> it was observed in figure 66 that increasing perimeters/infill overlap percentage led to an increase in the bonding between the perimeters and infill. However, it showed over extrusion that decreased the effect of the perimeter. Thus, faster drug release obtained. F1 and f2 calculated and it was observed that tablets that have perimeters/infill overlap with a percentage of 200% were similar and bioequivalence to tablets that have perimeters/infill overlap with a percentage of 250%, (see table 20).
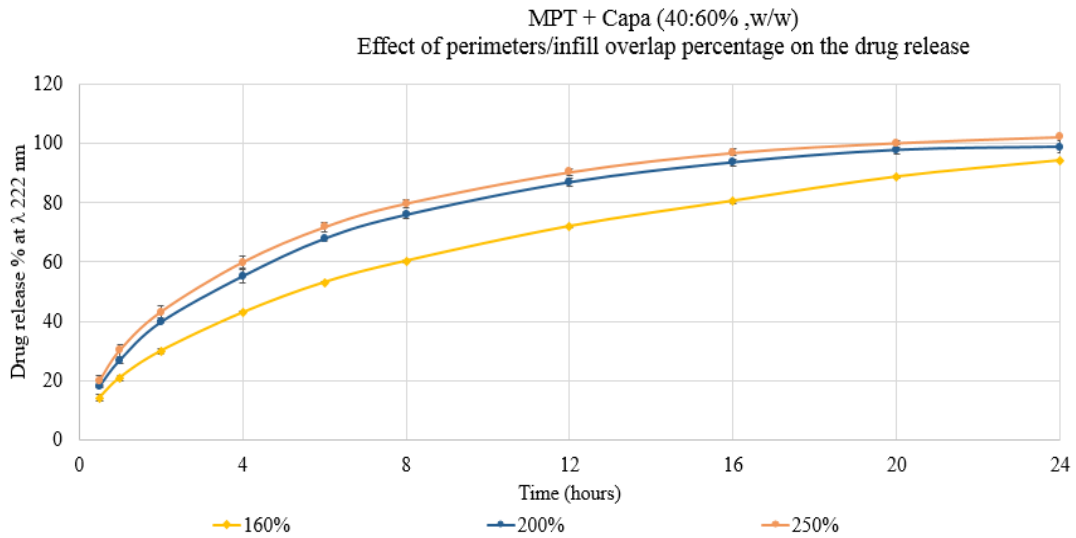
Figure 66: Overlap effect on dissolution, (n=3)

Table 20: differences and similarity factors of dissolution curves

Case	F1	F2	Results
Number of solid layers	21.533	44.115	Not similar and bioequivalent
Number of walls3-2	16.923	48.306	Not similar and bioequivalent
Number of walls 3-5	9.830	60.270	similar and bioequivalent
Number of walls 2-5	6.317	64.135	similar and bioequivalent

Overlap 160-200	18.597	47.553	Not similar and bioequivalent
Overlap 160-250	24.709	41.8447	Not similar and bioequivalent
Overlap 200-250	5.153	71.998	similar and bioequivalent

Based on the above results, tablets with 100% infill, 160% perimeters/infill overlap, 5 top and 5 bottom layer, 3 perimeters, and 0.15mm layer height, solid layer every 2 layers, concentric infill pattern and 0.6mm elephant leg compensation with printing speed 80mm/s was chosen as the best formula for SR tablets. Since it achieved a semi-linear curve and slowest dissolution rate 94.11% of the drug released within 24 hours.

For Immediate release tablets two formulas printed (MPT: Klucel EF 25:75% w/w) and (MPT: Eudragit EPO: POLYOX^{TM} 25:52.5:22.5% w/w) then dissolution test performed for them. Both formulations printed with the same parameters with 50% infill, 25% perimeters/infill overlap,3 top and 3 bottom layer, 2 perimeters, and 0.15mm layer height, solid layer every 0 layers, grid infill pattern and 0.6mm elephant leg compensation was chosen as the best formula for IR tablets. However, MPT: Klucel (25:75%, w/w) filament printed at lower speed 20mm/s compared with MPT: Eudragit EPO: POLYOX^{TM} (25:52.5:22.5% w/w) Filament that printed at 80mm/s.

Compared with Sustained release formulation, in immediate-release, the infill pattern changed from concentric which is the most complicated infill pattern with lowest gaps and channels to Grid infill pattern that has the most gaps/holes and channels. Moreover, the overlap percentage was reduced to adjust the dose and the infill ratio to achieve faster dissolution.

MPT+ Klucel EF (25:75%, w/w) had slower dissolution rate approximately 100% of the drug released within 1 hour as shown in Figure 67.
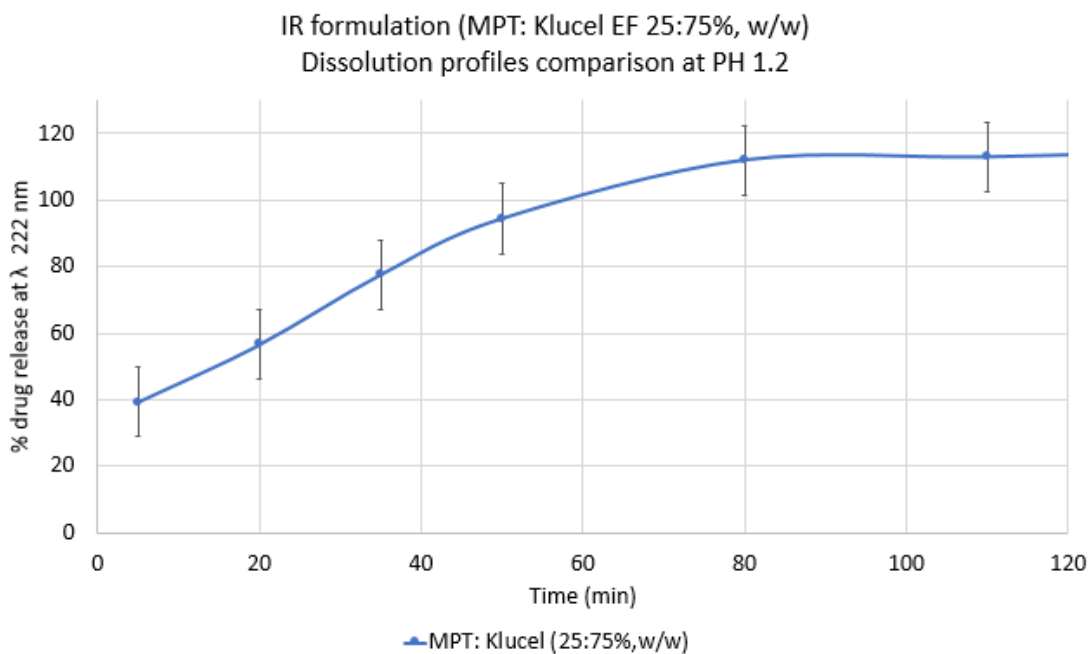
Figure 67: MPT: Klucel EF (25:75%, w/w) dissolution profile, (n=3)

While MPT: Eudragit EPO: POLYOX™ (25:52.5:22.5%, w/w) showed complete drug release within 15 minutes as shown in Figure 68. That happened because Eudragit

EPO was more hydrophilic so it dissolved faster. Since Eudragit EPO has the dimethyl aminoethyl group that can ionized, resulting fast solvation of the polymer in the low PH [84]. As well as due to its amorphous phase, since it had crystallinity percentage less than 10% as shown from the DSC curves (see figure 61).
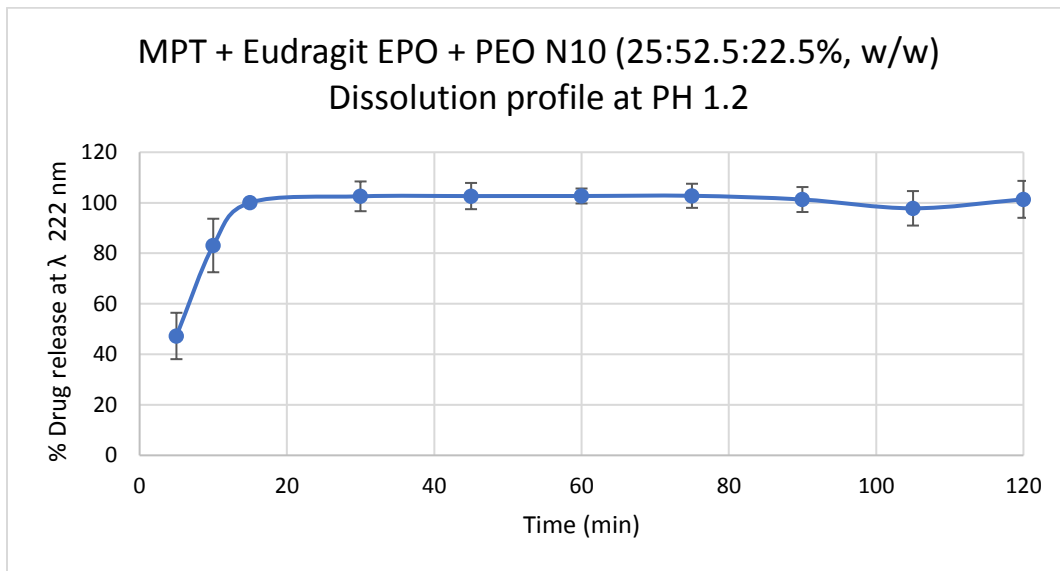
Figure 68: MPT + Eudragit EPO + POLYOX^M (25:52.5:22.5%, w/w) Dissolution profile, (n=3)

A comparison between the two IR formulation presented in Figure 69. It was clear that using Eudragit, which is one of the most hydrophilic polymers, and POLYOX™ as a pore former in the formula beside the solid dispersion technique resulted a fast drug release.
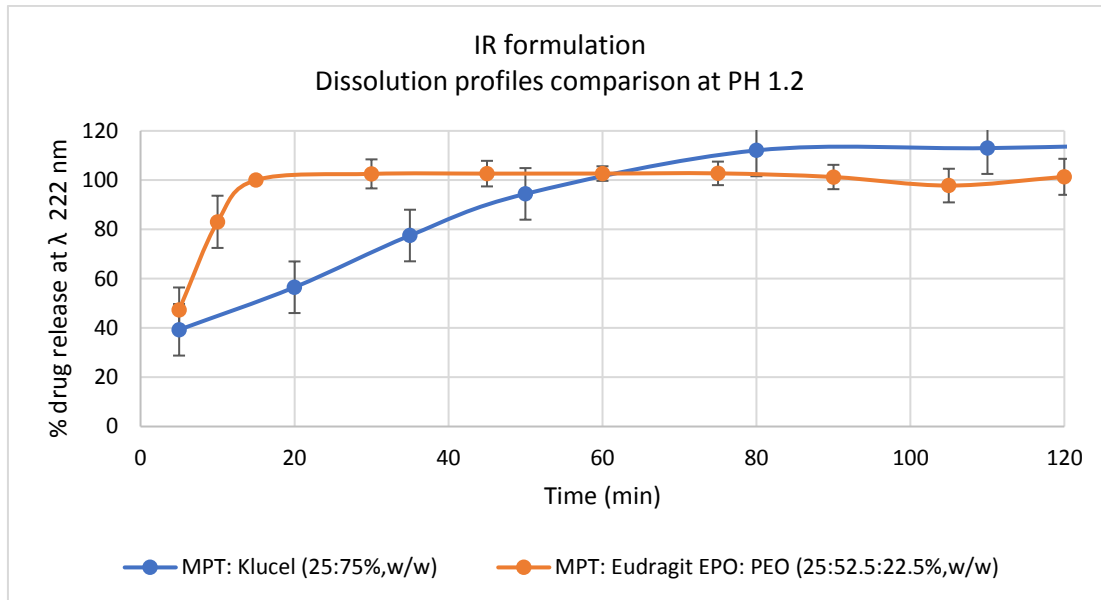
Figure 69: Immediate-release tablets dissolution profile, (n=3)

After the sustained and immediate release formulation selected. Bilayer tablet printed from MPT: CAPA® 6506 (40:60%, w/w) and MPT: Eudragit EPO: POLYOX™ (25:52.5:22.5%, w/w/w) filaments and in-vitro dissolution test applied.

Metoprolol tartrate from bilayer tablets released with 87% within 24 hours as shown in figure 70. Where HCl buffer with PH 1.2 used in the first two hours then it was substituted with phosphate buffer PH 6.8 for 22 hours.

It was observed that 40% of the API released within the first hour as a loading dose and that was matched with the release from each curve of the mono tablet. since in IR tablets all the API released within 16 min so 25% MPT released in the first hour, regards SR tablets 20% of MPT released within the first hour. Thus, the total release

from the two mono tablet curves was 45% while it was 41.6% from the bilayer tablet. Considering that the surface area for water penetration of the bilayer tablet is smaller than the mono tablets.

Considering the release in the second hour, it was 55% from the mono tablets (25% from the IR and 30% from the SR) where it was 56% from the bilayer tablet. Also, it was 87% from the mono tablets (25% from the IR and 53% from the SR) while it was 65.2% from the bilayer tablet. Considering that the surface area of the bilayer tablet is smaller than the mono tablets. Since the water penetrate the mono tablet from four sides, but the bilayer tablet from three sides since the fourth side covered with the other layer.
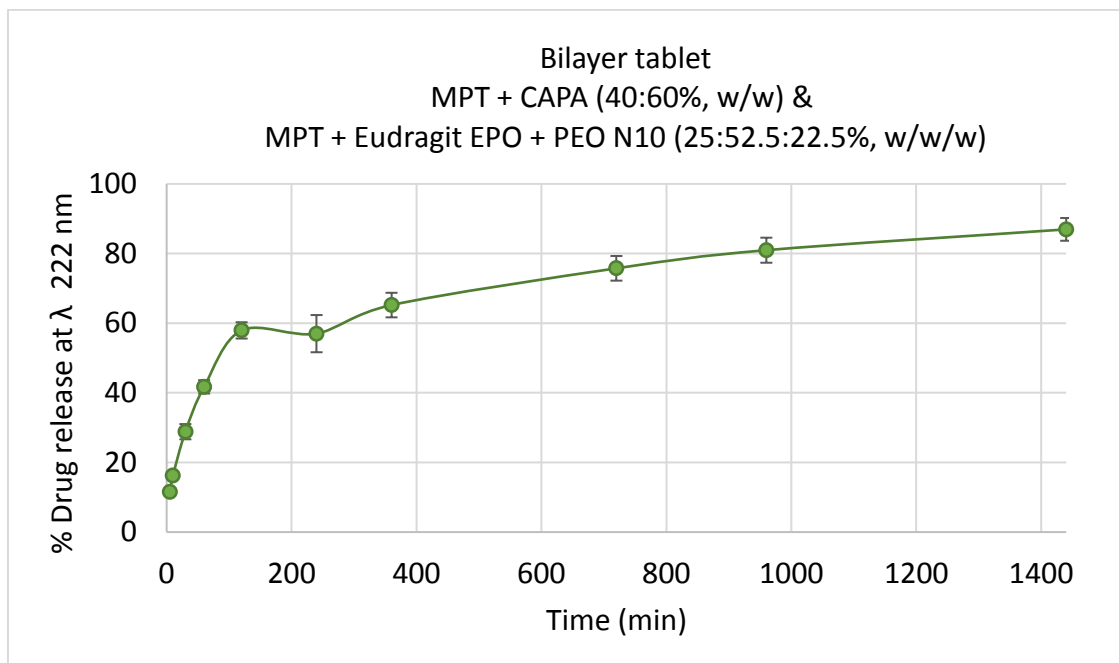
Figure 70: Bilayer tablet dissolution profile, (n=3)

On the other side, in vitro dissolution test for MPT: Capa® 6506 (40:60%, w/w) tablets in acidic medium PH1.2 applied. It was found that 64% of the drug released within the first two hours (see figure71). It indicated a fast drug release compared with using phosphate buffer (PH 6.8) since approximately 30% was released within the first two hours (see figure 63).
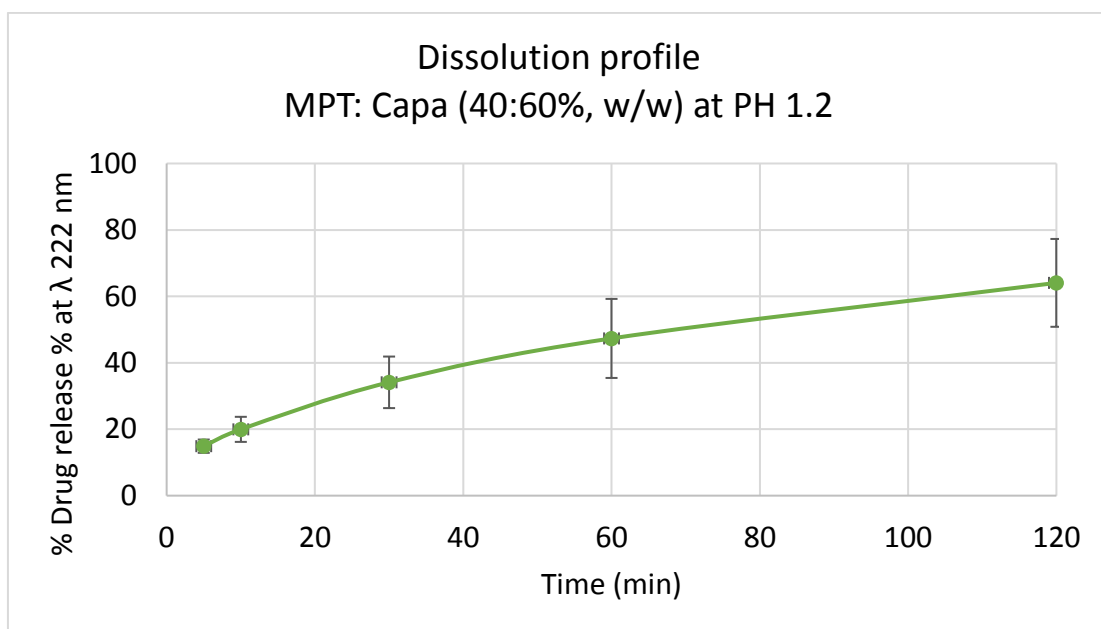
Figure 71: Dissolution profile of MPT: Capa® 6506 (40:60%, w/w) at PH 1.2,(n=3)

That might happen due to the decomposition of polycaprolactone filament since it became carboxylic acid at PH <3. Mechanism of polycaprolactone degradation in acidic media shown in figure 72. Or because the MPT pKa (strongest acid) 14.09 and pKa(strongest base) 9.67 [139]. Thus, more investigation is needed.
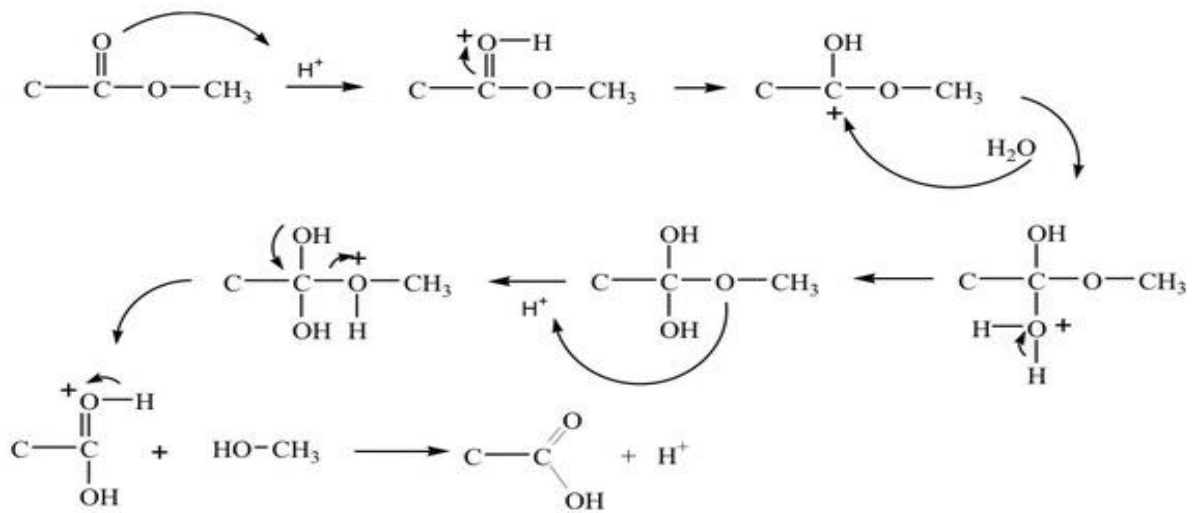
Figure 72: polycaprolactone degradation in acidic media PH <3

5.4.9 Dissolution kinetics

To study the mechanism of Metoprolol tartrate release kinetics in vitro dissolution for sustained release mono tablets. Data fitted at the following models: zero and first orders, Higuchi, Hixson- Crowell and Korsmeyer- Peppas. The correlation coefficient value (R^2) used to determine the best model that the formula fitted in. Table 21 showed the tablets' results.

It was observed that sustained-release formulation followed Korsmeyer- Peppas. It means that the drug released in the diffusion mechanism with anomalous release model due to coupled diffusion and/or relaxation of the polymer [108],[140].

Also, the release mechanism of the drug studied when the printing parameters changes such as the perimeters/infill overlap percentage, number of perimeters, and

number of solid layers ([see in vitro dissolution section]). From the obtained results it was found that increasing the overlap percentage led to change the release mechanism from anomalous release model to Fickian diffusion release model as shown in table 22.

On the other hand, it was observed that the number of perimeters and number of solid layers had no effect on the release kinetics since all of them followed anomalous release model as shown in tables 23 & 24.

Table 21: Kinetics data for MPT from SR tablets

	Zero-order		First- order		Higuchi		Hixson- Crowell		Korsmeyer- Peppas	
	Y equation	r^2	Y equation	r^2	Y equation	r^2	Y equation	r^2	n	r^2
SR	Y=3.32x+24.97	0.9240	Y=0.067x+3.22	0.7604	Y=0.50x+3.00	0.9893	Y=0.080x+2.94	0.8250	0.49	**0.9967**

Table 22: Effect of overlap percentage on the release kinetics

	Zero-order		First- order		Higuchi		Hixson- Crowell		Korsmeyer- Peppas	
	Y equation	r^2	Y equation	r^2	Y equation	r^2	Y equation	r^2	n	r^2
160%	Y=3.32x+24.97	0.9240	Y=0.067x+3.22	0.7604	Y=0.50x+3.00	0.9893	Y=0.080x+2.94	0.8250	0.49	**0.9967**
200%	Y=0.52x+6.34	0.8332	Y=0.059x+3.51	0.6810	Y=0.50x+3.23	0.8796	Y=0.073x+3.25	0.7376	0.45	**0.9788**
250%	Y=3.22x+39.10	0.8076	Y=0.055x+3.60	0.6610	Y=0.50x+3.28	0.8058	Y=0.070x+3.35	0.7152	0.42	**0.9720**

Table 23: Effect of number of perimeters on release kinetics

	Zero-order		First- order		Higuchi		Hixson- Crowell		Korsmeyer-Peppas	
#	Y equation	r^2	Y equation	r^2	Y equation	r^2	Y equation	r^2	n	r^2
3 perimeters	Y=3.32x+24.97	0.9240	Y=0.067x+3.22	0.7604	Y=0.50x+3.00	0.9893	Y=0.080x+2.94	0.8250	0.49	**0.9967**
2 perimeters	Y=3.44x+32.86	0.8275	Y=0.064x+3.41	0.6722	Y=0.50x+3.18	0.9260	Y=0.078x+3.16	0.7307	0.49	**0.9759**
5 perimeters	Y=3.19x+31.18	0.8613	Y=0.062x+3.39	0.6908	Y=0.50x+3.14	0.9286	Y=0.079x+3.16	0.7551	0.47	**0.9810**

Table 24: effect of number of solid layers on the release kinetics

	Zero-order		First- order		Higuchi		Hixson- Crowell		Korsmeyer-Peppas	
Solid every	Y equation	r^2	Y equation	r^2	Y equation	r^2	Y equation	r^2	n	r^2
2 two layers	Y=3.32x+24.97	0.9240	Y=0.067x+3.22	0.7604	Y=0.50x+3.00	0.9893	Y=0.080x+2.94	0.8250	0.49	**0.9967**
1 layer	Y=3.41x+35.50	0.8179	Y=0.061x+3.50	0.6653	Y=0.50x+3.23	0.8959	Y=0.076x+3.24	0.7227	0.67	**0.9737**

5.5 Direct compression and tablets dissolution

Direct compression (DC) is one of the best tablets manufacturing methods since it needs a few preparation stages. Nevertheless, the physical mixture requires good flowability and compressibility properties to be convenient for direct compression [141]. Where compressibility is correlated to the materials` bulk density and flow properties [142]. Particularly bulk density, tapped density, size distribution, particle size, compressibility, and flow properties play a significant role in tablets manufactured by DC [142].

Direct compression used to produce bilayer tablets like those manufactured by HME and FDM. An identical ratio of MPT: Capa® 6506 (40:60%, w/w) and MPT: Eudragit EPO: POLYOX^{TM} (25:52.5:22.5%, w/w/w) physical mixtures used for sustained and immediate-release formulations, respectively.

It was found that the sustained release formulation MPT: Capa® 6506 (40:60%, w/w) was not compressible until 20KN. A 220mg tablet obtained but it was weak and broken by hands (see figure 73). No previous studies had shown that a formula of MPT and PCL or pure PCL were compressible.

Figure 73: MPT: Capa (40:60%, w/w) tablet manufactured by DC technology

That happened because polycaprolactone is ductile and has high elongation breakage, thus creating good elasticity [143]. And when the bulk modulus (elasticity) of a material increase, its compressibility decrease [144]. Upon that MPT: Capa® 6506 (40:60%, w/w) formulation was not compressible and high compressible grade excipients should be used [142].

Upon Immediate release formulation MPT: Eudragit EPO: POLYOX^{TM} (25:52.5:22.5%, w/w/w), it was compressible at 20KN. Obtained tables were strong, thus dissolution test performed and it was found that 100% of the drug released in 30 min, where 43% released with the first 5 minutes while 94% released within the first 15 minutes (see figure 74).
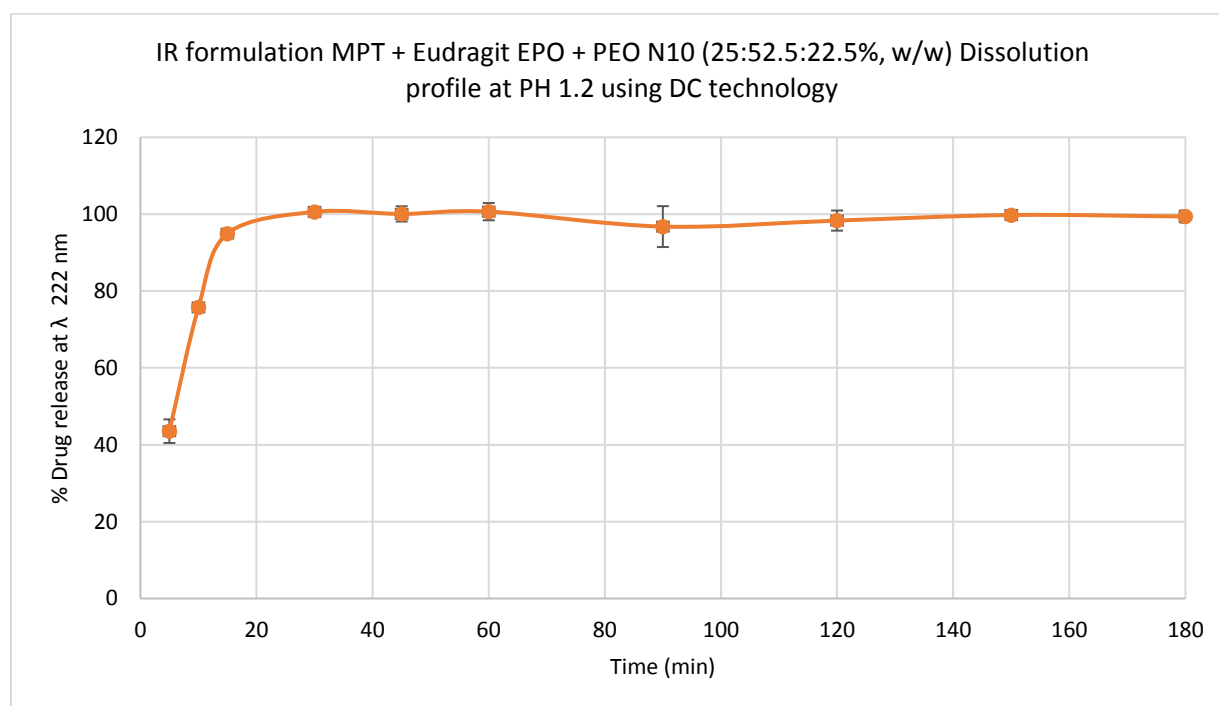
Figure 74: IR formulation MPT + Eudragit EPO + POLYOX^{TM} (25:52.5:22.5%, w/w) Dissolution profile at PH 1.2 using DC technology, (n=3)

To compare the results obtained from FDM and DC tablets a comparison curve plotted (see figure 75). It resulted from differences and similarity factors (f1 and f2) that the release rate from FDM

tablets and DC tablets were the same (see table 25). Where FDM were a bit faster. That happened due to solid dispersion, where the material became more soluble thus the release was faster [137].
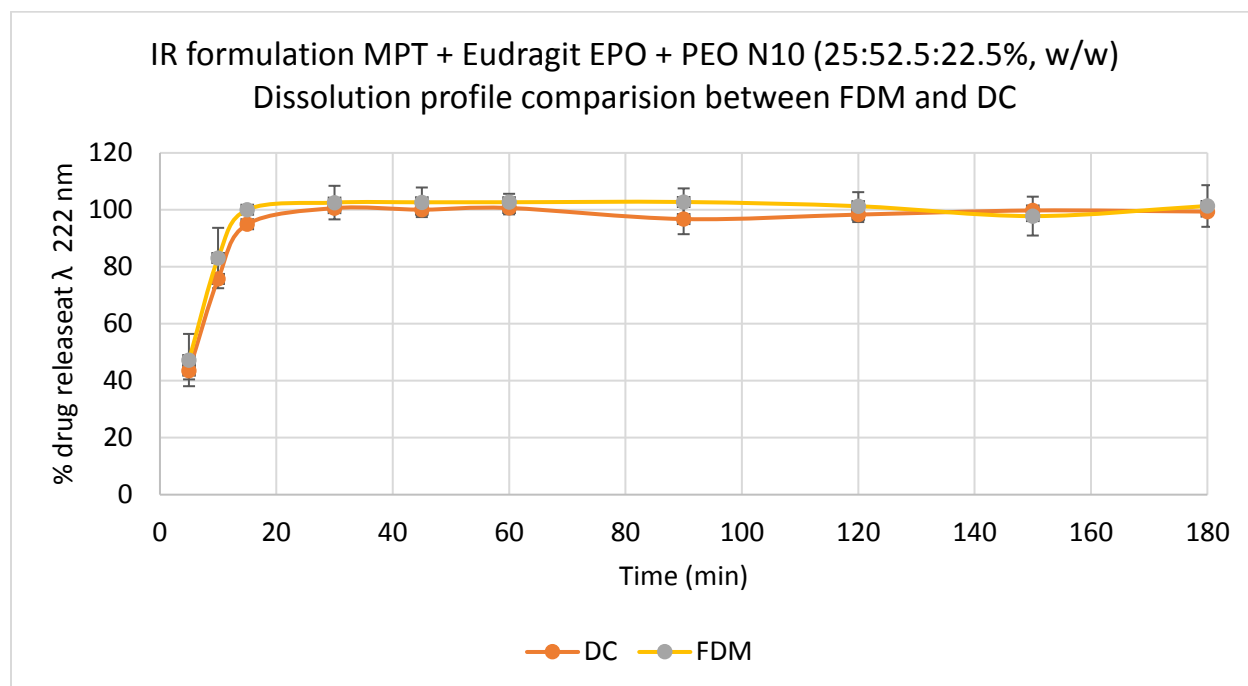
Figure 75: IR formulation MPT + Eudragit EPO + POLYOX™ (25:52.5:22.5%, w/w) Dissolution profile comparison between FDM and DC, (n=3)

Table 25: difference and similarity factors (f1 and f2) for MPT IR tablets produced by FDM and DC

F1	F2	results
3.778	69.207	similar and bioequivalent

6. Conclusion

Metoprolol tartrate (MPT) bilayer tablets manufactured by using 3D printing technology, fused deposition modelling (FDM) technique. The main idea of using the 3DP is to manufacture individualized medicine, since the dose may vary due to gender, weight, genetics profile … etc.

MPT used as a model drug since it is highly water soluble and permeable material and classified in class I in BCS. Also, because it was not manufactured in direct compression or as capsules before, because those are the main techniques that are used in hospitals and pharmacies to produce individualized medicine. Moreover, MPT has a low melting point compared with other drugs and it is a challenge to be manufactured using extrusion and 3DP.

MPT has a short half-life (4-5 hours), so patients take more than one tablet per day as immediate release formulation. For sustained release formulation, generally, metoprolol succinate used. In this work bilayer tablet was manufactured because the patients need the loading dose and the maintenance dose and they can get them through the IR and SR layers respectively.

For SR formulations, the hydrophobic polymers Capa® 6506 and Ateva 1850 used as carriers. While for IR formulations different hydrophilic polymers such as Eudragit EPO, Kollidon K12, Kollicoat IR, Klucel ELF, and POLYOX^{TM} and copolymers used as carriers. All the SR polymers extruded below 120°C, since the T_m for MPT is 120°C and above that temperature the material become more amorphous. while IR polymers extruded below 150°C, since the degradation of MPT starts at 155°C.

Filaments diameters measured using the caliber, since it is one of the most important factors in 3DP. All the filaments had good diameters which is acceptable and near the commercial filaments

diameter which is 1.75 ± 0.05mm. However, it was observed die swelling in Klucel EF and ELF filaments due to their viscoelastic behavior.

The extruded filaments must have good mechanical, rheological, and thermal properties to be printable. Moreover, different materials parameters (melt rheology, mechanical flexibility), machine parameters (nozzle diameter, filament diameter, motor step size and bed leveling), and process parameters (nozzle temperature, bed temperature, printing speed and layer thickness) should be taken into consideration while printing.

Upon that the mechanical properties of the filaments, tensile test applied using the texture analyzer. The flexibility profile obtained from stress-strain curve. Filaments stiffness, breaking distance, ultimate tensile strength, and toughness calculated. It resulted that all the filaments were brittle thus they were broken between the feeding gears. Except MPT: Capa® 6506 (40:60%, w/w) and MPT: Klucel EF (25:75%, w/w) and MPT: Eudragit EPO: POLYOX^{TM} (25:52.5:22.5%, w/w/w).

Upon the thermal properties, SR printable filament was printed below 120°C and for IR they were printed below 150°C. DSC test applied to check the crystallinity loss because the filaments face the heat twice. The first time when they were extruded and second one when they were printed. It was found that there was no great crystallinity loss in MPT in SR formulation. It was resulted that the crystallinity percentage of filaments and tablets were 96.89 and 94.83% respectively. Where for IR formulations, they were 9.86 % and 6.69%, respectively. That happened due to solid dispersion because MPT: Eudragit EPO: POLYOX^{TM} (25:52.5:22.5%, w/w/w) extruded and printed above 120°C.

Tablets dimensions, weight variation, friability, and content uniformity for the printed tablets studied and they showed compatible and acceptable results. Tablets hardness could not be measured because the tablets wee intact and they had not been broken I the device. Instead, indentation hardness recommended to be applied. Upon the tablets` morphology, different tablets with different printing parameters studied under the microscope.

Upon the disintegration test, all the tablets (n=6) disintegrated in less than 10 min. Upon in vitro dissolution, it was applied for sustained release formulation MPT: Capa® 6506 (40:60%, w/w) tablets for 24 hours using phosphate buffer PH 6.8 and they showed a semi linear curve with 94.6% drug release in 24 hours.

For immediate release formulation two of them were printable [(MPT: Klucel 25:75%, w/w) and (MPT: Eudragit EPO: POLYOX^{TM} (25:52.5:22.5%, w/w/w)] the test implemented for 3 hours using HCl buffer PH 1.2. MPT: Klucel 25:75%, w/w) showed a complete release within 1 hour, where (MPT: Eudragit EPO: POLYOX^{TM} (25:52.5:22.5%, w/w/w) showed a complete release within the first 15 minutes. Regards that it was chosen for the IR layer in the bilayer tablets.

Upon the release from the bilayer tablet, it showed that 41.7% of the drug released within the first hour as a loading dose where 86.9% of the drug released within 24 hours. Long while HCl PH 1.2 used for the first two hours and phosphate buffer PH 6.8 used for the last 22 hours as a dissolution medium according to USP method A.

The release from the bilayer tablet needs more investigation, since it was shown when MPT: Capa® 6506 (40:60%, w/w) tablets placed in acidic medium HCl buffer PH 1.2 that 60% of the

drug was released within 3 hours. That might happen due to the pKa of API or degradation of PCL in the acidic media < PH3.

On the other side, different printing parameters modified to see the effect on the dissolution profile and rate and it was found that some parameters had significant change and others did not show a critical change when differences and similarity factors (f1 and f2) applied. Number of perimeters, perimeters/infill overlap percentage, and number of solid layers were the parameters that changed with different percentage.

After that the kinetics of the SR formulation studied and it showed that the tablets followed Korsmeyer- Peppas drug release model with anomalous release because of coupled diffusion and/or relaxation of the polymer.

Additionally, it was proven that increasing the perimeters/infill overlap percentage resulted a change in the kinetics considering it resulted Fickian diffusion release model. Other printing parameters such as number of perimeters and number of solid layers showed no critical effects on the drug kinetics.

At the end, the same physical mixtures as used for the printable tablets prepared and compressed using Styl`One machine. It was resulted that MPT: Capa® 6506 (40:60%, w/w) was not compressible until 20KN where MPT: Eudragit EPO: POLYOX^{TM} (25:52.5:22.5%, w/w/w) was compressible. Dissolution test applied and it showed slower release than 3D printed tablet. Because, by using extrusion at high temperature above the T_m of the API solid dispersion formed which leads to increase the drug release consequently the drug bioavailability.

To sum up, this research demonstrated that FDM is an appropriate method to manufacture individualized medicine with different drug release profiles and kinetics. MPT bilayer tablets are a useful idea for those patients who take that drug since they can get there loading dose and maintenance one in one tablet that is specialized for them.

Capa® 6506 is a good hydrophobic polymer for sustained release tablets. where Eudragit EPO with PEO are good hydrophilic polymers for immediate release tablets that manufactured with FDM. However, more investigation is needed regarding the dissolution of Capa® 6506 in Acidic medium PH <3.

This work can be a baseline for future researches to manufacture bilayer tablets using FDM technique and a lot of research and work can be done in the future around it.

7. Future work

Future work for this study can be summarized in, First, manufacture 3D printed core and shell tablets using FDM technique and compare the dissolution profile of them both.

Second, Implement a rheology study for the filaments. Third, perform chemical and physical stability study for both filaments and printed tablets to study the degradation and crystallinity loss where X-Ray, FTIR, DSC, tomography and electronic scanning microscope can be used for characterization.

Fourth, tablet properties should be studied before and after invitro dissolution test applied such as swelling percentage, porosity, and dimensions. Fifth, full characterization must be done for all possible interactions that may happen in the system. Sixth, sink conditions must be studied. Seventh, perform a comparison between dissolution profiles and kinetics of capsules that have pure MPT, capsules that contains the physical mixtures, MPT tablets available in market and MPT tablets produced by FDM technique. Then, perform the Assay for filaments and tablets. Moreover, HPLC can be used in the analysis instead of UV and a validation method should be verified.

References

[1]   J. Goole and K. Amighi, "3D printing in pharmaceutics: A new tool for designing customized drug delivery systems," *Int. J. Pharm.*, vol. 499, no. 1–2, pp. 376–394, 2016.

[2]   L. V Allen and H. C. Ansel, "Ansel ' s Pharmaceutical Dosage Forms and Drug Delivery Systems," *Chief Int. J. Pharm. Compd.*, p. 537, 2011.

[3]   S. S. Montoto and M. E. Ruiz, "Routes of Drug Administration: Design, and Pharmacotherapy Success," *ResearchGate*, no. January, 2018.

[4]   R. Goyena, "Dosage Forms, Routes of Administration, and Dispensing Medications," in *Journal of Chemical Information and Modeling*, vol. 53, no. 9, 2019, pp. 1689–1699.

[5]   C. B. Andriy Dashevskiy,Bernhard Fussnegger, "New Sustained Release Formulation Solutions Overcome Challenges of Alcohol-Induced Dose Dumping," *BASF*.

[6]   M. M. and A. N. Deck Khong Tan, "Advanced pharmaceutical applications of hot-melt extrusion coupled with fused deposition modelling (FDM) 3D printing for personalised drug delivery," *Pharmaceutics*, vol. 10, no. 4, 2018.

[7]   X. Feng and F. Zhang, "Twin-screw extrusion of sustained-release oral dosage forms and medical implants," *Drug Deliv. Transl. Res.*, vol. 8, no. 6, pp. 1694–1713, 2018.

[8]   M. Williams, Y. Tian, D. S. Jones, and G. P. Andrews, "Hot-melt extrusion technology: Optimizing drug delivery," *Eur. J. Parenter. Pharm. Sci.*, vol. 15, no. 2, pp. 61–63, 2010.

[9]   J. Breitenbach, "Melt extrusion: from process to drug delivery technology," *European Journal of Pharmaceutics and Biopharmaceutics*, vol. 54, no. 2. pp. 107–117, Sep-2002.

[10]   L. Zema, A. Melocchi, A. Maroni, and A. Gazzaniga, "Three-Dimensional Printing of Medicinal Products and the Challenge of Personalized Therapy," *J. Pharm. Sci.*, vol. 106, no. 7, pp. 1697–

1705, 2017.

[11]   J. Zhang, X. Feng, H. Patil, R. V. Tiwari, and M. A. Repka, "Coupling 3D printing with hot-melt

extrusion to produce controlled-release tablets," *Int. J. Pharm.*, vol. 519, no. 1–2, pp. 186–197,

2017.

[12]   D. Markl *et al.*, "Supervisory Control System for Monitoring a Pharmaceutical Hot Melt Extrusion

Process," vol. 14, no. 3, pp. 1034–1044, 2013.

[13]   A. Gmbh, "Melt extrusion : from process to drug delivery technology," vol. 54, pp. 107–117,

2002.

[14]   M. R. Thompson, "Twin screw granulation-review of current progress," *Drug Development and

Industrial Pharmacy*, vol. 41, no. 8. Informa Healthcare, pp. 1223–1231, 01-Aug-2015.

[15]   K. Kohlgrüber, "General Overview of the Compounding Process: Tasks, Selected Applications, and

Process Zones," in *Co-rotating Twin-Screw Extruders: Fundamentals, Technology and

Applications*, G. Dr.-Ing. Klemens Kohlgrüber, Bayer Technology Services GmbH, D-51368

Leverkusen, Ed. Hanser, 2008, pp. 57–87.

[16]   B. S. Robertson and B. Sc, "Hot Melt Extrusion in the Pharmaceutical and Food Industries," pp. 1–

9, 2019.

[17]   M. M. Crowley *et al.*, "Pharmaceutical applications of hot-melt extrusion: Part I," *Drug Dev. Ind.

Pharm.*, vol. 33, no. 9, pp. 909–926, 2007.

[18]   H. Patil, R. V. Tiwari, and M. A. Repka, "Hot-Melt Extrusion: from Theory to Application in

Pharmaceutical Formulation," *AAPS PharmSciTech*, vol. 17, no. 1, pp. 20–42, Feb. 2016.

[19]   M. A. Repka *et al.*, "Pharmaceutical Applications of Hot-Melt Extrusion: Part II," *Drug Dev. Ind.

Pharm.*, vol. 33, no. 10, pp. 1043–1057, Jan. 2007.

[20]   S. G. edited by Abdul W. Basit, "3D Printing of Pharmaceuticals - Google Books." [Online].

Available:

https://books.google.be/books?id=RYdnDwAAQBAJ&pg=PA19&lpg=PA19&dq=Breitenbach+J.+M

elt+extrusion:+from+process+to+drug+delivery+technology.+Eur+J+Pharm+Biopharm.+2002;54(2

):107–

17.&source=bl&ots=JpdasMLM2q&sig=ACfU3U3n3j23fKk4YUehFfvFrGOpfYn3mg&hl=en&sa=X&v

ed=2ahUKEwjDwfSNsuLlAhVJNOwKHSR6DuIQ6AEwAXoECAUQAQ#v=onepage&q=Breitenbach J.

Melt extrusion%3A from process to drug delivery technology. Eur J Pharm Biopharm.

2002%3B54(2)%3A107–17.&f=false. [Accessed: 11-Nov-2019].

[21]   D. Khong Tan, M. Maniruzzaman, and A. Nokhodchi, "pharmaceutics Advanced Pharmaceutical

Applications of Hot-Melt Extrusion Coupled with Fused Deposition Modelling (FDM) 3D Printing

for Personalised Drug Delivery."

[22]   S. B. Repka, M.A.; Majumdar, S.; Battu, S.K.; Srirangam, R.; Upadhye, *APPLICATIONS OF HOT-

MELT EXTRUSION FOR DRUG DELIVERY*, vol. 176, no. 5. 2017.

[23]   M. Ravindar Reddy, A. R. Subrahmanyam, M. Maheshwar Reddy, J. Siva Kumar, V. Kamalaker, and

M. Jaipal Reddy, "X-RD, SEM, FT-IR, DSC Studies of Polymer Blend Films of PMMA and PEO," in

Materials Today: Proceedings, 2016, vol. 3, no. 10, pp. 3713–3718.

[24]   S. A. Khaled *et al.*, "Extrusion 3D Printing of Paracetamol Tablets from a Single Formulation with

Tunable Release Profiles Through Control of Tablet Geometry," *AAPS PharmSciTech*, vol. 19, no.

8, pp. 3403–3413, 2018.

[25]   C. Voura *et al.*, "Printable medicines: A microdosing device for producing personalised

medicines," *Pharm. Technol. Eur.*, vol. 23, no. 1, pp. 32–36, 2011.

[26]   S. A. Khaled *et al.*, "3D extrusion printing of high drug loading immediate release paracetamol

tablets," *Int. J. Pharm.*, vol. 538, no. 1–2, pp. 223–230, 2018.

[27]   Sau (Larry) Lee, "Modernizing the Way Drugs Are Made: A Transition to Continuous

Manufacturing," *U.S Food and Drug administration*, 2017. .

[28]   S. A. Khaled, J. C. Burley, M. R. Alexander, and C. J. Roberts, "Desktop 3D printing of controlled

release pharmaceutical bilayer tablets," *Int. J. Pharm.*, vol. 461, no. 1–2, pp. 105–111, 2014.

[29]   S. Lamichhane *et al.*, "Complex formulations, simple techniques: Can 3D printing technology be

the Midas touch in pharmaceutical industry?," *Asian J. Pharm. Sci.*, no. xxxx, 2019.

[30]   D. J. Horst, "3D Printing of Pharmaceutical Drug Delivery Systems," *Arch. Org. Inorg. Chem. Sci.*,

vol. 1, no. 2, pp. 1–5, 2018.

[31]   L. Luxminarayan, S. Neha, V. Amit, and M. P. Khinchi, "3D PRINTING OF PHARMACEUTICALS – A

POTENTIAL TECHNOLOGY IN DEVELOPING PERSONALIZED MEDICINE," *Asian J. Pharm. Res. Dev.*,

vol. 5, no. 2, pp. 1–8, 2017.

[32]   M. R. P. Araújo, L. L. Sa-Barreto, T. Gratieri, G. M. Gelfuso, and M. Cunha-Filho, "The digital

pharmacies era: How 3D printing technology using fused deposition modeling can become a

reality," *Pharmaceutics*, vol. 11, no. 3, 2019.

[33]   B. O. G.*, G. V. S., S. B. K., D. R. C., G. S. A., and G. P. S., "3D Printing & Pharmaceutical

Manufacturing: Opportunities and Challenges," *Int. J. Bioassays*, vol. 5, no. 01, p. 4723, 2016.

[34]   L. K. Prasad and H. Smyth, "3D Printing technologies for drug delivery: a review," *Drug Dev. Ind.

Pharm.*, vol. 42, no. 7, pp. 1019–1031, 2016.

[35]   J. Aho, J. P. Bøtker, N. Genina, M. Edinger, L. Arnfast, and J. Rantanen, "Roadmap to 3D-Printed

Oral Pharmaceutical Dosage Forms: Feedstock Filament Properties and Characterization for

Fused Deposition Modeling," *J. Pharm. Sci.*, vol. 108, no. 1, pp. 26–35, 2019.

[36]   B. C. Gross, J. L. Erkal, S. Y. Lockwood, C. Chen, and D. M. Spence, "Evaluation of 3D printing and its potential impact on biotechnology and the chemical sciences," *Anal. Chem.*, vol. 86, no. 7, pp. 3240–3253, 2014.

[37]   G. Verstraete *et al.*, "3D printing of high drug loaded dosage forms using thermoplastic polyurethanes," *Int. J. Pharm.*, vol. 536, no. 1, pp. 318–325, 2018.

[38]   J. M. Nasereddin, N. Wellner, M. Alhijjaj, P. Belton, and S. Qi, "Development of a Simple Mechanical Screening Method for Predicting the Feedability of a Pharmaceutical FDM 3D Printing Filament," *Pharm. Res.*, vol. 35, no. 8, 2018.

[39]   X. Wang, M. Jiang, Z. Zhou, J. Gou, and D. Hui, "3D printing of polymer matrix composites: A review and prospective," *Compos. Part B Eng.*, vol. 110, pp. 442–458, 2017.

[40]   S. Hwang, E. I. Reyes, K. sik Moon, R. C. Rumpf, and N. S. Kim, "Thermo-mechanical Characterization of Metal/Polymer Composite Filaments and Printing Parameter Study for Fused Deposition Modeling in the 3D Printing Process," *J. Electron. Mater.*, vol. 44, no. 3, pp. 771–777, 2015.

[41]   M. Sadia, B. Arafat, W. Ahmed, R. T. Forbes, and M. A. Alhnan, "Channelled tablets: An innovative approach to accelerating drug release from 3D printed tablets," *J. Control. Release*, vol. 269, pp. 355–363, 2018.

[42]   J. Norman, R. D. Madurawe, C. M. V. Moore, M. A. Khan, and A. Khairuzzaman, "A new chapter in pharmaceutical manufacturing: 3D-printed drug products," *Adv. Drug Deliv. Rev.*, vol. 108, pp. 39–50, 2017.

[43]   S. J. Tren, A. Awad, A. Goyanes, S. Gaisford, and A. W. Basit, "3D Printing Pharmaceuticals : Drug Development to Frontline Care," *Trends Pharmacol. Sci.*, 2018.

[44] A. Goyanes, U. Det-Amornrat, J. Wang, A. W. Basit, and S. Gaisford, "3D scanning and 3D printing as innovative technologies for fabricating personalized topical drug delivery systems," *J. Control. Release*, vol. 234, pp. 41–48, 2016.

[45] A. A. Konta, M. García-Piña, and D. R. Serrano, "Personalised 3D printed medicines: Which techniques and polymers are more successful?," *Bioengineering*, vol. 4, no. 4, 2017.

[46] M. Preis, J. Breitkreutz, and N. Sandler, "Perspective: Concepts of printing technologies for oral film formulations," *Int. J. Pharm.*, vol. 494, no. 2, pp. 578–584, 2015.

[47] C. I. Gioumouxouzis, O. L. Katsamenis, N. Bouropoulos, and D. G. Fatouros, "3D printed oral solid dosage forms containing hydrochlorothiazide for controlled drug delivery," *J. Drug Deliv. Sci. Technol.*, vol. 40, pp. 164–171, Aug. 2017.

[48] J. Skowyra, K. Pietrzak, and M. A. Alhnan, "Fabrication of extended-release patient-tailored prednisolone tablets via fused deposition modelling (FDM) 3D printing," *Eur. J. Pharm. Sci.*, vol. 68, pp. 11–17, 2015.

[49] J. Zhao, X. Xu, M. Wang, and L. Wang, "A new model of a 3D-printed shell with convex drug release profile," *Dissolution Technol.*, vol. 25, no. 1, pp. 24–28, 2018.

[50] A. Goyanes, A. B. M. Buanz, A. W. Basit, and S. Gaisford, "Fused-filament 3D printing (3DP) for fabrication of tablets," *Int. J. Pharm.*, vol. 476, no. 1, pp. 88–92, 2014.

[51] A. Goyanes *et al.*, "3D Printing of Medicines: Engineering Novel Oral Devices with Unique Design and Drug Release Characteristics," *Mol. Pharm.*, vol. 12, no. 11, pp. 4077–4084, 2015.

[52] A. Goyanes, P. Robles Martinez, A. Buanz, A. W. Basit, and S. Gaisford, "Effect of geometry on drug release from 3D printed tablets," *Int. J. Pharm.*, vol. 494, no. 2, pp. 657–663, 2015.

[53] W. Jamróz, J. Szafraniec, M. Kurek, and R. Jachowicz, "3D Printing in Pharmaceutical and Medical

Applications – Recent Achievements and Challenges," *Pharm. Res.*, vol. 35, no. 9, 2018.

[54]   C. J. H. Brenan, "3-D-Printed Pills: A New Age for Drug Delivery [From the Editor]," *IEEE Pulse*, vol. 6, no. 5, p. 3, 2015.

[55]   D. Evaluation, "Medical review(s)," *Cent. DRUG Eval. Res.*, 2015.

[56]   M. A. Alhnan, T. C. Okwuosa, M. Sadia, K. W. Wan, W. Ahmed, and B. Arafat, "Emergence of 3D Printed Dosage Forms: Opportunities and Challenges," *Pharm. Res.*, vol. 33, no. 8, pp. 1817–1832, 2016.

[57]   S. A. Khaled, J. C. Burley, M. R. Alexander, J. Yang, and C. J. Roberts, "3D printing of tablets containing multiple drugs with defined release profiles," *Int. J. Pharm.*, vol. 494, no. 2, pp. 643–650, 2015.

[58]   S. A. Khaled, J. C. Burley, M. R. Alexander, J. Yang, and C. J. Roberts, "3D printing of five-in-one dose combination polypill with defined immediate and sustained release profiles," *J. Control. Release*, vol. 217, pp. 308–314, 2015.

[59]   F. A. Maulvi, M. J. Shah, B. S. Solanki, S. P. Patel, Akanksha, T. G. Soni, and D. O. Shah, "Application of 3D Printing Technology in the Development of Novel Drug Delivery Systems," *Int. J. Drug Dev. Res.*, vol. 9, no. 1, pp. 1–5, 2017.

[60]   G. F and A. Velez, "3D Pharming: Direct Printing of Personalized Pharmaceutical Tablets," *Polym. Sci.*, vol. 2, no. 1, pp. 1–10, 2016.

[61]   N. G. Solanki, M. Tahsin, A. V. Shah, and A. T. M. Serajuddin, "Formulation of 3D Printed Tablet for Rapid Drug Release by Fused Deposition Modeling: Screening Polymers for Drug Release, Drug-Polymer Miscibility and Printability," *J. Pharm. Sci.*, vol. 107, no. 1, pp. 390–401, 2018.

[62]   M. Edinger, J. Jacobsen, D. Bar-Shalom, J. Rantanen, and N. Genina, "Analytical aspects of printed

oral dosage forms," *Int. J. Pharm.*, vol. 553, no. 1–2, pp. 97–108, 2018.

[63]   F. R. Vogenberg, C. I. Barash, and M. Pursel, "Personalized medicine - Part 1: Evolution and development into theranostics," *P T*, vol. 35, no. 10, 2010.

[64]   A. Zajicek *et al.*, "A report from the pediatric formulations task force: Perspectives on the state of child-friendly oral dosage forms," *AAPS J.*, vol. 15, no. 4, pp. 1072–1081, 2013.

[65]   B. N. Turner, R. Strong, and S. A. Gold, "A review of melt extrusion additive manufacturing processes: I. Process design and modeling," *Rapid Prototyping Journal*, vol. 20, no. 3. Emerald Group Publishing Ltd., pp. 192–204, 2014.

[66]   E. Fuenmayor, M. Forde, A. V Healy, D. M. Devine, C. Mcconville, and I. Major, "Material Considerations for Fused-Filament Fabrication of Solid Dosage Forms," pp. 1–27, 2018.

[67]   M. Alhijjaj, P. Belton, and S. Qi, "European Journal of Pharmaceutics and Biopharmaceutics An investigation into the use of polymer blends to improve the printability of and regulate drug release from pharmaceutical solid dispersions prepared via fused deposition modeling (FDM) 3D printin," *Eur. J. Pharm. Biopharm.*, vol. 108, pp. 111–125, 2016.

[68]   C. Bellehumeur, L. Li, Q. Sun, and P. Gu, "Modeling of bond formation between polymer filaments in the fused deposition modeling process," *J. Manuf. Process.*, vol. 6, no. 2, pp. 170–178, 2004.

[69]   S. F. Costa, F. M. Duarte, and J. A. Covas, "Estimation of filament temperature and adhesion development in fused deposition techniques," *J. Mater. Process. Technol.*, vol. 245, pp. 167–179, Jul. 2017.

[70]   J. Roesler, H. Harders, and M. Baeker, *Mechanical Behavior of Enginerring Materials*. 2006.

[71]   "Differential Scanning Calorimeters – TA Instruments." [Online]. Available:

https://www.tainstruments.com/products/thermal-analysis/differential-scanning-calorimeters/.
[Accessed: 25-Nov-2019].

[72]   S. Baghel, H. Cathcart, and N. J. O'Reilly, "Polymeric Amorphous Solid Dispersions: A Review of Amorphization, Crystallization, Stabilization, Solid-State Characterization, and Aqueous Solubilization of Biopharmaceutical Classification System Class II Drugs," *J. Pharm. Sci.*, vol. 105, no. 9, pp. 2527–2544, 2016.

[73]   P. Hub, F. Macro, and H. Thermodynamics, *Thermal Physics and Thermal Analysis*. Springer New York LLC, 2017.

[74]   A. Heimowska, M. Morawska, and A. Bocho-Janiszewska, "Biodegradation of poly(ϵ-caprolactone) in natural water environments," *Polish J. Chem. Technol.*, vol. 19, no. 1, pp. 120–126, 2017.

[75]   M. Abedalwafa, F. Wang, L. Wang, and C. Li, "Biodegradable poly-epsilon-caprolactone (PCL) for tissue engineering applications : A review BIODEGRADABLE POLY-EPSILON-CAPROLACTONE (PCL) FOR TISSUE ENGINEERING APPLICATIONS : A REVIEW," no. December, 2012.

[76]   "Chemistry of EVA - Celanese Healthcare and Life Sciences." [Online]. Available: https://healthcare.celanese.com/products/ateva-g/chemistry-of-eva.aspx. [Accessed: 22-Nov-2019].

[77]   N. Genina, J. Holländer, H. Jukarainen, E. Mäkilä, J. Salonen, and N. Sandler, "Ethylene vinyl acetate (EVA) as a new drug carrier for 3D printed medical drug delivery devices," *Eur. J. Pharm. Sci.*, vol. 90, pp. 53–63, 2016.

[78]   C. Schneider, R. Langer, D. Loveday, and D. Hair, "Applications of ethylene vinyl acetate copolymers (EVA) in drug delivery systems," *J. Control. Release*, vol. 262, no. July, pp. 284–295,

2017.

[79]   M. Brogly, M. Nardin, and J. Schultz, "Effect of vinylacetate content on crystallinity and second-order transitions in ethylene—vinylacetate copolymers," *J. Appl. Polym. Sci.*, vol. 64, no. 10, pp. 1903–1912, Jun. 1997.

[80]   I. Erukhimovich and M. O. de la Cruz, "Phase equilibria and charge fractionation in polydisperse polyelectrolyte solutions," pp. 2864–2879, 2004.

[81]   A. Almeida *et al.*, "Ethylene vinyl acetate as matrix for oral sustained release dosage forms produced via hot-melt extrusion," *Eur. J. Pharm. Biopharm.*, vol. 77, no. 2, pp. 297–305, 2011.

[82]   A. Arsac, C. Carrot, and J. Guillet, "Determination of primary relaxation temperatures and melting points of ethylene vinyl acetate copolymers," *J. Therm. Anal. Calorim.*, vol. 61, no. 3, pp. 681–685, 2000.

[83]   P. Eur, "EUDRAGIT ® E 100, EUDRAGIT ® E PO and EUDRAGIT ® E 12,5 Specification and Test Methods Solution of EUDRAGIT ® E 100 with 12.5 % (w/w) dry substance in a mixture of," 2015.

[84]   T. Parikh, S. S. Gupta, A. Meena, and A. T. M. Serajuddin, "Investigation of thermal and viscoelastic properties of polymers relevant to hot melt extrusion - III : Polymethacrylates and polymethacrylic acid based polymers Investigation of thermal and viscoelastic properties of polymers relevant to hot melt extrusi," *J. Excipients Food Chem.*, no. April 2017, 2014.

[85]   M. Sadia, B. Arafat, W. Ahmed, R. T. Forbes, and M. A. Alhnan, "Channelled tablets: An innovative approach to accelerating drug release from 3D printed tablets," *J. Control. Release*, vol. 269, no. November 2017, pp. 355–363, 2018.

[86]   M. Sadia, A. So, B. Arafat, A. Isreb, and W. Ahmed, "Adaptation of pharmaceutical excipients to FDM 3D printing for the fabrication of patient-tailored immediate release tablets," *Int. J. Pharm.*,

vol. 513, pp. 659–668, 2016.

[87]   J. Pratik, T. Rupesh, and S. Raosaheb, "A brief review on Kollidon," *J. Drug Deliv. Ther.*, vol. 9, no. 2, pp. 493–500, 2019.

[88]   W. Kempin *et al.*, "Immediate Release 3D-Printed Tablets Produced Via Fused Deposition Modeling of a Thermo-Sensitive Drug," 2018.

[89]   N. N. Mohammed *et al.*, "Klucel^{TM} EF and ELF polymers for immediate-release oral dosage forms prepared by melt extrusion technology," *AAPS PharmSciTech*, vol. 13, no. 4, pp. 1158–1169, 2012.

[90]   S. Onoue *et al.*, "Improved dissolution and pharmacokinetic behavior of cyclosporine A using high-energy amorphous solid dispersion approach," *Int. J. Pharm.*, vol. 399, no. 1–2, pp. 94–101, Oct. 2010.

[91]   Ashland Inc., "Klucel TM Hydroxypropylcellulose in Hot-melt Extrusion Applications," 2010.

[92]   Ashland Inc., "Klucel hydroxypropylcellulose physical and chemical properties (Datasheet)," p. 24, 2017.

[93]   S. Ali, "Kollicoat® IR: Minimizing the Risks for Oxidative Degradation of Drugs," *J. Anal. Pharm. Res.*, vol. 2, no. 3, pp. 8–12, 2016.

[94]   J. Paul and G. Van Den Mooter, "The use of a new hydrophilic polymer , Kollicoat IR ® , in the formulation of solid dispersions of Itraconazole," vol. 0, pp. 288–294, 2006.

[95]   A. G. K. Kolter, M. Karl, *Hot-Melt Extrusion with BASF pharma polymers*, 2nd editio. BASF, 2012.

[96]   A. Melocchi, F. Parietti, A. Maroni, A. Foppoli, A. Gazzaniga, and L. Zema, "Hot-melt extruded filaments based on pharmaceutical grade polymers for 3D printing by fused deposition

modeling," *Int. J. Pharm.*, vol. 509, no. 1–2, pp. 255–263, 2016.

[97]   G. Wypych, "PEO poly(ethylene oxide)," in *Handbook of Polymers*, Elsevier, 2016, pp. 390–393.

[98]   R. N. Patel and P. D. Bharadia, "Formulation and Evaluation of Dual Component Tablets of Metoprolol tartrate AND," vol. 1, no. 2, pp. 514–522, 2012.

[99]   G. Mosca, J. Schumpeter, W. Mills, T. Skocpol, R. Miliband, and N. Poulantzas, "metoprolol tartrate tablets, USP metoprolol," no. 1, pp. 1–10, 2011.

[100]   J. R. Luch, "Metoprolol Tartrate," *Analytical Profiles of Drug Substances and Excipients*, 1983. [Online]. Available: https://pubchem.ncbi.nlm.nih.gov/compound/Metoprolol-tartrate.

[101]   T. Quinten, T. De Beer, C. Vervaet, and J. P. Remon, "Evaluation of injection moulding as a pharmaceutical technology to produce matrix tablets," *Eur. J. Pharm. Biopharm.*, vol. 71, no. 1, pp. 145–154, 2009.

[102]   "Metoprolol tartrate | C34H56N2O12 - PubChem." [Online]. Available: https://pubchem.ncbi.nlm.nih.gov/compound/Metoprolol-tartrate#section=NLM-Curated-PubMed-Citations. [Accessed: 04-Nov-2019].

[103]   United State Pharmacopeia, "<905> UNIFORMITY OF DOSAGE UNITS." [Online]. Available: http://ftp.uspbpep.com/v29240/usp29nf24s0_c905h.html. [Accessed: 09-Mar-2020].

[104]   D. Sharma, "Formulation Development and Evaluation of Fast Disintegrating Tablets of Salbutamol Sulphate for Respiratory Disorders," *ISRN Pharm.*, vol. 2013, pp. 1–8, 2013.

[105]   P. K. J, T. Ramarao, K. N. Jayaveera, D. V. R. N. Bhikshapathi, and M. R. Y, "Design and In vivo evaluation of Metoprolol Tartrate bilayer floating tablets in healthy human volunteers," vol. 6, pp. 14–23, 2014.

[106]   "< 701> DISINTEGRATION," pp. 2–5, 2020.

[107]   "Reagents: Buffer Solutions." [Online]. Available:

http://www.uspbpep.com/usp29/v29240/usp29nf24s0_ris1s119.html. [Accessed: 30-May-2020].

[108]   H. Naseef, A. Samaro, M. S. Qurt, H. Nakhleh, R. Moqadi, and M. Enaya, "Formulation and

evaluation of oral biphasic drug delivery system of Metronidazole using HPMC polymer," vol. 5,

no. 7, pp. 22–30, 2016.

[109]   P. M. V. and C. J. P. Chirag M Lakhani, Braden T Tierney, Arjun K Manrai1, Jian Yang, "Influence of

degassing on hot-melt extrusion process.," *Eur J Pharm Sci*, vol. 176, no. 3, pp. 139–148, 2019.

[110]   H. Akdogan, "Pressure, torque, and energy responses of a twin screw extruder at high moisture

contents," *Food Res. Int.*, vol. 29, no. 5–6, pp. 423–429, 1996.

[111]   "V23_259_280.Pdf." .

[112]   A. M. Henderson and A. Rudin, "Effects of die temperature on extrudate swell in screw

extrusion," *J. Appl. Polym. Sci.*, vol. 31, no. 2, pp. 353–365, Feb. 1986.

[113]   Kenneth J. Anusavice, *Phillips' Science of Dental Materials*, Eleventh Edition. Elsevier Health

Sciences, 2003.

[114]   J. Holländer *et al.*, "Three-Dimensional Printed PCL-Based Implantable Prototypes of Medical

Devices for Controlled Drug Delivery," *J. Pharm. Sci.*, vol. 105, no. 9, pp. 2665–2676, 2016.

[115]   G. Kollamaram, D. M. Croker, G. M. Walker, A. Goyanes, A. W. Basit, and S. Gaisford, "Low

temperature fused deposition modeling (FDM) 3D printing of thermolabile drugs," *Int. J. Pharm.*,

vol. 545, no. 1–2, pp. 144–152, 2018.

[116]   W. Kempin *et al.*, "Development of a dual extrusion printing technique for an acid- and thermo-

labile drug," *Eur. J. Pharm. Sci.*, vol. 123, pp. 191–198, 2018.

[117] X. H. X. Chen, "Melt-spun PVDF hollow fiber membrane with PEO as pore formation agent,"

researchgate, 2009. [Online]. Available:

https://www.researchgate.net/publication/282321340_Melt-

spun_PVDF_hollow_fiber_membrane_with_PEO_as_pore_formation_agent. [Accessed: 27-Mar-

2020].

[118] "3D Printing: Elephant's Foot – Easy Fixes | All3DP." [Online]. Available:

https://all3dp.com/2/elephant-s-foot-3d-printing-problem-easy-fixes/. [Accessed: 11-Mar-2020].

[119] J. William D. Callister, "Callister - Materials Science and Engineering." John Wiley & Sons, Inc.,

2007.

[120] M. Alhijjaj, J. Nasereddin, P. Belton, and S. Qi, "Impact of Processing Parameters on the Quality of

Pharmaceutical Solid Dosage Forms Produced by Fused Deposition Modeling (FDM)," 2019.

[121] R. Singh, R. Kumar, and M. S. J. Hashmi, "Friction Welding of Dissimilar Plastic-Based Material by

Metal Powder Reinforcement," in *Reference Module in Materials Science and Materials

Engineering*, Elsevier, 2017.

[122] "Melt Index." [Online]. Available: https://polymerdatabase.com/polymer physics/Melt

Flow.html. [Accessed: 11-Mar-2020].

[123] "<1217> TABLET BREAKING FORCE." [Online]. Available:

https://www.drugfuture.com/Pharmacopoeia/USP32/pub/data/v32270/usp32nf27s0_c1217.ht

ml. [Accessed: 11-Mar-2020].

[124] Y. C. G. G. Z. Z. L. L. W. P. Yihong Qiu, Ed., *Developing Solid Oral Dosage Forms: Pharmaceutical

Theory and Practice - Google Books*, 2nd ed. USA: Elsevier, 2009.

[125] S. Prasanthi *et al.*, "Formulation and Evaluation of Sitagliptin Phosphate and Simvastatin

Bilayered Tablets," *Artic. INFO Abstr. Artic. Hist. Indo Am. J. Pharm. Res.*, vol. 2015, no. 08, p. 5,

2015.

[126] United State Pharmacopeia, "<1216> TABLET FRIABILITY," 2016.

[127] F. Osei-Yeboah and C. C. Sun, "Validation and applications of an expedited tablet friability

method," *Int. J. Pharm.*, vol. 484, no. 1–2, pp. 146–155, Apr. 2015.

[128] H. Liu *et al.*, "Design space determination and process optimization in at-scale continuous twin

screw wet granulation," *Comput. Chem. Eng.*, vol. 125, no. April, pp. 271–286, 2019.

[129] M. A. Azad, D. Olawuni, G. Kimbell, A. Z. M. Badruddoza, M. S. Hossain, and T. Sultana, *Polymers

for extrusion-based 3D printing of pharmaceuticals: A holistic materials–process perspective*, vol.

12, no. 2. 2020.

[130] H. M. Heidemann, M. E. R. Dotto, J. B. Laurindo, B. A. M. Carciofi, and C. Costa, "Cold plasma

treatment to improve the adhesion of cassava starch films onto PCL and PLA surface," *Colloids

Surfaces A Physicochem. Eng. Asp.*, vol. 580, p. 123739, Nov. 2019.

[131] F. Awaja, M. Gilbert, G. Kelly, B. Fox, and P. J. Pigram, "Adhesion of polymers," *Progress in

Polymer Science (Oxford)*, vol. 34, no. 9. Pergamon, pp. 948–968, 01-Sep-2009.

[132] S. L. Messimer, A. E. Patterson, N. Muna, A. P. Deshpande, and T. Rocha Pereira,

"Characterization and Processing Behavior of Heated Aluminum-Polycarbonate Composite Build

Plates for the FDM Additive Manufacturing Process," *J. Manuf. Mater. Process.*, vol. 2, no. 1, p.

12, Feb. 2018.

[133] Adeline Siew, "Analyzing Content Uniformity," *Pharm. Technol.*, vol. 42, no. 2, 2018.

[134] W. E. Katstra, R. D. Palazzolo, C. W. Rowe, B. Giritlioglu, P. Teung, and M. J. Cima, "Oral dosage

forms fabricated by Three Dimensional Printing(TM)," *J. Control. Release*, vol. 66, no. 1, pp. 1–9, 2000.

[135] J. M. Jaroslav Š, Pavel H, "Glassy, Amorphous and Nano-Crystalline Materials: Thermal Physics, Analysis, Structure and Properties," *Springer*, 2011.

[136] R. D. Aleksandar Aleksovski, Pieter-Jan Van Bockstal, Robert Roškar, Tamás Sovány, Géza Regdon jr., Thomas De Beer, Chris Vervaet, "COMPARISON OF METOPROLOL TARTRATE MULTIPLE-UNIT LIPID MATRIX SYSTEMS PRODUCED BY DIFFERENT TECHNOLOGIES," *Eur. J. Pharm. Sci.*, pp. 233–245, 2016.

[137] Bart Claeys, "Non-conventional polymers as matrix excipients for hot melt extruded oral-release formulations," *researchgate*, 2015.

[138] "Metoprolol tartrate vs. succinate: Differences in uses and effects." [Online]. Available: https://www.medicalnewstoday.com/articles/324175. [Accessed: 19-Mar-2020].

[139] "Metoprolol tartrate - DrugBank." [Online]. Available: https://www.drugbank.ca/salts/DBSALT000862. [Accessed: 31-Mar-2020].

[140] H. Baishya, "Application of Mathematical Models in Drug Release Kinetics of Carbidopa and Levodopa ER Tablets," *J. Dev. Drugs*, vol. 06, no. 02, pp. 1–8, 2017.

[141] O. Cantin, "PEO hot melt extrudates for controlled drug delivery Oriane Cantin To cite this version : HAL Id : tel-01540630 Faculté des Sciences Pharmaceutiques et Biologiques Thesis submitted to obtain the degree of Doctor in Pharmaceutical Sciences," 2017.

[142] S. M. Rahman, T. Saha, Z. U. Masum, and J. A. Chowdhury, "Evaluation of Physical Properties of Selected Excipients for Direct Compressible Tablet," *Bangladesh Pharm. J.*, vol. 20, no. 1, pp. 34–38, 2017.

[143]   X. Zhang, X. Peng, and S. W. Zhang, "Synthetic biodegradable medical polymers: Polymer blends," in *Science and Principles of Biodegradable and Bioresorbable Medical Polymers: Materials and Properties*, Elsevier Inc., 2017, pp. 217–254.

[144]   "(181) Bulk Modulus of Elasticity and Compressibility - Fluid Mechanics - Physics Practice Problems - YouTube." [Online]. Available: https://www.youtube.com/watch?v=ugxgSIGIHrg. [Accessed: 18-Mar-2020].

[145]   "Americas Gastrointestinal Drugs Market Key Players: Abbott Laboratories, Valent Pharmaceuticals, Evoke Pharma, Takeda Pharmaceutical, Janssen Biotech, GlaxoSmithKline. | Medgadget." [Online]. Available: https://www.medgadget.com/2019/06/americas-gastrointestinal-drugs-market-key-players-abbott-laboratories-valent-pharmaceuticals-evoke-pharma-takeda-pharmaceutical-janssen-biotech-glaxosmithkline.html. [Accessed: 01-Mar-2020].
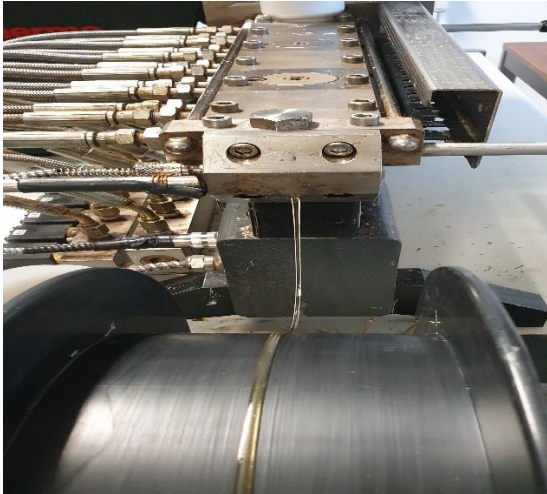
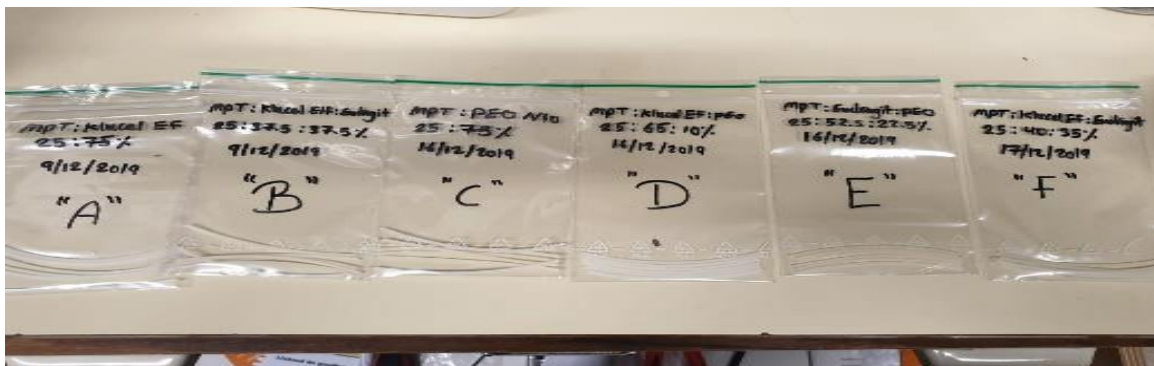Photos from the work

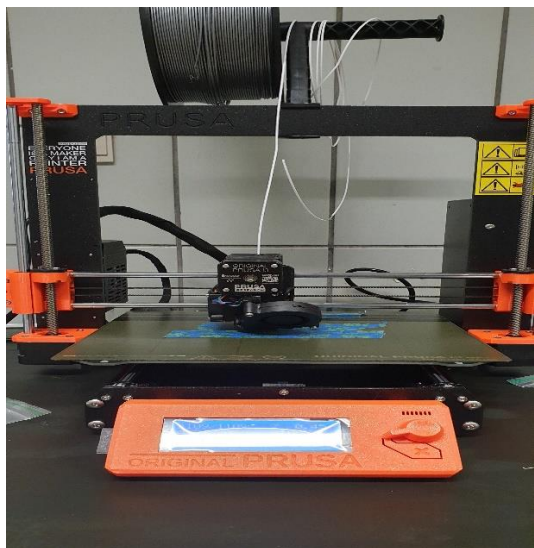Extruder Feeder

Extruder Screws

Extuder

One of the printed filaments (MPT: Capa 40:60%, w/w)
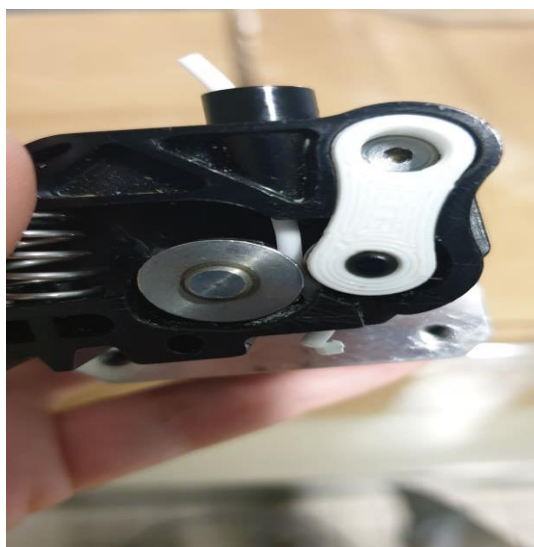

Extruder Monitor screen

Filaments Ready For Tensile Test
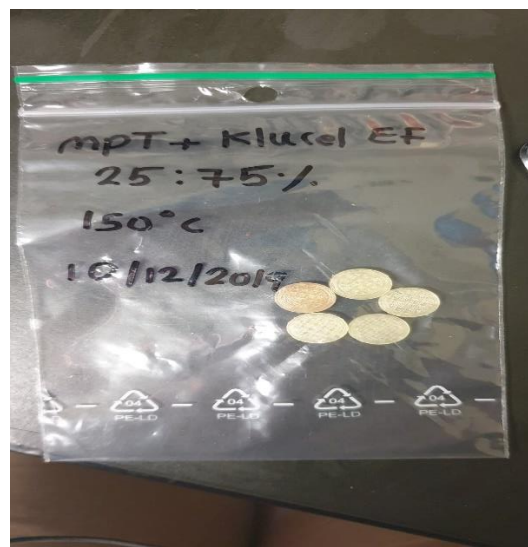
FDM, 3D Printer

Microscope

Brittle filament broken between the counter

Rotating Wheels

Trials during printing Mono Tablets

3D Printed Bilayer Tablet